AN ABSTRACT OF THE THESIS OF

Bernhard H. Geierstanger for the degree of Master of Science in Biophysics and Biochemistry presented on July 6, 1990.

Title: Base specific binding of copper(II) to Z-DNA:
1.3 Å single crystal structure for d(m^5CGUAm^5CG) soaked with $CuCl_2$

Redacted for Privacy

Abstract approved:

The structure of the self-complementary hexamer sequence d(m^5CGUAm^5CG) soaked with copper(II) chloride was solved to atomic (1.3 Å) resolution. The structure was found to be nearly identical to the Z-DNA conformation of the native d(m^5CGUAm^5CG) structure. A comparison of the ions revealed that four potential copper binding sites were present in an asymmetric unit, as defined by the hexamer duplex. The sum of the partial occupancies at each copper binding site showed that a total of 1.3 copper ions were present per hexamer duplex, nearly identical to the value of 1.1 copper ion per hexamer duplex determined from atomic absorption and UV absorbance measurements.

Each of the four guanine bases along the hexamer chain were shown to be modified by a covalent coordinate bond formed between its N7 nitrogen and a copper ion. The specific partial occupancies and geometries were dependent on the accessibility and the potential interactions at the site as determined by the local environment. One copper was shared between a guanine and an adenine base, each on different hexamer duplexes. The adenine that sits in an open solvent channel was not susceptible to copper modification. This suggests that the adenines of Z-DNA, and most likely all other conformations of duplex DNA, are immune to covalent modification by copper(II) in dilute DNA solution. In the more densely packed environment of the nuclear matrix in a cell, however, additional and perhaps specific DNA-DNA interactions may render the N7 nitrogen of adenine more prone to copper binding.

In addition, the solvent structure of this copper-soaked crystal was compared with those of the native d(m^5CGUAm^5CG) and the d(m^5CGTAm^5CG) Z-

DNA crystals. This showed that the magnesium complex at the internal d(UA) dinucleotide of the native d(m^5CGUAm^5CG) structure was primarily responsible for the continuity of the spine of water in the minor groove crevice that stabilizes Z-DNA. The presence of the copper ions in the current structure dislodged the magnesium cluster at the major groove surface, resulting in a narrowing of the minor groove crevice. This acted to "squeeze" the waters in the crevice and disrupted the continuity of the water network. The minor groove was not, however, as narrow as that of the d(TA) dinucleotide and, therefore, no waters were actually excluded from the crevice. Thus, the water structure in the minor groove crevice was shown to be determined by the structure of the narrow crevice in Z-DNA, and not vice versa.

Base Specific Binding of Copper(II) to Z-DNA: 1.3 Å Single Crystal Structure of d(m^5CGUAm^5CG) Soaked with $CuCl_2$

by

Bernhard H. Geierstanger

A THESIS

submitted to

Oregon State University

in partial fulfillment of
the requirements for the
degree of

Master of Science

Completed July 6, 1990

Commencement June 1991

APPROVED:

Redacted for Privacy

Professor of Biophysics in charge of major

Redacted for Privacy

Chairman of the Department of Biochemistry and Biophysics

Redacted for Privacy

Dean of Graduate School

Date thesis is presented July 6, 1990

ACKNOWLEDGEMENT

I thank Professor Gary J. Quigley, Department of Chemistry, New York University, NY, for performing the X-ray diffraction measurements, Mark Keller, Department of Agricultural Chemistry, Oregon State University, for providing copper(II) standard solutions for atomic absorption measurements, and the Department of Agricultural Chemistry, OSU for allowing me to use their atomic absorption spectrometer.

My special thanks, and also apology, to Dr. Jeanne R. Small, Dr. Mike Schimerlik and Dr. Douglas Barofsky for having them read this very extended thesis.

I also would like to thank my fellow lab colleagues Todd Kagawa and Guangwen Zhou for their cooperation. Guangwen Zhou solved the structure of the native (copper free) d(m^5CGUAm^5CG) Z-DNA crystal. Todd Kagawa solved the Z-DNA crystal structure of the copper(II)-soaked d$(CG)_3$ hexamer duplex. The comparison of these structures with the present copper(II)-soaked d(m^5CGUAm^5CG) structure yielded to the conclusions presented in this thesis.

I am especially thankful for the guidance and advice supplied by Dr. Pui Shing Ho, my major professor. Discussions with him steadily improved my understanding of X-ray crystallography applied to deoxyribonucleic acids. It was a pleasure to work with Dr. Pui Shing Ho, Todd Kagawa and Guangwen Zhou.

I am graceful for a partial stipend from the Fulbright Kommission, Bonn, West Germany. I also thank my roommate Eric Hanson for proofreading this thesis.

TABLE OF CONTENTS

LIST OF FIGURES

LIST OF TABLES

Base Specific Binding of Copper(II) to Z-DNA: 1.3 Å Single Crystal Structure of d(m^5CGUAm^5CG) Soaked with $CuCl_2$

INTRODUCTION

A number of biochemical processes in the nuclear matrix of a cell have been shown to be involved or be adversely affected by copper ions. Copper was among the metals found to be associated with deoxyribonucleic acid (DNA) extracted from cells (see Sissoëff *et al.*, 1976, Zimmer *et al.*, 1971 for references) and was found to bind preferentially to the bases of DNA (Eichhorn and Shin, 1968). *In vitro* studies have shown that copper and other ions facilitate the crosslinking of a considerable number of proteins to DNA (Wedrychowski *et al.*, 1986). Evidence for this process was also found *in vivo* (see Sissoëff *et al.*, 1976 for review and references).

One of the more important effects of copper on DNA, at least in terms of environmental causes of carcinogenesis, is its role in a number of DNA damaging mechanisms. The DNA bound copper is believed to function as a localized redox center that generates a non-diffusible oxygen radical in concert with hydrogen peroxide. With the highest binding affinity among divalent metal ions for the bases of DNA and its reactivity as a transition metal, copper may be unique in its interactions with and subsequent effects on DNA.

Recently two solution studies (Sagripanti and Kraemer, 1989, Yamamoto and Kawanishi, 1989) revealed that DNA cleavage in the presence of copper(II) and hydrogen peroxide was specific for sequences of guanines (GG and GGG). Kagawa *et al.* (unpublished) solved the Z-DNA crystal structure of $d(CG)_3$ soaked with $CuCl_2$ to atomic resolution. Copper(II) was observed to form a covalent coordinate bond to the N7 nitrogens of all guanine bases. No direct binding to the anionic phosphate groups of DNA was detected. Consequently, the question arose as to whether copper(II) binds exclusively to the guanine bases or whether its binding is general for all purine bases of DNA.

This thesis focuses on this question by extending the crystallographic studies to the sequence d(m^5CGUAm^5CG) that contains adenine bases as well as guanine bases. The results will show that copper binding appears to be specific for guanines for DNA in solution but may be not as specific in the cellular matrix.

In the remainder of the introduction, the specific role that copper(II) ions play in the induction of carcinogenesis and, ironically, in attempts to treat cancer will be discussed in order to emphasize the importance of this metal in a biological system. This will also serve to focus the discussion on the relevance of the specific metal-DNA interactions for this metal. The known chemistry and biochemistry of these interactions will be discussed in terms of the phenomenological base specificity and the models to explain this specificity of copper binding to DNA .

Copper(II) ions have been shown to be mutagenic to phage and bacterial DNA, and tumorigenic in animal tissue (Sissoëff *et al.*, 1976 for references). At the molecular level, this transition metal plays a role in the control of replication, gene amplification and transcription (see Sissoëff *et al.*, 1976 for review and references). The effect of copper on these molecular processes appears to be the root of the phenotypic responses observed at the cellular level. In at least one case, the absence of copper adversely affects the molecular biology of DNA in a cell. When rats were fed a diet containing 2 % cuprizone, a potent copper chelating agent, their liver cells exhibited abnormally large, or "giant" mitochondria. An analysis of the mitochondrial DNA and comparison to that of normal cells showed that a short DNA sequence had either been deleted or multiply duplicated. This led to the conclusion that copper(II) ions play a role in the initiation of mitochondrial DNA amplification (Sissoëff *et al.*, 1976).

The effect of copper(II) ions on these molecular events in the nuclear matrix appears to involve direct interactions of the metal with the DNA, regardless of whether it is acting at the level of controlling elements (enzymes and proteins involved in DNA replication and transcription) or the structure of the DNA itself. For example, deoxyribonuclease I (DNAase I), which normally causes single-strand breaks in DNA, caused double-strand breaks in the presence of copper(II). This appears to be associated with a change in the conformation of the DNA induced by metal binding (Sissoëff *et al.*, 1976 for review and references). The specificity of DNAase I is also affected by copper ions. The enzyme is generally considered to be a relatively nonspecific DNA cleavage agent. The preferential binding of copper(II) to guanine bases (to be discussed later), however, inhibits cleavage of DNA by DNAase I at guanine sites (see Marzille *et al.*, 1980 for references).

At the DNA level, copper binding has been shown to influence the actual helical structure of the molecule in terms of the denaturation and renaturation of

base pairs, as well as the conformation of the double helix (see Zimmer *et al.*, 1971, Sissoëff *et al.*, 1976 for review and references). These effects clearly would influence the chemistry and biology of DNA in the cell.

1. Copper(II) induced DNA damage

In addition to the effect of copper(II) on the functioning of biochemical processes in the nuclear matrix, the metal ion itself appears to play an important role in aging and in mutagenesis, and can result in the development of cancer. This process generally involves the copper(II) catalyzed oxidative cleavage of DNA (Schaaper *et al.*, 1987). Ironically, the same mechanism has been exploited in the design and synthesis of antitumor agents.

A large variety of therapeutic anticancer agents act by damaging the DNA of rapidly proliferating cancer cells. The exact mechanism for DNA cleavage by these agents is not entirely understood. The basic principle appears to involve the generation of an oxygen radical from hydrogen peroxide and a copper(I) species. The resulting radical is not readily diffusible and thus reacts in the immediate area of its copper center origin. The following discussions will center on the known properties of these copper-dependent antitumor agents, from which the basic mechanisms of copper-dependent DNA cleavage reactions were developed. This will be followed by a synopsis of what is currently understood concerning the requirements for direct DNA cleavage by copper ions.

1.1 Copper as a co-factor for antitumor drugs

Copper is a co-factor for a variety of DNA damaging drugs, such as 4'-(9-acridinylamino)-methanesulfon-m-aniside (mAMSA), bleomycin, rifamycin, 1,10-phenantroline and camptothecin (see Table 1 for references). A number of these drugs have antiviral and anticancer activity, which is supposedly due to their ability to damage DNA. They have in common the requirement for the presence of copper ions in order to cleave DNA.

The drugs listed in Table 1 are clinically used or have potential applications for cancer treatment. Human acute leukemia, lymphomas and carcinoma of the breast can be effectively treated using the highly active antitumor drug mAMSA. Bleomycins are a group of antitumor antibiotics that are used clinically in the

Table 1.

Drugs, cleaving DNA in reactions catalyzed by copper and oxygen radicals (especially hydrogen peroxide).

Reagent:	Sequence specific cleavage:	References:
4'-(9-acridinylamino)-methanesulfon-m-aniside (mAMSA)	Not investigated	Wong *et al.*, 1986
Bleomycins	Cleavage at C at 3' side of Pu in PyGCPu	Hecht, 1986, Rabow *et al.*, 1990a and 1990b
Rifamycin	not investigated	Quinlan and Gutteridge, 1987
1,10-Phenanthroline (Phen)	Double-helical structure required; cleaves at all nucleotides, predominant at A in TAT, preference: TAT>>TGT=TAC>>CAT,CAC >CGT,CGC	Marshall *et al.*, 1981, Marshall *et al.*, 1982, Graham *et al.*, 1980, Goldstein and Czapsk, 1986 and ref. herein, Veal and Rill, 1988, Veal and Rill, 1989
Camptothecin	Nonspecific; cytosines at the 3' side of adenines somewhat prefered	Kuwahara *et al.*, 1983

treatment of certain malignancies, including squamous cell carcinomas and malignant lyphomas (Hecht, 1986). Camptothecin (CPT), a cytotoxic alkaloid isolated from a tree in South China, is believed to inhibit nucleic acid synthesis rather than protein synthesis. The 10-hydroxy derivative of CTP has been successfully used in China for the treatment of liver carcinoma and head-neck cancer (Kuwahara *et al.*, 1983). Phenanthroline inhibits DNA polymerase I and other polymerases through the cleavage of DNA initiated by the binding of a (1,10-phenanthroline)$_2$Cu(I) complex to DNA. The resulting cleavage reaction products are what ultimately inhibit the function of polymerase I from *Escherichia coli* (Marshall *et al.*, 1982). Rifamycin SV inhibits the initiation of bacterial DNA-dependent RNA synthesis by a mechanism similar to that of the metal chelating agent 1,10-phenanthroline (Quinlan and Gutteridge, 1987). The lipophilic antibiotic rifamycin SV substantially degrades DNA molecules in the presence of copper or iron ions.

The antitumor activity of these drugs is believed to be a result of their ability to cause DNA strand scission in the presence of copper. In the case of phenanthroline and rifamycin, the cleavage products may be responsible for the antitumor activity. A common feature of these molecules is that they all bind to DNA. The drug mAMSA, for example, is a strong DNA intercalator (Wong *et al.*, 1986). The formation of a partially intercalated (1,10-Phenanthroline)$_2$Cu(I) complex was proposed as the initial step of DNA cleavage by phenanthroline (Veal and Rill, 1989). Bleomycins have been shown to be fully or partially intercalated into double-stranded DNA (see Levy and Hecht, 1988 for references). This strongly implicates DNA as the most likely target molecule for the antitumor activity of these drugs.

The incubation of DNA with the drugs in Table 1 in the presence of copper resulted in oxidative DNA damage. The sequence specificity of the DNA cleavage reaction catalyzed by the drug/copper complexes is summarized in Table 1. The complexes do not exhibit the same degree of sequence specificity as do biological DNAases (Marshall *et al.*, 1982). Whenever a preference for cleavage at particular bases was apparent, such as for bleomycin (Hecht, 1986) and phenanthroline (Veal and Rill, 1988, Veal and Rill, 1989), DNA cleavage occurred at or next to a purine base. Copper(II) was reported to preferentially bind to purine bases, with binding affinities in the order G>A>C>T (Eichhorn and Shin, 1968). This suggests that

binding of the copper/drug complexes to DNA involves copper binding to the purine bases. The interaction of the organic function from the copper/drug complex with DNA constrains the geometry of the copper/drug/DNA complex and plays, therefore, a role similar, if not more significant, to that of copper binding in the determination of the sequence specificity of the cleavage reactions.

The metal dependence of these anticancer drugs varies. Bleomycin exhibits DNA cleavage activity under aerobic conditions in the presence of Fe(II), Mn(II) or VO(IV) (Hecht, 1986). Camptothecin complexed with Mn(II), Fe(II), Co(II), Ni(II), Zn(II), Fe(III) or Co(III) was unable to break DNA or inactivate phage infectability (Kuwahara *et al.*, 1983). For both drugs copper(I) and copper(II) resulted in full DNA cleavage activity. This suggests that copper may be unique in its redox chemistry and/or its interactions with DNA in the functions of these drugs.

Single- and double-strand scission were observed when DNA was incubated with the drugs in Table 1 in the presence of copper. In the case of bleomycins, the therapeutically significant Fe(II)-Bleomycin complex was shown to cleave double-stranded DNA by oxidation at the C4' of the ribose moiety leading to a C4' radical (hydrogen abstraction) (Hecht, 1986). At elevated O_2 concentrations, base propenals are released and nucleoside 3'-(phosphoro-2"-O-glycolates) are formed at the 3' end of the oligonucleotides upon cleavage (Hecht, 1986). Under anaerobic conditions, and to lesser extent under aerobic conditions, free bases and alkali-labile sugar-phosphate sites in the backbone are generated by the drug. These can be subsequently cleaved by free hydroxide ion. The copper(II)-bleomycin complex is believed to react in the same manner with DNA. This drug forms an equimolar complex of molecular oxygen to copper to bleomycin that attacks the DNA. The resulting reaction products from the copper complex have not, however, been as well characterized as those from the ferrous complex (Hecht, 1986, Rabow *et al.*, 1990a+b). Copper(II) was also shown to enhance the unwinding of plasmid DNA by bleomycin A2. Copper therefore does not only function as a reaction center for oxygen activation, but also plays an important role in DNA/drug interaction (Levy and Hecht, 1988). The degradation of DNA by rifamycin likely proceeds by a mechanism similar to that of the bleomycins. The fragments released contain aldehyde groups and a highly reactive hydroxyl radical that supposedly facilitates the degradation of the deoxyribose (Quinlan and Gutteridge, 1987).

Treatment of DNA with 1,10-phenanthroline in the presence of copper(II) and/or copper(I) resulted in the generation of free bases and 5'- and 3'-end phosporylated DNA fragments (Marshall *et al.*, 1982). The 3'-phosphorylated fragments are responsible for the inhibition of *Escherichia coli* DNA polymerase I. A furan derivative (3'-phospho-5-methylfuranone intermediate) was also proposed at the 3' termini of the cleavage products (Marshall *et al.*, 1982). Its formation is believed to result from a hydroxyl radical attack at the C1' of the ribose. Similarly 3'-phosphoglycolates were produced by the attack at the C4' (Sigman, 1986, Veal and Rill, 1989). Aldehydes were not found in the digest (Marshall et. al., 1982) as was the case for bleomycins.

From the cleavage products, the mechanism of DNA cleavage by the drugs in the presence of copper appears to follow a similar pattern, although the actual cleavage reactions may vary somewhat. The formation of a copper/drug complex with DNA is the first step (Marshall *et al.*, 1981, Hecht, 1986) of the cleavage reaction. The reactive copper form for all the drug/copper complexes is always copper(I), which is generated by the reduction of copper(II) by reducing agents such as mercaptopropionic acid (for phenanthroline reaction (Marshall *et al.*, 1981)), hydrogen peroxide (Marshall *et al.*, 1981, Hecht, 1986, Rabow *et al.*, 1990a+b) or by UV light (in camptothecin reaction) (Kuwahara *et al.*, 1983). In the case of mAMSA an electron transfer reaction between mAMSA and copper(II) yields mAQDI (N1-methylsulfonyl-N4-(9-acridinyl)-3-methoxy-2,5-cyclohexadiene-1,4-diimine) and copper(I). The resulting mAQDI and copper(I) are the reactive species in the cleavage mechanism (Wong *et al.*, 1986), as shown by the correlation of the kinetics of DNA cleavage by mASMA and copper(II) and the production of both copper(I) and mAQDI (Wong *et al.*, 1986).

The next step in the cleavage mechanism appears to be the formation of hydrogen peroxide. All the drug/Cu(I) complexes can generate hydrogen peroxide from molecular oxygen under aerobic conditions by a reaction similar to (Marshall *et al.*, 1981 and references herein):

$$2\ H^+ + O_2 + 2\ (Phen)_2Cu(I) \text{ -------> } H_2O_2 + 2\ (Phen)_2Cu(II)$$

Under anaerobic conditions, DNA cleavage is significantly inhibited, consistent with the involvement of molecular oxygen in the formation of hydrogen

peroxide. Furthermore, the addition of reducing agents to an aerobic reaction enhances DNA cleavage by recycling the copper(II) species back to copper(I) (Marshall *et al.*, 1981).

Direct involvement of hydrogen peroxide in DNA scission was demonstrated by, first, the observed enhancement of the cleavage rate resulting from the addition of hydrogen peroxide to an aerobic reaction (Marshall *et al.*, 1981). Under anaerobic conditions, the rate of DNA damage by phenanthroline and copper was identical to that under aerobic conditions when hydrogen peroxide and mercaptopropionic acid (a reductant to regenerate copper(I)) was added (Marshall *et al.*, 1981). Secondly, the action of these drugs is inhibited by catalase (an hydrogen peroxide degrading enzyme) and bathocuprione (a copper(I) specific chelator). Together these results clearly indicate that both hydrogen peroxide and copper(I) are essential for the cleavage of DNA by these copper-dependent antitumor drugs.

The possible reactive species generated from copper(I) and hydrogen peroxide include superoxide, hydroxyl radicals, or other undefined oxygen radical species. The effect of free radical scavengers such as superoxide dismutase, a superoxide anion scavanger, on the DNA cleavage reactions varies considerably depending on the specific drug tested. Although superoxide anion radicals are formed during the aerobic oxidation of $(Phen)_2Cu(I)$ (Marshall *et al.*, 1981. Graham *et al.*, 1980) and rifamycin SV (Quinlan and Gutteridge, 1987), freely diffusible superoxide is not directly involved in the cleavage reactions as indicated by their insensitivity to inhibition by superoxide dismutase. Superoxide anions may, however, affect cleavage reactions by increasing the steady-state levels of hydrogen peroxide and the drug/Cu(I) complex via the following reaction (Marshall *et al.*, 1981, Graham *et al.*, 1980):

$$2\ O_2^{\cdot -} + 2\ H^+ \text{ -------> } O_2 + H_2O_2$$

$$(Phen)_2Cu(II) + O_2^{\cdot -} \text{ --------> } O_2 + (Phen)_2Cu(I)$$

It is more likely that the reactive species is generated by copper(I) and hydrogen peroxide in a Fenton-type redox cycle (Johnson *et al.*, 1985, Masarwa *et al.*, 1988):

$$Cu(I) + H_2O_2 \longrightarrow \cdot OH + OH^- + Cu(II)$$
$$Cu(II) + H_2O_2 \rightleftharpoons Cu(I) + HO_2 + H^+$$

In the case of phenanthroline, hydroxyl radical and singlet oxygen traps were not effective in inhibiting cleavage (Marshall *et al.*, 1981). The hydroxyl radical was proposed as the reactive species in the cleavage of DNA with rifamycin, but the degradation was only poorly inhibited by hydroxyl radical scavengers such as formate, thiourea, and mannitol (Quinlan and Gutteridge, 1987). This is believed to be evidence for a site-specific radical reaction with the DNA molecule, where the oxygen radical responsible for cleavage is in fact either not freely diffusible or is bound to the copper(I). Generally, the cutting efficiency would be enhanced by short diffusion distances for the free radicals from their formation site (Wong et. al., 1986).

Other proposed oxygen radicals that may be responsible for the cleavage mechanism include the $[Cu(I)H_2O_2]^+$ complex (Ponganis *et al.*, 1980) and copper(III). Although less reactive (Ponganis *et al.*, 1980, Johnson *et al.*, 1985), these species could cleave DNA without the need for a hydroxyl radical. Summarizing the findings of the studies, a non-diffusible oxygen radical, which is generated close to the DNA cleavage site by a reaction dependent on hydrogen peroxide and copper(I), is the reactive radical species responsible for the DNA cleavage by drug/copper complexes.

1.2 Copper ion as a DNA cleavage agent

As previously discussed, copper is believed to function as a reaction center for the generation of a site-specific oxygen radical during DNA cleavage reactions by copper/drug complexes. It is therefore not surprising that, under certain conditions, copper itself can cause DNA strand cleavage. DNA cleavage by copper generally requires the presence of a reducing agent such as reducing sugars (Nanjou *et al.*, 1985, Morita *et al.*, 1985), hydrogen peroxide (Sagripanti and Kraemer, 1989, Yamamoto and Kawanishi, 1989) or ascorbate (Chiou *et al.*, 1985, Fujimoto *et al.*, 1986). This suggests a DNA cleavage mechanism similar to that of the copper-dependent antitumor drugs.

DNA cleavage by ascorbate (vitamin C) in the presence of copper is presumably the reason for the antitumor activity of ascorbate. Studies using cell

culture indicate that ascorbate in the presence of copper is preferentially cytotoxic for malignant melanoma cells (Bram *et al.*, 1980), presumably due to the elevated copper concentrations in these cells. Regularly proliferating cells are only slightly affected. The copper/ascorbate combination can therefore be considered an antitumor drug.

The major difference from the class of DNA cleaving drugs described previously, however, is that ascorbate does not form a drug/copper complex with DNA. The involvement of ascorbate (Chiou *et al.*, 1985, Fujimoto *et al.*, 1986) and various other reducing agents such as reducing sugars (Nanjou *et al.*, 1985, Morita *et al.*, 1985), and hydrogen peroxide (Sagripanti and Kraemer, 1989, Yamamoto and Kawanishi, 1989) in causing DNA cleavage, is to lead to the conversion of copper(II) to copper(I), which in turn generates oxygen radicals that are responsible for the observed DNA damage.

Recent studies on direct DNA damage caused by copper(II) ions (Sagripanti and Kraemer, 1989, Yamamoto and Kawanishi, 1989) have focused on the nature of the reactive oxygen species and on the sequence specificity of the DNA cleavage reaction.

Yamamoto and Kawanishi (1989) studied the cleavage reaction of a (^{32}P) 5' end-labeled 261-base pair fragment with a well defined sequence (from plasmid pbcNI). Both copper(II) and hydrogen peroxide were required to break the phosphate backbone, and, in addition, lead to base modifications and base release. The complete inhibition of these reactions by diethylenetriaminepentaacetic acid (DTPA, a copper chelator) supports the involvement of copper(II), while the complete inhibition by bathocuproine (a copper(I) specific chelator) implicates copper(I) involvement in the reaction mechanism. This suggests a redox mechanism similar to the copper/drug complexes for copper alone affecting DNA cleavage.

Electron paramagnetic resonance (EPR) experiments showed that both hydroxyl radicals and singlet oxygen are formed in the reaction of copper(II) with hydrogen peroxide. The singlet oxygen scavengers sodium azide and 1,4-diazobicyclo[2,2,2]octane (Dabco) were highly effective inhibitors for the cleavage reaction. Hydroxyl radical scavengers, such as ethanol and mannitol, did not inhibit the DNA cleavage reaction. Tert-butyl alcohol, a weak hydroxyl radical scavenger, however, significantly inhibited (60%) the reaction. Thus, the authors concluded

that DNA damage was not caused by the hydroxyl radicals generated from the copper(II)-hydrogen peroxide reaction, but rather by copper-peroxide complexes that mimic singlet oxygen and/or hydroxyl radical reactivities.

As an alternative to the generally assumed Fenton-type reaction for copper(II) and hydrogen peroxide, Yamamoto and Kawanishi proposed a model whereby two DNA-bound copper(II) ions are bridged by a single hydrogen peroxide to form a hydroperoxo-dicopper(II) complex. The reaction results in the reduction of both coppers to copper(I). One of the copper(I) ions reacts then with hydrogen peroxide generating a DNA-Cu(I)$^{\cdot}$ OOH^{-} radical complex which would eventually lead to DNA damage. This model is based on kinetic studies on reactions involving low-valent transition-metal complexes with hydrogen peroxide (Masarwa *et al.*, 1988). In these model studies, copper(I) reacted with hydrogen peroxide to form a $Cu^{+}\cdot O_2H^{-}$ complex in the presence of an alcohol substrate. Only in the absence of the substrate does this complex lead to aqueous copper(II) and hydroxyl free radicals. The properties of this copper-peroxy complex are consistent with the effects of radical scavengers on the DNA cleavage reaction by copper(II) and hydrogen peroxide as well as by copper/drug complexes. The $Cu^{+}\cdot O_2H^{-}$ complex, therefore, appears most likely to be the reactive oxygen species in DNA cleavage reactions by copper ions or copper/drug complexes.

Finally, the inhibitors that were effective at arresting general DNA scission by copper(II) and hydrogen peroxide did not inhibit the reaction at guanine sites. In addition, the DNA damage by this redox couple after piperidine treatment was observed to be preferential for thymine and guanine bases that were 5' of two or more adjacent guanine nucleotides. Cleavage at adenines was rarely observed. This suggests that copper(II) binds specifically to guanine bases and that, in the absence of piperidine, cutting of DNA at the guanines may involve a base specific reaction mechanism, while general cleavage involves a nonspecific mechanism.

Sagripanti and Kraemer (1989) basically confirmed these findings for larger DNA sequences. When they reacted supercoiled plasmid DNA with copper(II) and hydrogen peroxide, as little as 10^{-6} M copper(II) in the presence of 10^{-5} M hydrogen peroxide lead to DNA breakage and the loss of transforming ability of the plasmid. Concentrations up to 10^{-2} M of either copper(II) or hydrogen peroxide alone did not cause DNA damage. Studies on the effects of radical scavengers and chelators on this reaction indicated that copper(II), copper(I), and hydrogen

peroxide were involved in the cleavage mechanism. They found, however, that hydroxyl free radical scavengers did inhibit the DNA cleavage reaction. The effective radius of hydroxyl free radical cutting function was assumed to be very short because the inhibition was only partial. Piperidine-labile sites were specifically generated at stretches of two or more guanine nucleotides suggesting guanine specific base damage by copper and an oxygen radical. Although copper(I) caused DNA damage as well, no base specificity was observed after piperidine treatment; again, this indicated a specific copper(II)-guanine interaction.

Earlier studies had suggested that the oxidative degradation of DNA by copper had a strong preference for certain bases. DNA cleavage in the presence of excess ascorbate was specific for short stretches of purine nucleotides cutting at the 3' side of guanine and at both the 3' and 5' ends of adenines (Chiou *et al.*, 1985). There was only minimal damage to stretches of pyrimidine bases. A similar study that monitored the release of free bases after aerobic reaction of DNA with copper(II) and ascorbic acid showed that adenine was preferentially released over guanine, thymine, and cytosine bases (Fujimoto *et al.*, 1986). Stoewe and Prütz (1987) found that adenine and guanosine triphosphate could effectively inhibit cleavage of DNA by copper(II), hydrogen peroxide, and ascorbic acid. Guanosine triphosphate was more efficient at inhibiting the reaction (90 % inhibition) when compared to free adenine (44 % inhibition), suggesting that the inhibition of cleavage was a result of competitive binding of copper ions by the free nucleotide and nucloside bases, in much the same way that metal chelators inhibited this reaction.

Thus, the observed specificity of the copper cleavage reaction, under conditions of excess ascorbic acid, appeared to favor adenine bases. This contrasts the more recent results (Sagripanti and Kraemer, 1989, and Yamamoto and Kawanishi, 1989) that suggest a preference for copper induced damage at the guanine bases of DNA. Although all these studies indicate that pyrimidines remain immune to DNA damage, the question of which purine base in DNA is susceptible to cleavage by copper, and the origin of this specificity, remains unresolved. One approach to address these questions is to search for the structural basis for the specific binding of copper species to DNA.

2. Structural studies on binding of copper and other transition metals to DNA and its components

DNA, as a polyelectrolyte, has a large variety of potential sites for binding transition metals. Since metals in solution are cationic, they are electrophilic and will, therefore, search out those atoms or functions with the highest density of negative electrical charges. The most obvious functions along the DNA duplex that meet this general criteria are the phosphodiester linkages of the DNA backbone. Metal binding to the phosphates, however, would not confer base specificity. The most recent studies, and the rest of this discussion, therefore, focused on the properties of the DNA bases that are responsible for the base specificity for binding transition metals, and for binding copper ions in particular.

A good initial indicator of the electric potential of an atom or functional group is its pK_a value. The more basic an atom (i. e., the higher its pK_a), the more it prefers to hold on to its proton, indicating a more electronegative site, and therefore, the site most susceptible to electrophilic attack by a transition metal. The site with the highest pK_a value in both adenine and guanine is the N9 nitrogen of the free bases (Barton and Lippard, 1980, Marzille *et al.*, 1980). In DNA, the N9 nitrogen is covalently bound to the ribose moiety of the nucleotide component of the polymer. This site is, therefore, not available for metal binding to DNA.

Of the sites available for metal binding, the N1 nitrogen is the most basic in the adenine base, followed by the N7 nitrogen. In the guanine base the order is N7 followed by O6. For completeness, the N3 nitrogen of pyrimidine bases is the most basic site followed by the O4 and O2 oxygens of uridine, and the O2 oxygen of cytosine (Barton and Lippart, 1980, Marzille *et al.*, 1980).

From calculations of the electrostatic potentials of all the nucleotides, Pullman and Pullman (1981) found that, as expected, the negatively charged phosphates were the most electronegative group, and the ribose moiety was the least electronegative. The bases fell in the middle showing broad regions of electronegativity. While a wider electronegative surface was calculated for guanine that stretches from the O6 oxygen to the N7 nitrogen (with a distinct minimum at the N7), that of adenine was smaller, narrower, and not as electronegative. The adenine base also exhibited a large electropositive potential at the N6 amino nitrogen.

When placed into the context of a DNA polymer, the distribution of electronegative sites changes (Pullman and Pullman, 1981). The most negative electrostatic potential in double helical B-DNA occurs at the N7 nitrogen of guanine (-683 kcal/mole), followed by the N3 nitrogen of guanine (-670 kcal/mole) and of adenine (-669 kcal/mole), the O2 oxygen of thymine (-654 kcal/mole), the O6 oxygen of guanine (-650 kcal/mole), and the N7 nitrogen of adenine (-650 kcal/mole). In contrast, the potential at the oxygens of the phosphate groups was calculated to be about -600 kcal/mole. This reverses the expected order of electronegativity between the bases and the phosphate making the major groove of B-DNA much more electronegative. This is mainly due to the additive effects of the electrostatic potentials of the negatively charged phosphate groups surrounding the major groove. The addition of counter ions to the polymer lowers the absolute magnitude of each potential but not the order. For GC base pairs the most electronegative site is the N7 nitrogen of the guanine base in the major groove, while in AT base pairs the N3 position in the minor groove is most electronegative. The accessibility of the minor groove in B-DNA is, however, much lower than that of the major groove. The N7 position of adenine is not only less electronegative than the N7 of guanine, but its accessibility is also slightly lower (Pullman and Pullman, 1981). B-DNA in solution, therefore, would have its most susceptible site for metal binding at the major groove of the d(CG) base pairs around the N7 of the guanine bases.

The effect of DNA conformation on this selectivity changes. For example, in left-handed Z-DNA the most electronegative potential was placed in the minor groove crevice of the d(GC) base pairs. When counter ions were considered in the calculations, the major groove surface near the N7 of guanine was again the most electronegative site. In any case, the inaccessibility of the Z-DNA minor groove suggests that, even in this conformation, the sites that would be most susceptible to direct metal binding are the N7 nitrogens of the guanine bases. These electrostatic calculations, therefore, predict that copper(II) binding should be specific for the N7 nitrogens of guanine at the major groove of polymeric DNA. It should be stressed, however, that this would be a prediction of the relative binding affinities, and not whether a copper would bind at one site exclusively.

A number of single crystal studies have been performed on isolated nucleosides and nucleotides bound to various transition metals. These studies

support the results of the electropotential calculations in that the most basic atoms of the purine bases are the N1 and the N7 nitrogens. Studies on 9-methyladenine showed that a silver(I) complex and an organic copper(II) complex bound specifically to the N7 of adenine (Marzille *et al.*, 1980). In the latter structure, the copper is in a square planar coordination geometry. An aqueous complex of nickel(II) ions was also observed to bind to the N7 of the adenine base of AMP. These crystallographic results on the complexes of isolated bases and nucleotides would suggest that, contrary to the electronegativity calculations, it is the N7 nitrogen and not the N3 nitrogen of adenine that is most susceptible to metal binding. In contrast, the crystal structure of a polymeric copper(II) complex of guanosine-5'-monophosphate (GMP) showed that the copper(II) was coordinated to the N7 nitrogen of the base and the oxygens of the phosphate group (Aoki *et al.*, 1976), as predicted by the electrostatic potential calculations. For isolated purine nucleotides and nucleosides the most susceptible site for metal binding, particularly copper(II) binding, appears to be the N7 of the bases, regardless of whether it is an adenine or a guanine base.

For polymeric DNA, an extrapolation of these small molecule crystal structures suggests that both adenine and guanine would be susceptible to electrophilic attack at the major groove surface. Kagawa *et al.* (unpublished) solved the structure of a hexamer Z-DNA duplex ($d(CG)_3$) in the presence of copper(II) ions and showed that all the N7 nitrogens of the guanine bases formed covalent coordinate bonds to the copper(II) ions. The specific degree of modification and the coordination geometry defined by the water ligands of the cation were dependent on the local environment of each N7 nitrogen in the crystal.

The primary question to be addressed in this thesis is whether adenine bases in a DNA duplex behave similar to isolated adenine bases and nucleotides in that their N7 nitrogens are susceptible to covalent modification by copper(II) and, if so, to what degree and under what circumstances. The strategy for this study is to soak a single crystal of $d(m^5CGUAm^5CG)$ with copper(II) chloride and solve its crystal structure. This sequence crystallizes as Z-DNA in a space group that is isomorphous with the $d(CG)_3$ hexamer (Zhou and Ho, 1990). Thus, the binding of copper(II) ions to the guanine bases of the $d(m^5CGUAm^5CG)$ structure can be directly compared to that of the $d(CG)_3$ structure. This comparison acts as an internal control to ensure that the C5-methyl of the cytosine bases does not affect

copper binding at the purine bases, and to determine whether the specificity of copper binding is dependent on the local base effects or on overall sequence effects. The percentage of copper(II) modification at each guanine base in the crystal (i. e., the partial occupancy of each copper ion) will be compared between the d(m^5CGUAm^5CG) and the d(CG)$_3$ structures in the presence of copper(II) chloride. If the partial occupancy of each guanine base follows the same trend along each hexamer chain in both structures then the C5-methyl groups of the pyrimidine bases will be shown to not directly affect copper binding to the purine bases and that changing the internal two base pairs from d(CG) to d(UA) does not affect the ability of individual guanine base to bind copper(II).

A comparison of the partial occupancy of any copper(II) at the N7 nitrogen of the adenine bases will determine the degree and the circumstances to which an adenine in duplex DNA is modified. The high resolution (better than 1.3 Å) of these Z-DNA crystals allows the assignment of accurate bond lengths and distances, and the coordination geometry around each copper(II) ion. These will be the major criteria for determining whether a copper(II) ion has been bound to a DNA base. The recognition of a regular symmetric coordination geometry is one of the strongest indicators of a row II or transition metal in aqueous solution. By these criteria, the present study suggests that an adenine base of DNA in solution would not be modified by copper(II) ions. However, specific DNA-DNA interactions possibly found in the nuclear matrix of the cell could induce copper(II) binding to the N7 of adenine bases.

In the present crystal one of the adenine bases sits in an open solvent channel, while the second adenine is located at an interface between two hexamer duplexes. Each of the four guanine bases along the hexamer chain were shown to be modified by a covalent coordinate bond formed between its N7 nitrogen and a copper ion. The specific partial occupancies and geometries were dependent on the accessibility and the potential interactions at the site as determined by the local environment. One copper was shared between a guanine and an adenine base, each on different hexamer duplexes. The adenine that sits in an open solvent channel was not susceptible to copper modification. This suggests that the adenines of Z-DNA, and most likely all other conformations of duplex DNA, are immune to covalent modification by copper(II) in dilute DNA solution. In the more densely packed environment of the nuclear matrix in a cell, however, additional and perhaps

specific DNA-DNA interactions may render the N7 nitrogen of adenine more prone to copper binding.

Finally, this copper(II) structure will serve to enhance the understanding of the factors that stabilize Z-DNA. A magnesium water complex was found to be bound at the major groove surface of the d(UA) dinucleotides in the native d(m^5CGUAm^5CG) crystal. This magnesium water complex stabilizes Z-DNA by affecting the major groove surface and the water structure of the minor groove crevice. The analogous d(TA) containing sequence did not exhibit these Z-DNA stabilizing characteristics. The present structure will show that the copper(II) cations displace this magnesium complex from the d(UA) major groove surface, making it more analogous to that of the d(TA) surface.

A comparison of the solvent structure of this copper-soaked crystal with that of the native d(m^5CGUAm^5CG) and the d(m^5CGTAm^5CG) Z-DNA crystals showed that the magnesium complex at the internal d(UA) dinucleotide of the native d(m^5CGUAm^5CG) structure was primarily responsible for the continuity of the spine of water in the minor groove crevice that stabilizes d(UA) as Z-DNA. The presence of the copper ions in the current structure dislodged the magnesium cluster at the major groove surface, resulting in a narrowing of the minor groove crevice. This acted to "squeeze" the waters in the crevice and disrupted the continuity of the water network. The minor groove was not, however, as narrow as that of the d(TA) dinucleotide and, therefore, no waters were actually excluded from the crevice. Thus, the water structure in the minor groove crevice was shown to be determined by the structure of the narrow crevice in Z-DNA, and not vice versa.

MATERIALS AND METHODS

1. Materials

The hexanucleotide d(m^5CGUAm^5CG) was synthesized on an Applied Biosystems DNA synthesizer at the Center of Gene Research and Biotechnology at Oregon State University. The coupling efficiency was estimated to be better than 90 %. The DNA was purified as described in the Methods section.

Sephadex G10 for gel filtration, ammonium acetate, HPLC grade acetonitrile, copper(II) chloride (99.999% pure), magnesium chloride hexahydrate (99.999% pure), sodium cacodylate ($(CH_3)_2As(O)ONa*xH_2O$) (98% purity) and 2-methyl-2,4-pentanediol (MPD) (gold label and reagent grade=99%) were obtained from Aldrich Chemical Company, Milwaukee, Wisconsin. Gold label MPD was used for the preparation of the precipitating solution added to the crystallization wells, while reagent grade MPD was used in the reservoir of the crystal setups. All solutions were prepared using destilled and deionized water.

The standard copper solutions for the atomic absorption spectroscopy measurements were dilutions of a 1000 ppm copper standard from Varian techtron ($CuSO_4$ in diluted H_2SO_4), and provided by Mark Keller, Department of Agricultural Chemistry, Oregon State University.

2. Methods

2.1 Purification of oligonucleotides

The dry d(m^5CGUAm^5CG) hexanucleotide sample (approximately 1000 nmole) from the DNA synthesizer was typically dissolved in 100 µl distilled and deionized water, and loaded onto a wet 120 mm x ∅10 mm Sephadex G-10 size exclusion chromatography column to remove blocking agents and precursors. The elution of the DNA with water was monitored at 260 nm with a Hewlett-Packard HP 8452A diode array spectrometer. The sample was lyopholized under vacuum and redissolved in water. The oligonucleotide was further purified by high pressure liquid chromatography (HPLC) using an Alltech C6000 B C-18 (reverse phase) column. The HPLC system consisted of an ISCO model 2360 gradient maker, an ISCO model 2350 HPLC pump and an ISCO V^4 absorbance detector. The detector was set to

260 nm and the gradient program listed in Table 2 was used. For later crystal setups, the HPLC purification step was replaced by recrystallization as described below. The purified material was lyopholized and redissolved in deionized and filtered water to obtain the desired concentration.

2.2 Estimation of DNA concentration

All DNA concentrations were estimated by measuring the UV absorbance at 260 nm using a Hewlett-Packard HP 8452A diode array spectrometer. The molar extinction coefficient of the hexamer d(m^5CGUAm^5CG) in solution (B-form DNA) is 8950 M^{-1} cm^{-1} (per base) as measured by Ho *et al.* (1990). This value is equivalent to a molar extinction coefficient (ε) of $107.4*10^3$ M^{-1} cm^{-1} (per hexamer), or that 1 OD = $9.314*10^{-6}$ M. Using a molecular weight of approximately 3794 g/mole for the hexamer, 1 mg/ml = 28.3 OD. This molar extinction coefficient was used for all calculations of DNA concentration.

2.3 DNA Crystal growth

The hexanucleotide was crystallized at room temperature by vapor diffusion against an aqueous 2-methyl-2,4-pentanediol (MPD) solution (Wang *et al.*, 1984, Kim *et al.*, 1973). In this method, a dichlorodimethylsilane coated Pyrex spot plate with nine wells was placed in a plastic container sealed with vacuum grease. A large volume of aqueous MPD solution was placed at the bottom of the container, acting as a reservoir for equilibrating the vapor pressure inside the container. The crystallization solutions (similar to the conditions previously reported for the d(m^5CGUAm^5CG) hexamer duplex (Zhou and Ho, 1990)) were added into the wells in the following order:

5 µl 100 mM Sodium cacodylate buffer (pH 6.96)
5 µl 600 mM Magnesium chloride hexahydrate
10 µl 4.74 mM purified d(m^5CGUAm^5CG) hexanucleotide
5 µl 10% v:v MPD (in distilled and filtered water)

The initial concentration of MPD in the reservoir was typically 25 %, or approximately 10 times higher than the MPD concentration in the crystallization wells. Because MPD has a low vapor pressure relative to water, the difference in MPD concentration in the wells versus the reservoir is balanced by reducing the

Table 2. Purification of oligonucleotides by reverse phase high performance liquid chromatography: HPLC gradient.

Time in min:	Mobile phase:
0 to 5	95% A 5% B
5 to 35	95% A 5% B to 55% A 45% B
35 to 40	55% A 5% B to 95% A 5% B

A 0.1 M Ammonium acetate (pH 7.0)

B 50% Acetonitrile in A

Solutions were filtered through a 0.45 μm Nylaflo Nylon Membrane filter (Gelman Sciences Inc.) before use in the HPLC system.

volume of water in the wells. Upon equilibration the concentration of MPD, and all components including DNA, are effectively increased in the crystallization wells. The MPD concentration was further increased by 5 % increments, to give a final concentration of 50 % . The setup was allowed to reequilibrate for 48 hours after each addition of MPD. The final concentration of MPD in the wells, therefore, was 50 %, resulting in an overall decrease in solution volume of 35-fold. The decreased solubility of DNA in the more concentrated alcohol solution, in conjunction with the increase in DNA concentration, drives the molecule out of solution. Under optimal conditions, the DNA comes out of solution in an ordered fashion as large, regularly formed crystals. If the conditions are suboptimal, the DNA crystallizes as a shower of minute and/or irregular crystals, or as a noncrystalline precipitate. The large, well formed crystals are suitable for X-ray diffraction studies. The smaller and/or irregular crystals were harvested and redissolved for additional crystallization attempts (see 'DNA recrystallization'), or for copper soaking and subsequent atomic absorption and spectroscopic studies (see 'Copper binding').

DNA recrystallization

The small crystals resulting from multiple nucleation events were harvested, dissolved, and subsequently used for additional crystallization setups. The following is a description of a typical recrystallization procedure.

The MPD concentration in the reservoir was increased to 100% one day prior to harvesting the crystals in order to crystallize all free DNA. The crystals were transferred, along with the mother liquid in the well, into an Eppendorf tube. The crystals were centrifuged in an Eppendorf microcentrifuge (Centrifuge 5412, 15000 r. p. m.) for 10 minutes. The supernatant was used to wash the well of the crystal setup to recover all the crystals. The wash solution was than transferred back into the Eppendorf tube with the crystals, the transfer capillary rinsed with approximately 20 µl water, and the solution in the Eppendorf tube was again centrifuged for 10 minutes. The supernatant was discarded and the crystals were washed twice with 20 µl of cold, distilled, deionized water. Finally, 40 µl of water were added to the crystals and the solution was heated to about 85^{o} C to dissolve the crystals. The solution was slowly cooled to room temperature and the DNA

concentration was estimated from the UV absorption at 260 nm as previously described.

2.4 Copper binding to d(m5CGUAm5CG) crystals

The large DNA crystals obtained were soaked with copper by incremental additions of copper(II) chloride solution (concentration: 10 mM to 100 mM). The crystals were allowed to reequilibrate for 48 hours after each addition.

Atomic absorption spectroscopy (AAS) was used to determine the copper content in the crystals. A copper soaked crystal, which was not suitable for X-ray diffraction studies, but identically soaked with copper as the crystals used for diffraction data collection, was transferred with very little liquid into an Eppendorf tube. This crystal was redissolved in 600 µl deionized and distilled water by heating to about 90^{o} C for several hours. The DNA concentration was estimated by measuring the UV absorption of the dissolved crystal at 260 nm. The amount of copper in the 600 µl solution was measured using a Perkin Elmer 403 atomic absorption spectrometer using an acetylene/air flame for ionization. The instrument was set to 20 mA for the current through the hollow cathode lamp, slit width setting 4 (0.7 nm) and UV wavelength at 325 nm. The wavelength was fine adjusted to maximum sensitivity (copper line at 324.8 nm). According to the user manual of the instrument the sensitivity is about 0.09 µg copper/ml at 1% absorption and the working range for copper is linear up to concentrations of approximately 5 µg/ml in aqueous solution. The copper(II) standard solutions in diluted aqueous H_2SO_4 were provided by Mark Keller, Department of Agricultural Chemistry. To his knowledge there is no interference of absorption lines from other elements with the copper absorption line.

2.5 X-ray diffraction measurements

The copper soaked DNA crystals which were suitable for X-ray diffraction studies were mounted in a quartz capillary. The mounted crystals were sent to Professor Gary J. Quigley, Department of Chemistry at the New York University, for diffraction data collection. The X-ray diffraction measurements were performed on a Enraf-Nonius diffractometer with a rotating copper anode. The power setting for the electron cathode was 45 kV at 80 mA. The space group of the copper-soaked

crystals was $P2_12_12_1$ (No. 19, system type 3), identical to that of the native d(m^5CGUAm^5CG) crystal (Zhou and Ho, 1990).

2.6 Structure refinement

X-ray diffraction allows the determination of the molecular structure of biomolecules in crystals. Although the properties of the crystal lattice can be easily obtained from the diffraction pattern, the distribution of the electron density within the unit cell (the electron density map) is difficult to determine (see Cantor and Schimmel, 1980 for review). In order to calculate the electron density map of a crystal unit cell, the X-ray diffraction data must be transformed to structure factors (F). The structure factors for the diffraction spots with the reciprocal space indicies (h, k, l), are complex numbers ($|F| * e^{i\Phi}$), where |F| is the amplitude and $e^{i\Phi}$ a phase term. The intensity I (h,k,l), which is proportional to $|F|^2$ can be measured directly. The phase term $e^{i\Phi}$ is, however, not experimentally observable. The structure factors eventually yield the electron density ρ (x,y,z); however, without the phase term the electron density distribution within the unit cell cannot be calculated. The literature refers to this situation as the "phase problem" of X-ray crystallography.

The phase problem was solved for the structure of single Z-DNA crystals using the method of multiple isomorphous replacement (see Cantor and Schimmel, 1980 for review). Since the phase can be calculated from the atomic coordinates of a molecule or molecules in a unit cell, this solution to the structure of Z-DNA provides the phase information for the atoms in Z-DNA in the space group of the original crystal unit cell. These phases can be used as the first guess for the phases of any other Z-DNA structure in an isomorphous crystal. The differences in the DNA and solvent structures between a new crystal and the original crystal can be treated as perturbations to the structure, and therefore to the phases of the original crystal structure. Thus modifications of the original Z-DNA coordinates can be used to solve the structure of subsequent Z-DNA crystals by a method known as molecular replacement. In this method the model (a modification of a known structure) is used as an initial guess for the phases of the unit cell. The model is subsequently altered by shifting the atomic coordinates of the model and/or by adding or removing atoms (primarily solvent atoms) to the unit cell to fit the structure factors calculated from the model (F_{cal}) to the structure factors from X-

ray diffraction data (F_{obs}). This process, therefore, refines the original model to fit the observed data.

For the present study the crystal structure of the copper-free d(m^5CGUAm^5CG) hexamer (Zhou and Ho, 1990) was used as the starting model for the refinement process. This model provided the phases for the observed diffraction intensities associated with the DNA. The Konnert-Hendrickson protein nonlinear least squares (PRLS) constrained refinement routine (Hendrickson and Konnert, 1981) for nucleic acids in space group 19 (PRLS19) was used to refine the model to the X-ray diffraction data.

The refinement process requires the operator to visually examine the electron density maps ($2F_{obs}$-F_{cal} maps), to compare the fit of the model to the electron density, and to add solvent molecules and ionic complexes accordingly. After each modification the structure must be re-refined by several runs of the refinement program. The process of re-refining the model after changes by the operator is termed a 'refinement step' for the following discussion. The refinement program itself modifies the model by repositioning the assigned atoms during each cycle in order to fit the calculated structure factors to the observed structure factors. The operator, however, controls the resolution limits, the constraint and the number of refinement cycles for each run of the refinement program according to an overall structure refinement scheme. Before this overall procedure of refining a crystal structure is explained, the principle function of the refinement program will be described.

2.6.1 The refinement program

The function of the refinement program is summarized in Figure 1. From the coordinates of the model, the diffraction intensities $I_{cal}(h,k,l)$ and corresponding phases $\Phi_{cal}(h,k,l)$ are calculated. The structure factors $F_{cal}(h,k,l)$ are calculated from these model values. The structure factors $F_{obs}(h,k,l)$ associated with the X-ray data are calculated from the observed intensities $I_{obs}(h,k,l)$ of the diffraction data using the phases from the model $\Phi_{cal}(h,k,l)$. By comparison of $F_{cal}(h,k,l)$ with $F_{obs}(h,k,l)$ from the diffraction data the refinement program modifies the model and recalculates the structure factors. This process is repeated for a given number of cycles.

Figure 1. Schematic showing the workings of one run of PRLS19, a constrained structure refinement program developed by Konnert and Hendrickson (1981), over a defined set of refinement cycles. The flow of the program routines are shown by the arrows. The functions of the program are enclosed in the rounded boxes, the input information (X-ray diffraction data, structural model, ideal structure libraries for constraint, and operator controls) are enclosed in rectangular boxes, the conditional decisions (in this case to continue or end the refinement run) are enclosed in a diamond box, and the end of the refinement run (labeled as 'Refined model') is in the elliptical box.

Figure 1.

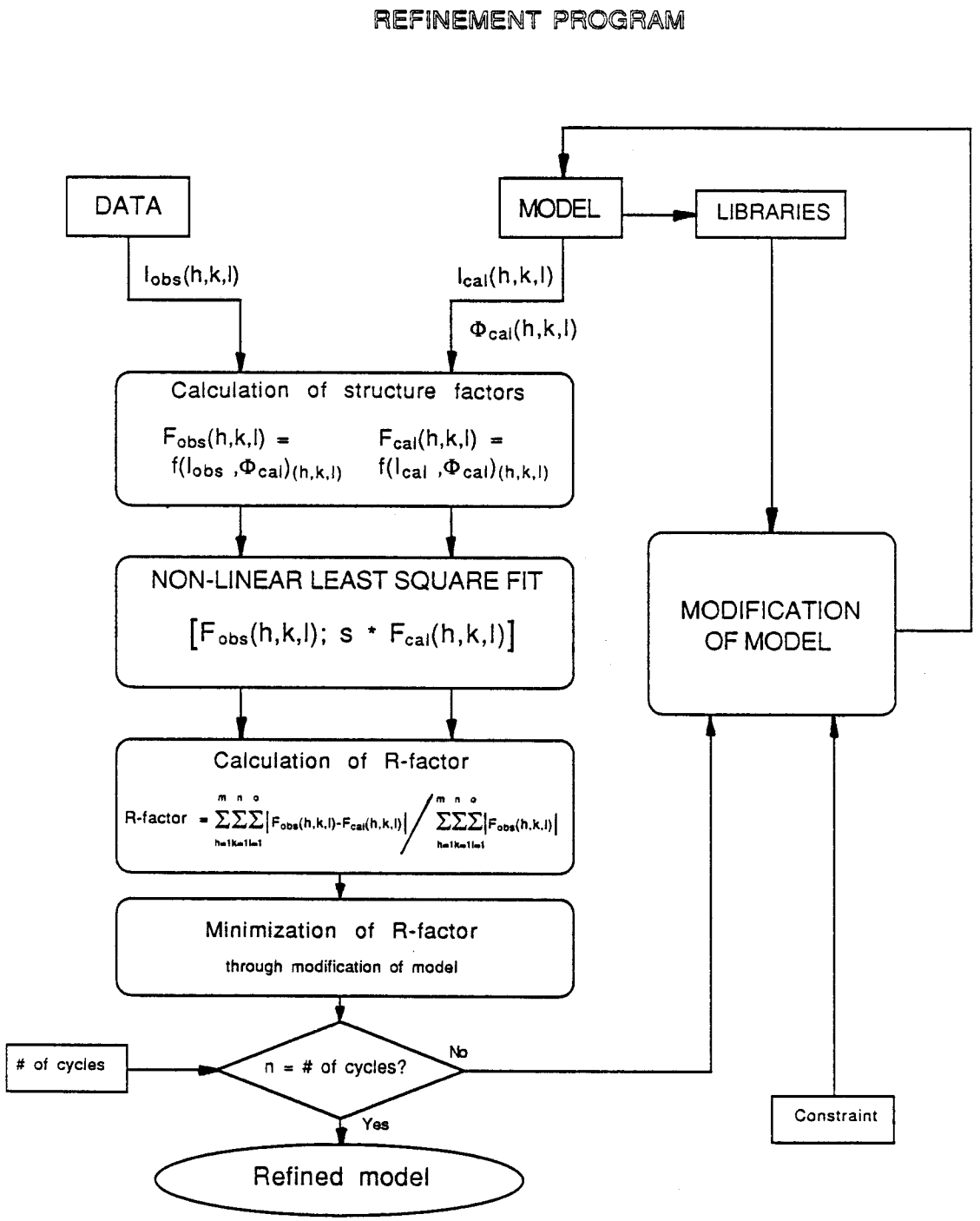
REFINEMENT PROGRAM
DATA
MODEL
LIBRARIES
$I_{obs}(h,k,l)$
$I_{cal}(h,k,l)$
$\Phi_{cal}(h,k,l)$
Calculation of structure factors
$F_{obs}(h,k,l) = f(I_{obs}, \Phi_{cal})_{(h,k,l)}$
$F_{cal}(h,k,l) = f(I_{cal}, \Phi_{cal})_{(h,k,l)}$
NON-LINEAR LEAST SQUARE FIT
$[F_{obs}(h,k,l);\ s * F_{cal}(h,k,l)]$
MODIFICATION OF MODEL
Calculation of R-factor
R-factor $= \sum_{h=1}^{m}\sum_{k=1}^{n}\sum_{l=1}^{o} |F_{obs}(h,k,l) - F_{cal}(h,k,l)| \Big/ \sum_{h=1}^{m}\sum_{k=1}^{n}\sum_{l=1}^{o} |F_{obs}(h,k,l)|$
Minimization of R-factor
through modification of model
# of cycles
n = # of cycles?
No
Yes
Constraint
Refined model

The observed and calculated structure factors are compared through a non-linear least square fit, using a scale factor S to normalize differences in the overall intensities of $F_{obs}(h,k,l)$ and $F_{cal}(h,k,l)$ (Figure 1). The residual factor R, (Cantor and Schimmel, 1980) is a measure for the goodness of a non-linear least squares fit of model and diffraction data. The definition of the R-factor is shown in Eq. 1, where h, k and l are the Miller indicies in reciprocal space and m, n and o are the maximum indicies as determined by the resolution cut-off.

$$\text{R-factor} = \sum_{h=1}^{m}\sum_{k=1}^{n}\sum_{l=1}^{o}\left|F_{obs}(h,k,l)-F_{cal}(h,k,l)\right| \Big/ \sum_{h=1}^{m}\sum_{k=1}^{n}\sum_{l=1}^{o}\left|F_{obs}(h,k,l)\right| \qquad \text{(Eq. 1)}$$

The resolution improves when more diffraction data is included in the refinement. The R-factor can assume values between 1.0 and 0.0. While a R-factor of 1.0 indicates that there is no fit between the diffraction data and the model, the value for a perfect fit (R = 0.0) can never be reached. Generally, R-factors of 0.2 (20%) or better indicate a good fit. During the refinement cycles the program tries to minimize the R-factor by adjusting the molecular model. The recalculated structure factors yield a new R-factor, and the model is modified again depending on the change of the R-factor.

Additional information on bond lengths, bond angles, dihedral angles, torsional angles, chirality, planarity of aromatic groups, and van der Waal's contacts (listed in a set of libraries) ensure that the model is adjusted only within the constraints imposed by the known chemical and steric properties of DNA (Figure 1). This is especially important at low resolution because the refinement program would try to fit the model to all the diffraction data including the diffraction from the oxygen atoms of the solvent molecules. Because the solvent molecules are homogeneously distributed and are not included in the model at low resolution, the molecular model would "blow up" without these constraints.

At the end of a particular run of the refinement program the refined model is analyzed by the operator. The R-factor and the bond distribution should asymptotically approach constant values during the last few refinement cycles of the refinement program. The number of cycles and the constraint is varied for the next run as described in the next section.

2.6.2 The overall refinement process

The mechanics of the refinement process is presented in the form of a flow chart in Figure 2. The X-ray diffraction data, in the form of scattering factors, and the molecular model are the input for the refinement program PRLS19. Model specific library files that contain additional information concerning the primary sequence, the bond lengths and the type of possible bonds, bond angles, dihedral angles, torsional angles, chirality, planarity of aromatic groups, and van der Waal's contacts are used to constrain the model during refinement. Refinement begins generally at low resolution where the positions of groups of atoms are defined. The number of refinement cycles and the constraint value for adjusting the model control the function of the refinement program for each run.

Generally, a refinement step starts with a high constraint, i. e. only small deviations of the model from the standard values for bond lengths and angles, etc. are allowed. Before the next run of the refinement program, the constraint is then relaxed, allowing the model to deviate from the ideal values in order to better fit the data. Assuming a Gaussian distribution around the average dimension for an ideal bond length or angle, approximately 20 % of the bonds should be within one standard deviation (SD), 10 % within two SD, and 5 % within three SD of the mean bond lengths. After refinement, the model should approximately exhibit this target distribution.

At subsequent refinement steps, more and more of the diffraction data is included to improve the resolution of the structure. Refinement at a new resolution shell starts again with a high constraint and is gradually relaxed during the following runs of the refinement program until the target bond distribution is reached.

Sections of the $2F_{obs}$-F_{cal} electron density map along the z-axis are printed onto overhead transparencies to build a three-dimensional electron density map. The fit of the molecular model to the electron density is visually examined by the operator. Solvent molecules and ions are added to the model once a resolution of 2 Å or better is reached. Solvent molecules may need to be removed from the model if the electron density disappears around the position of the assigned solvent molecule between subsequent refinement steps. The water ligands were assigned to the copper

Figure 2. Schematic showing the actual use of PRLS19 through the entire refinement process to obtain a final refined structure. The definition of the boxes are those described in Figure 1. The final complete structure that includes a refined DNA model and set of solvent molecules is designated as the 'Refined structure'.

Figure 2.

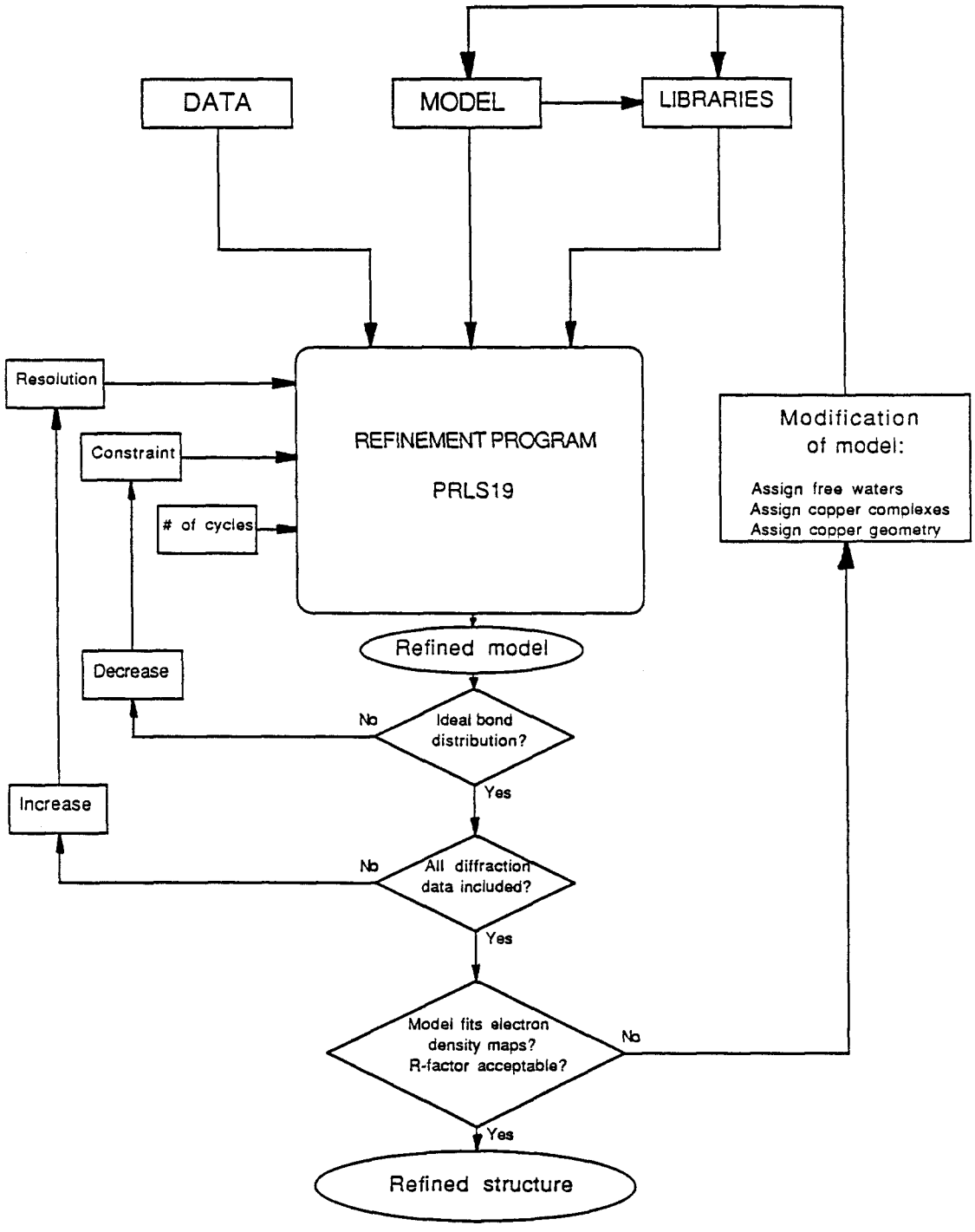
DATA
MODEL
LIBRARIES
Resolution
Constraint
# of cycles
REFINEMENT PROGRAM
PRLS19
Modification of model:
Assign free waters
Assign copper complexes
Assign copper geometry
Refined model
Decrease
No
Ideal bond distribution?
Yes
Increase
No
All diffraction data included?
Yes
Model fits electron density maps? R-factor acceptable?
No
Yes
Refined structure

ions in a geometry which fit the observed electron densities around the copper ions and conform to known coordination geometries of copper(II) ions.

When modifications of the model no longer improve the fit of the model to the electron density, and the final R-factor has asymptotically reached a constant value and the bond distribution is close to the ideal distribution, the end of the refinement is reached.

2.7 Calculation of atomic occupancies from electron density maps

The contour lines in the $2F_{obs}$-F_{cal} electron density map are a measure for the probability of finding scattering electrons in a particular space (x, y, z). The number of scattering electrons in this volume of space defines the electron density. The relative occupancy is the relative number of unit cells that actually contain a particular atom at a specific set of electron density. For example, a copper ion (Cu2+) has 27 electrons. Suppose at a particular copper site a set of electron density equivalent to the scattering of only 12 electrons was found, then the occupancy is approximately equal to 12 electrons/27 electrons $\approx$ 0.44 = 44 %. Therefore approximately 44 unit cells out of 100 contain a copper atom at this position.

The contour lines in the electron density map are generally given in units of electrons/$Å^3$. The units for the contour levels in the programs used are arbitrary but can be calibrated against the atoms of the DNA as discussed in the Results section. To determine the number of electrons at a site from the electron density map (x,y,z), one has to integrate the electron density ρ (x,y,z) over the volume of the electron density associated with the assigned atom.

$$\text{number of electrons} = \int_V \rho\ (x,y,z) * \partial V \qquad \text{(Eq. 2)}$$

This integral over the volume could be determined by summing the products of the contour level i and its area from each section along the z-axis of the map:

$$\text{number of electrons} \approx \sum_z \sum_{i=1}^{n} (\text{contour level})_i * A_i \qquad \text{(Eq. 3)}$$

The following approximation was used to circumvent this tedious integration of the electron density over the volume around an assigned atom. The number of contour lines for a standard increment (5 arbitrary units) were counted in the $2F_{obs}$-F_{cal} electron density map to determine the maximum contour level of the electron density distribution around this atom. The maximum contour level (number of contour lines) was multiplied by the volume of a sphere with an average diameter $d_{1/2}$ of the contour line at half the maximum contour level. This product is a relative measure for the number of electrons around a particular atom and is termed "ELECTRON COUNT" in this thesis. The units of the electron count are [contour lines*$Å^3$]. For the calculation of the electron count, the maximum contour level was used as an average contour level in this "atomic" volume. This method is most accurate if the electron distribution in each dimension around the center of the atom is a normal distribution and spherically symmetrical. Furthermore, the center of the set of electron density has to lie in the section of the electron map used to count the contour lines.

Figure 3 illustrates that, in a practical example, this method is reasonablly accurate in determining the number of electrons associated with a particular set of electron density in a electron density map. Figure 3 A shows a x,y-section of the $2F_{obs}$-F_{cal} electron density map at the copper Cu6 site in the d(m^5CGUAm^5CG) structure. The contour line at half the maximum peak height and the average diameter at half maximum peak height $d_{1/2}$ are marked. Figure 3 B shows the cross-section along line B in Figure 3 A through the density peak. The vertical axis is the electron density in arbitrary units. The minimum value for the electron density was set to 35 arbitrary units to assure that only contour levels above the noise level are included in this calculation. The area under the electron density distribution (panel B) is essentially equal to the area of a rectangle with $d_{1/2}$ as the length of one side and the maximum contour level as the second dimension. For a spherically symmetric set of electron density the integral of the electron density ρ over the volume of the set can, therefore, be reasonably estimated by the product of the maximum contour height (number of contour lines for a standard density increment, e. g. 5 arbitrary units) and the volume of a sphere with diameter $d_{1/2}$. This product, termed the electron count, is, therefore, a good relative estimate of the number of electrons in this set of density.

Figure 3. Calculation of the atomic "Electron count" from $2F_{obs}$-F_{cal} electron density map for copper Cu6 . An example is shown for how the electron count was estimated for a given atom, in this case the copper(II) ion bound to guanine G6. A. The electron density map for d(m^5CGUAm^5CG) is shown at the level 29.7 Å along the Z-axis, and contoured from 35 to 500 arbitrary units in increments of 25. The scale along the x-axis (vertical axis) and the y-axis (horizontal axis) is shown by the 1 Å bars. The vector labeled as $d_{1/2}$ represents the average diameter used to calculate the "atomic" volume of this copper ion. B. Cross-section of the electron density contours of copper Cu6 shown in A. along line B, where the vertical axis is the contour height and the horizontal axis is the dimension along line B in the map in Å. This panel demonstrates that the area of a rectangle with $d_{1/2}$ as one side and the maximum contour height as the second dimension approximates the total area of the contour cross section by compensating the lost areas below half the maximum height with the additional area calculated above the half maximal contour height. The product of the maximum contour height (number of contour lines) and the volume of a sphere with diameter $d_{1/2}$ gives the electron count of this particular atom.

Figure 3 A.

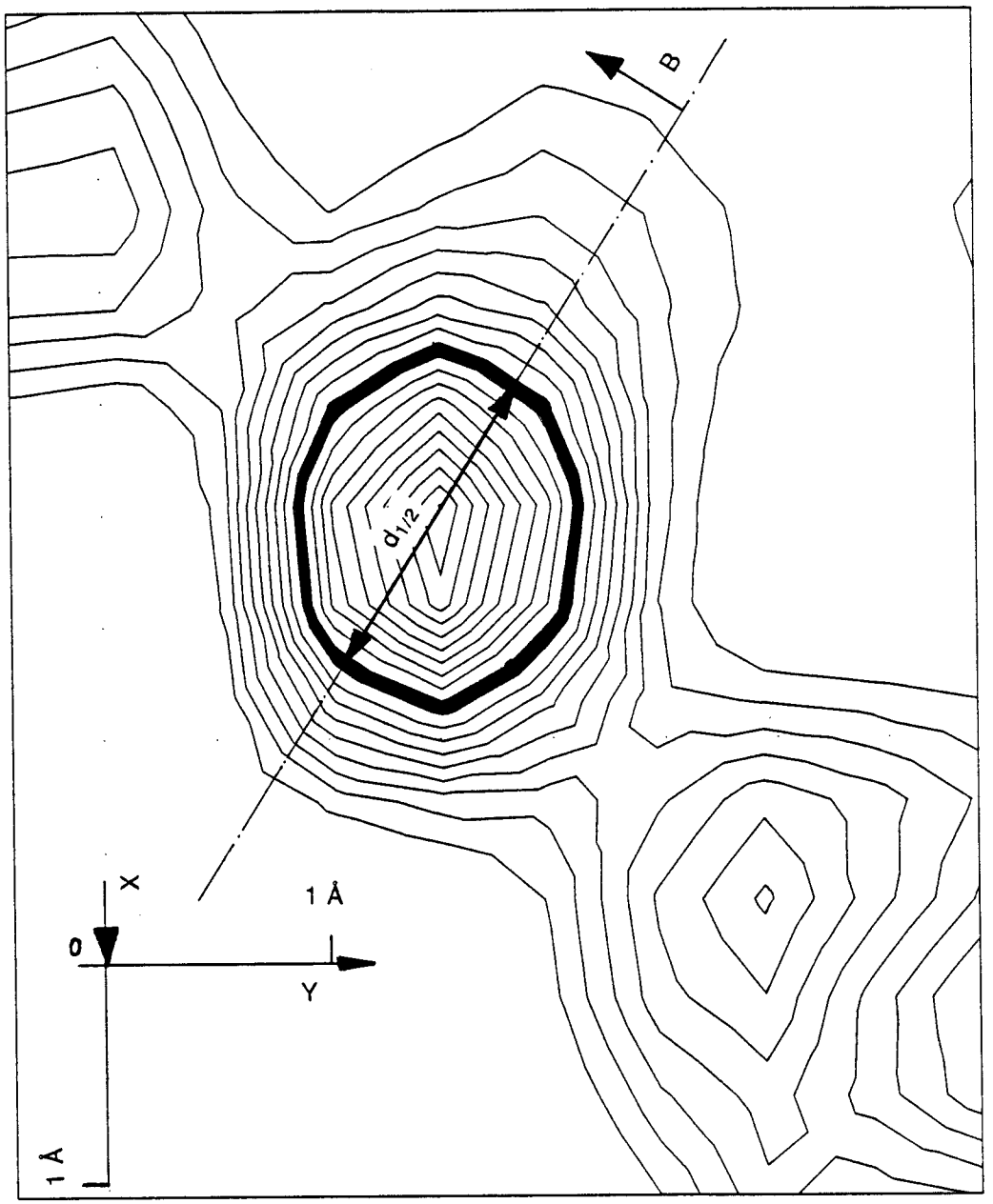

Figure 3 B.

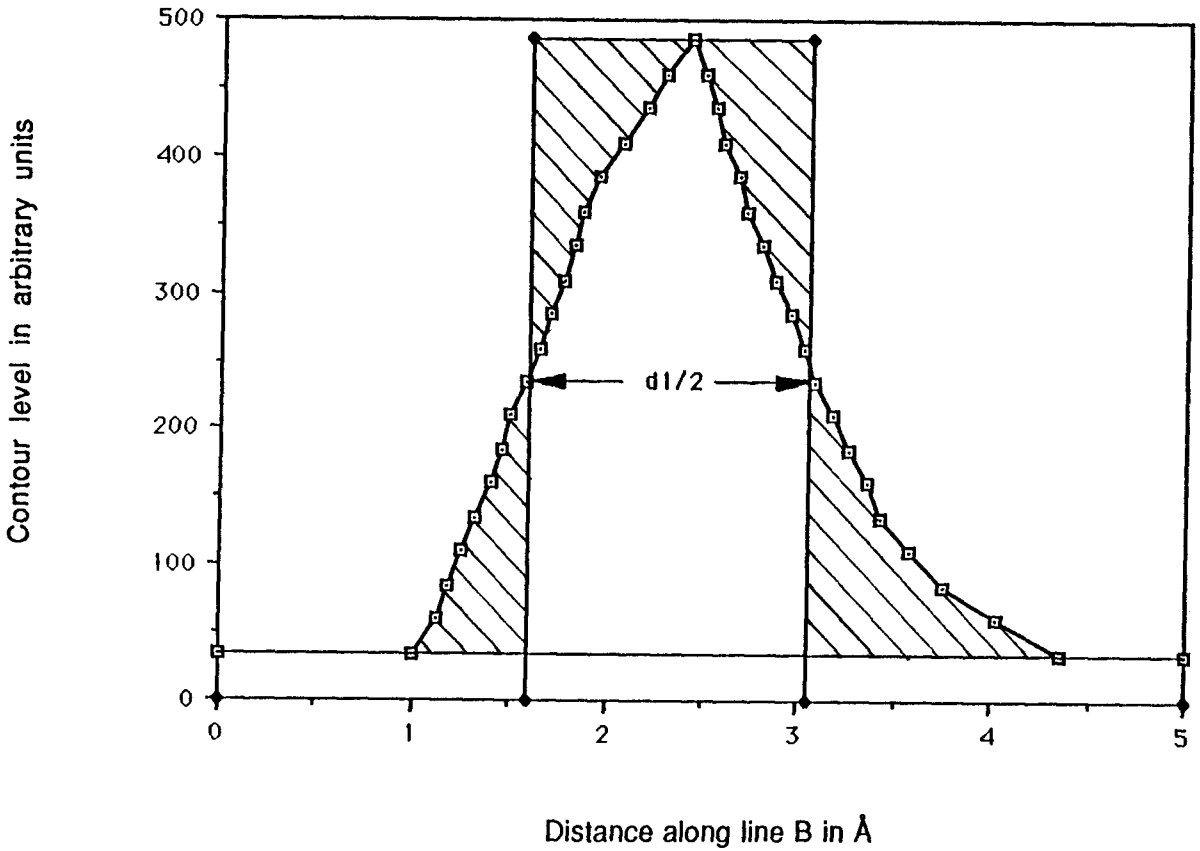
500
400
300
200
100
0
0
1
2
3
4
5
d1/2
Contour level in arbitrary units
Distance along line B in Å

The electron count, relative to the electron count of a fully occupied site, is a measure of the partial occupancy of a site. Some atoms are fixed more or less tightly in a certain position and, therefore, the electrons of each atom may be distributed in different volumes. The copper ions were observed to be covalently bound to the purine bases (Kagawa *et al.*, unpublished and Results section), and the positions of the bases do not fluctuate dramatically within the crystal. The thermal fluctuations of the coppers at each site were, therefore, assumed to be minimal, and the specific electron count at each copper site is believed to correspond to that of well fixed atoms in space.

In this thesis two definitions for % occupancy will be used. The first defines % occupancy at each site relative to a theoretical fully occupied site. The second definition defines % occupancy at each site relative to the total copper content in the asymmetric unit of the crystal. In the latter case the % occupancy is calculated as the electron count at a particular copper site i (E_i) divided by the sum of the electron counts for all copper sites as shown in Eq. 4.

$$\% \text{ occupancy} = \frac{E_i}{\sum_{i=1}^{n} E_i} \qquad \text{(Eq. 4)}$$

In equation Eq. 4, E_i is the electron count at the copper site i and n is the total number of copper sites in the asymmetric unit. The term E_i is calculated as the product of the number of contour lines and the 'volume' of the electron density at copper site i, respectively, as previously described. This latter definition allows each copper site in d(m^5CGUAm^5CG) crystal to be compared to the analogous sites in the $d(CG)_3$ crystal (Kagawa *et al.*, unpublished), regardless of the total copper content in the crystals.

As shown in the Results section the calculation of the electron count when applied to the atoms of the DNA bases can be used to calibrate the contour lines in the electron density map. This calibration can be used to calculate the number of copper ions per asymmetric unit from the sum of the electron counts of all copper sites from the electron density map. A comparison to the total copper content of the asymmetric unit determined by atomic absorption and UV spectroscopy yields an

internal test of the occupancy calculations (see Results section). The occupancy calculations also allow the assignment and the comparison of the different copper ion complexes bound to DNA. The specific definition used for % occupancy in the text or in the calculations in the Results section is explicitly indicated.

RESULTS

1. Crystals of d(m5CGUAm5CG) soaked with Copper(II) chloride

Crystals of the self-complementary sequence d(m^5CGUAm^5CG) were grown by vapor diffusion against 2-methyl-2,4-pentanediol (MPD) as previously described (Zhou and Ho, 1990). The conditions that provided diffraction quality crystals of this sequence are listed in Table 3. The resulting crystals were colorless with rectangular plane faces, similar to previous crystals of Z-DNA hexamers (see Jovin *et al.*, 1987 for references). The size of each crystals was carefully monitored for approximately one week to ensure that they were no longer growing. Approximately 210 nmoles of total copper ions were added to the crystallization wells by stepwise addition of a 100 mM stock copper(II) chloride solution. Each addition was allowed to equilibrate for 48 hours prior to the next addition. The color of the crystals changed to blue/green upon the addition of copper. The final molar ratio of copper ions to purine bases in the crystallization solution was estimated to be at least 3:2. Thus, at least in solution, the number of copper ions present exceeds the number of potential copper binding sites of the DNA duplex.

To determine the absolute quantity of copper ions bound to the DNA within a crystalline environment, one DNA crystal was sacrificed for metal ion analysis by atomic absorption spectroscopy (AAS). The total DNA content of the crystal was determined by ultraviolett (UV) spectroscopy. The two quantities together provided an estimate of the number of copper(II) ions bound to each DNA hexamer duplex.

A single copper-soaked DNA crystal was dissolved in 600 µl of distilled deionized water. The UV absorption spectrum was recorded and found to have an absorbance at 260 nm of 1.38 O.D. Using the molar extinction coefficient ε (260 nm) $=107.4*10^3$ M^{-1} cm^{-1} (per hexamer) (Ho *et al.*, 1990) the DNA concentration was estimated to be $12.9*10^{-6}$ M. The original crystal, therefore, contained 7.7 nmoles of hexamer duplex (the error of this calculation due to uncertainty from the ε (260 nm) value and volumetric measurements was estimated to be ± 5%).

The same copper-DNA solution was used to quantitate the absolute copper content within the crystal using atomic absorption spectroscopy. The spectrometer was standardized for copper absorption using 0.25 ppm to 2.0 ppm (1 ppm=

Table 3. Conditions for crystallizing the hexamer sequence d(m^5CGUAm^5CG) as Z-DNA

Initial conditions for setup: (3 wells)	
5 µl	100 mM Sodium cacodylate buffer (pH 6.96)
5 µl	600 mM $MgCl_2$*6 H_2O
15 µl	1.18 mM d(m^5CGUAm^5CG)
5 µl	10% MPD in water

The MPD concentration in the reservoir was increased from 25 % to 50 % in steps of 5% within 12 days. After three days at 50% MPD still no crystals had formed. Therefore 5 µl of 1.18 mM d(m^5CGUAm^5CG) was added to each well.

1μg/ml) copper(II) standard solutions (see section: Materials and Methods). The results of the standardization are shown in Figure 4. A linear least square fit of these data yielded a linear relationship with a slope of 0.212 absorbance units/ppm, a y-intercept of $2.61*10^{-3}$ absorbance units, and a correlation coefficient R = 0.999997. An absorbance of 0.032 ± 0.004 and 0.189 ± 0.007 was recorded for a 1:6 dilution and an undiluted copper-DNA solution, respectively. Taking into account the dilution factor, the two readings correspond to 0.83 ppm ± 0.03 ppm and 0.88 ppm ± 0.03 ppm (μg/ml) copper in the samples.

Because the diluted sample resulted in an absorbance outside of the calibration range, the reading of the undiluted sample was considered to be more accurate and this was used to determine the copper content of the crystal. From a molecular weight of 63.54 g/mole for copper and a total sample volume of 600 μl, the sample was calculated to contain 8.3 nmoles of copper. The relative uncertainty of this value was estimated to be at least 10 % due to errors in the volume measurements and AAS readings.

The UV spectrometric and AAS measurements indicated that 7.7 nmoles of hexamer duplex and 8.3 nmoles of copper(II) ion were present in the original copper soaked DNA crystal. The molar ratio of copper(II) ion to hexamer duplex was therefore approximately 1:1, or the copper(II) to potential binding sites of purine bases was 1:6. This is significantly lower than the 3:2 ratio calculated for the copper to purine base ratio in solution. The apparent difference can be reconciled by considering the volume of the crystal unit cell and the total copper within the unit cell. The volume of the unit cell in a Z-DNA crystal of d(m^5CGUAm^5CG) is approximately $2.52*10^{-23}$ l (unit cell dimensions from (Zhou and Ho, 1990) were approximately 17 Å * 33 Å * 45 Å). Since there are 4 hexamer duplexes/ unit cell and thus 4 copper(II) ions/ unit cell, the total copper(II) ion concentration in the crystal was estimated to be 0.26 M. If we assume that the vapor pressure of the crystallization solution has equilibrated with that in the reservoir, the final solution volumes in the crystallization wells were approximately 1 μl (35 μl of 1.43 % MPD equilibrated to 50% MPD), resulting in a 35-fold concentration of the solution. The equilibrium concentration of copper(II) in the crystallization solution was therefore 0.21 M (210 nmoles Cu(II) in 1 μl). The number of coppers per volume in both the crystal and the crystallization solution are thus identical.

Figure 4. Determination of copper content in the copper(II) chloride soaked single d(m^5CGUAm^5CG) crystal by atomic absorption spectroscopy. The absorption readings for the copper(II) standards are shown by the error bars. A linear least squares fit of the standards yielded a standard curve with the relationship Absorption = 0.212 * [Cu^{+2}] (ppm) + 0.0026, with a residual factor of R=0.999997. The absorption readings from the crystal dissolved in 0.6 ml of water and the 1:6 diluted sample from the dissolved crystal are shown by the open square data points. These correlate to 0.88 and 0.83 ppm copper(II) in the undiluted and diluted samples of the dissolved crystal, respectively.

Figure 4.

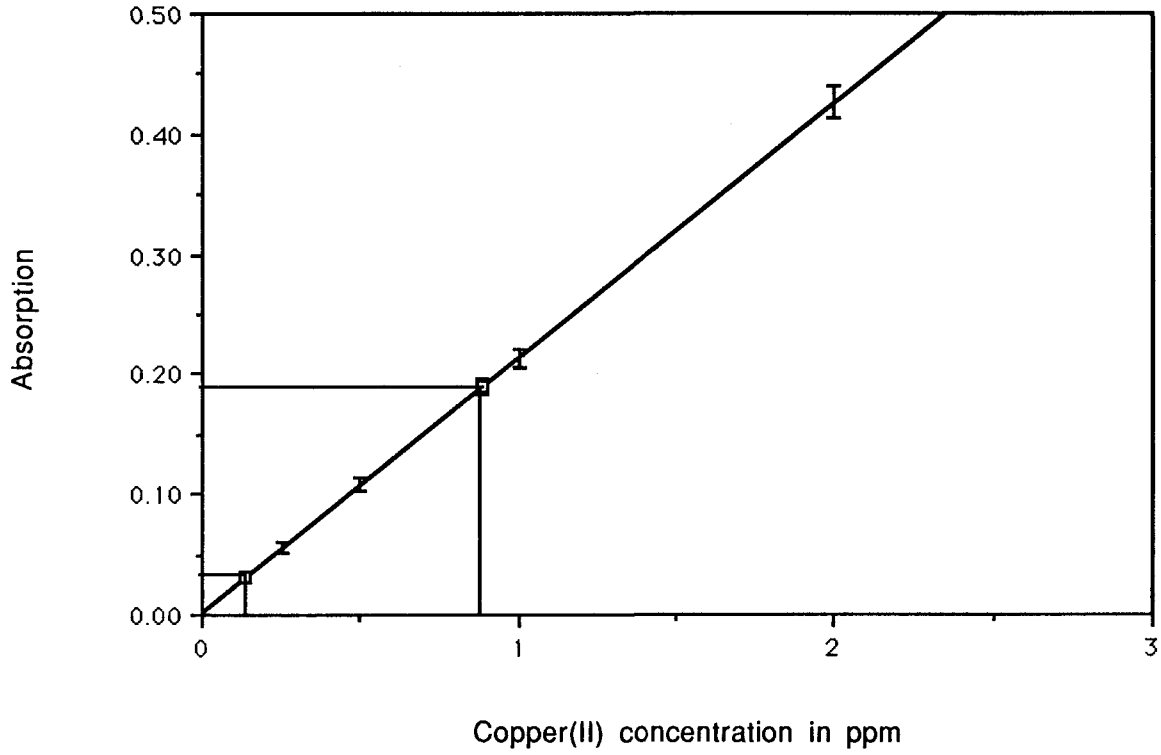
0.50
0.40
0.30
0.20
0.10
0.00
Absorption
0
1
2
3
Copper(II) concentration in ppm

The crystal environment, however, is not identical to that of the solution. The volume of "free solvent" in the crystal is much lower than the $2.52*10^{-23}$ l calculated for the volume of the unit cell. Within the unit cell the DNA constitutes nearly 71 % of the mass of the crystal (242 nonhydrogen atoms of the DNA were assigned in the asymmetric unit versus approximately 100 nonhydrogen atoms (mainly water oxygens) not associated with the DNA). Using a buoyant density of 1.72 g/ml for DNA containing 67% GC content (Lehninger, 1975) the hexamer duplexes were estimated to occupy over 40 % of the unit cell volume. The copper(II) ion concentration in the "free solvent" volume is therefore 0.44 M, or approximately twice that in the crystallization solution. Thus, the lower copper to purine base ratio in the crystal versus solution was not a result of the crystal lattice inhibiting copper diffusion but was a consequence of the nearly 10-fold higher DNA concentration in the crystal (0.26 M in crystal versus 0.023 M in the original solution). The higher apparent concentration of copper in the crystal can be accounted for by the accumulation of metal resulting from binding to DNA in the crystal.

2. X-ray diffraction study and structure refinement

The X-ray diffraction data of a large 0.45 mm x 0.25 mm x 0.20 mm crystal was collected on an Enraf-Nonius diffractometer by Professor Gary J. Quigley in the Department of Chemistry at the New York University, New York, NY.

In using copper K_α radiation to collect the x-ray diffraction data from the copper-soaked crystal, one would suspect that a significant portion of the incident radiation would be absorbed by the copper ions in the crystal, subsequently resulting in deterioration of the crystal integrity. This effect was measured as a function of time by collecting a set of five standard reflections every 20 minutes. The changes in intensity of these standard reflections monitor the stability of the crystal during data collection. These data were fit to single exponential decay models and the subsequent decay rate constant was used to correct the intensities of each reflection in the data set by a standard decay correction algorithm.

From the X-ray diffraction data the unit cell parameters were determined to be a= 17.590 Å, b= 30.583 Å and c= 44.519 Å in the orthorhombic space group $P2_12_12_1$ (no. 19, system type 3). A total of 4357 reflections were collected. Of

these, 2587 reflections were better than 2 σ in their intensity relative to the background and were thus included in the final refinement process.

The structure was solved by molecular replacement and subsequent refinement of the model using the Konnert-Hendrickson constrained refinement method (Hendrickson and Konnert, 1981). The Z-DNA structure from Zhou and Ho (1990) was used as the initial model for refinement. Atoms associated with the copper complexes and the solvent were added at 2 Å or better resolution. A total of 905 distances within the DNA and the solvent structure were refined. The final bond constraints are shown in Table 4. The final distribution of the bonds in the model were 25.5 % ± 4.1% within 1 σ, 8.7% ± 2.3% within 2 σ and 3.2% ± 1.4% within 3 σ of the mean bond length. This was sufficiently close to the target distribution, indicating that the refinement of the structure was complete.

The standard R-factor for the final refinement cycle was 20.9 %. Within the asymmetric unit, 242 atoms in the DNA hexamer and 71 free water molecules were assigned. In addition, four copper complexes were assigned as one $CuCl_2{*}H_2O$ complex, two $Cu{*}[H_2O]_5$ complexes and one $Cu{*}[H_2O]_4$ complex. Assignment of the free waters improved the R-factor of the 3.0 Å shell rapidly to a final value of 13.3 %. The R-factors for the 1.7 Å, and the 2.0 Å shell were significantly higher (29.9 %, and 24.5 %) than the overall R-factor. Reflections at this resolution were dominated by the diffraction from the copper complexes (bond lengths of 1.9 Å to 2.4 Å). Although the number of reflections observed at the 1.7 Å and 2.0 Å shell were higher than in any other range, the low occupancy of the coppers resulted in higher R-factors than are expected (see comparison to native structure). The high R factor of 39.9 % in the 1.2 Å range was due to the low number (62) of observed diffraction data at this shell. This suggests that the 1.2 Å resolution data did not contribute significantly to the structure. Therefore the maximum resolution of the structure was considered to be 1.3 Å. While further addition of free waters would not significantly improve the standard R-factor higher occupancies of the copper sites would.

In comparison, the R-factors of the native d(m^5CGUAm^5CG) crystal structure in the absence of copper bound to DNA were similar for the 1.2 Å, 1.5 Å, and 3.0 Å resolution shells. The R-factors in the shells 1.7 Å, 2.0 Å and 2.5 Å, were considerably smaller in the copper-free structure (25.2 %, 21.5 % and 18.5 %), reflecting the effect of the copper complexes. The R-factor in the structure

Table 4. Final bond constraints for the copper(II)-soaked d(m^5CGUAm^5CG) structure after Konnert-Hendrickson refinement.

Bond type	Constraint type	Total number of bonds constrained	Target distribution % 1 σ	2 σ	3 σ	Actual distribution % 1 σ	2 σ	3 σ*
I	Chiral atom to atoms	108	20	10	5	30	6.4	1.8
II	Nonchiral atoms to atoms	369	20	10	5	22	9.2	4.6
III	Bond angles	162	20	10	5	23	8.6	3.1
IV	Dihedral angles	220	20	10	5	21	11	4.5
V	Loosely constraint bonds, e.g. hydrogen bonds	46	20	10	5	35	26	13

* σ = standard deviation around the mean bond length or angle.

without copper for the 5 Å shell (20.1 % versus 16.4 %) is significantly larger and slightly higher for the 3 Å shell (water structure) (13.9 % versus 13.3 %). Thus, although the overall R-factors of both the copper-soaked and native d(m^5CGUAm^5CG) structures were nearly identical (20.9 % versus 20.8 %), they differed at each resolution level, reflecting the differences in the solvent and ion structure between the crystals.

3. DNA crystal structure

3.1 Crystal packing

The crystal packing of the d(m^5CGUAm^5CG) crystal soaked with copper was nearly identical to that of the native d(m^5CGUAm^5CG) crystal (Zhou and Ho, 1990). The unit cell consists of four hexamers, each defining a single asymmetric unit (Table 5). The hexamers are related by a two-fold screw axis along the helical axis, resulting in an end-to-end stacking that forms essentially continuous strands of Z-DNA parallel to the crystallographic c-axis. The "strands" are packed in an antiparallel arrangement along the b-axis and are staggered by two base pairs along the helical axis. The helical pitch within each "strand" is defined by the crystal packing as 12 base pairs/turn. The helical rise is defined as 3.71 Å per base pair by the crystal packing and the 44.5 Å unit cell length along the c-axis.

3.2 Overall DNA structure

Overall the structure of the DNA is very similar to the native d(m^5CGUAm^5CG) structure (Zhou and Ho, 1990) and to other Z-DNA hexamer structures in general. Figure 5 shows a Van der Waal's radii diagram of three hexamers aligned along the c-axis, giving 1.5 turns of Z-DNA. The phosphates along the backbone are connected to show the zig-zag pattern of Z-DNA. The major groove is a convex surface while the minor groove is a deep crevice. The copper complexes are shown as light grey clusters at the major groove surface.

3.3 Comparison of the overall structure of the copper-soaked and the native d(m5CGUAm5CG) crystal

A general comparison of the copper-soaked hexamer to that of the native structure showed very few major differences. This is consistent with the nearly

Table 5. Unit cell parameters for the copper(II)-soaked and the native d(m^5CGUAm^5CG) Z-DNA structure.

The space group for both structures is $P2_12_12_1$ (no. 19, system type 3).

Structure:	Unit cell parameters in Å			Unit cell volume in Å^3	Reference:
	a	b	c		
d(m^5CGUAm^5CG), copper(II)-soaked	17.590	30.583	44.519	23949	Present study
d(m^5CGUAm^5CG), native (no copper)	17.820	30.444	44.520	24153	Zhou and Ho, 1990

Figure 5. Van der Waal's diagram of one and one-half turns of copper(II)-soaked d(m^5CGUAm^5CG) as Z-DNA. Three hexamers are shown as they are aligned along the crystallographic c-axis to define 1.5 turns of Z-DNA along the molecular helix axis. Each hexamer duplex defines 1/2 turn of Z-DNA and are related by a 2-fold screw axis along the helical axis. The copper(II) atoms are shown exaggerated from their chemically defined ionic radii to better represent the larger atomic volumes observed in the electron density maps. Each copper is shown as fully occupied. The atoms of the copper complexes are shown as light shaded spheres, while those of the DNA are shown as dark shaded spheres.

Figure 5.

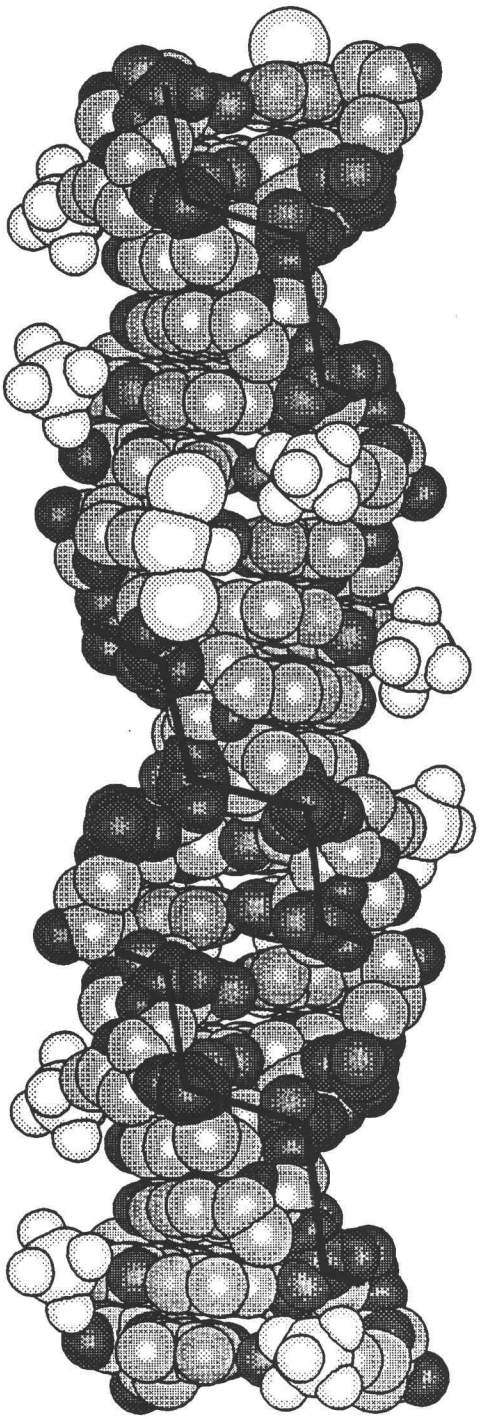

identical unit cell dimensions of the two crystals (Table 5). Figure 6 shows a comparison of the two DNA structures as a polar projection along the helical axes. The polar projection was generated by projecting the coordinates of the DNA atoms from the helical axis to a cylindrical surface wrapped around the DNA. When the cylinder is slit parallel to the helical axis and unrolled the backbone is laid out as a parallel ladder. The vertical axis is the rise along the helix while the horizontal axis is the rotation angle around the helix. The slant of the backbone from the upper left-hand corner to the lower right-hand corner shows that the DNA is left-handed. The base pairs are shown projected onto the major groove surface. The minor groove crevice is labeled as a groove. The thicker bonds represent the copper-soaked structure, while the thinner bonds represent the native structure. The nucleotides in the hexamer are numbered 1 to 6 in 5' to the 3' direction along one chain and 7 to 12 along the opposite strand. The copper soaked and native structure show good agreement in both the positions of the backbone and the base pairs. This is consistent with the small overall root mean square (RMS) deviation of 0.358 Å for the atoms between the two structures.

There are, however, some details of the copper-soaked DNA structure that differ significantly from the native structure. These are directly or indirectly related to specific copper binding to the DNA bases and their subsequent effects on the structure of the bases and the Z-DNA backbone. At the backbone, the ribose moiety of the G12 nucleotide has undergone an inversion of conformation from a 3' endo to a 2' endo pucker. The sugar puckers were determined by finding the ribose atom with the greatest distance from the mean square plane formed by the other four atoms (Table 6). This change in sugar conformation results in a rotation of the C5'- O5' bond. The phosphodiester bond linking adenine A4 with cytosine C5 was displaced, resulting in a slight narrowing of the major groove surface and concomitant widening of the minor groove crevice. Distortions of the phosphodiester bonds linking uracil U9 to adenine A10 and cytosine C5 to guanine G6 result in a narrower minor groove crevice near the end of the hexamer duplex. A slight displacement of the phosphodiester linking between nucleotide A4 and U3 causes narrowing of the minor groove crevice in the middle of the hexamer duplex. The distortion of the backbone at the d(UA) dinucleotides and its effect on the water structure will be discussed in detail in a later section. The effects of copper

Figure 6. Polar projection comparing the copper-soaked (current study) and the native (Zhou and Ho, 1990) d(m^5CGUAm^5CG) structure. A polar projection is developed by projecting the atoms of the molecule from the helical axis to a cylinder wrapped around the diameter of the DNA double helix. The cylinder is then slit parallel to the helical axis and unrolled. The resulting projection shows the relative relationships of all atoms in the major and minor grooves simultaneously of the DNA double helix. The copper(II)- soaked structure is shown in thick bonds while the native structure is shown in thin bonds. The minor groove crevice is labeled as 'Groove'. The nucleotide residues are numbered from 1-6 5' to 3' along one chain and 7-12 5' to 3' along the antiparallel strand. The vertical axis represents the rise along the helix and the horizontal axis is the rotation around the DNA duplex.

Figure 6.

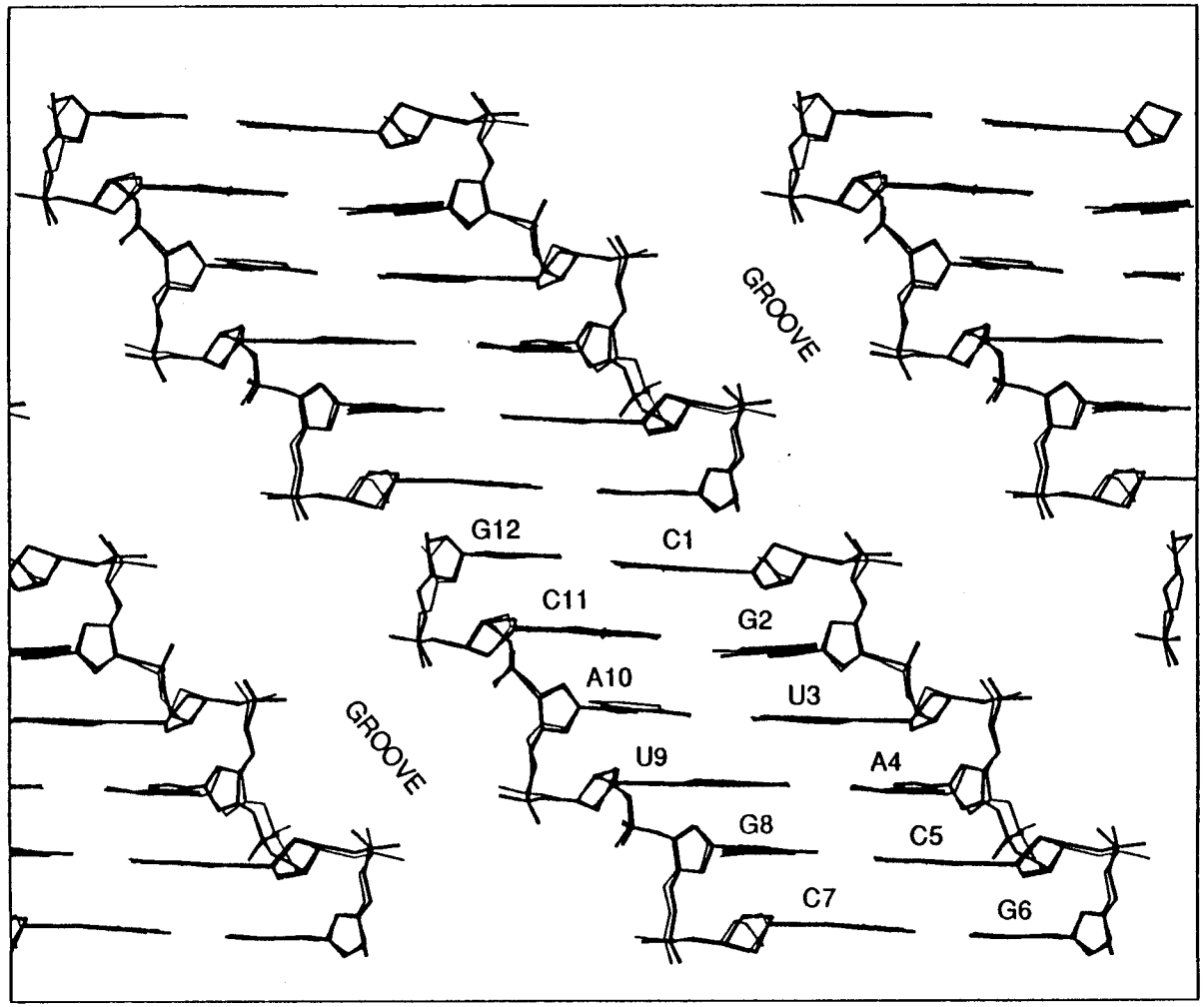

Table 6. Comparison of the sugar conformations in the copper(II)-soaked and native d(m^5CGUAm^5CG) Z-DNA crystal.

The sugar puckers were determined by calculating the maximum distance of a ribose atom from the mean square plane formed by the other four atoms of the ribose.

Nucleotide:	Sugar pucker		
	d(m^5CGUAm^5CG), copper(II)-soaked:	d(m^5CGUAm^5CG), native (no copper):	
C1	2'-endo	2'-endo	
G2	3'-endo	3'-end	
U3	2'-endo	2'-endo	
A4	3'-endo	3'-endo	
C5	2'-endo	2'-endo	
G6	2'-endo	2'-endo	
C7	2'-endo	2'-endo	
G8	3'-endo	3'-endo	
U9	2'-endo	2'-endo	
A10	2'-endo	2'-endo	
C11	2'-endo	2'-endo	
G12	2'-endo	3'-endo	<---- Inversion

binding on each of this backbone sites will be discussed in more detail in a later section.

Thus, even though the overall structures of the DNA hexamer duplexes were similar for both crystals, as defined by the crystal packing, some small, but significant distortions to the DNA structure were induced by copper binding.

4. Copper binding to the d(m5CGUAm5CG) crystal

The primary goal of the work in this thesis was to analyze the relative specificity of copper(II) binding to the purine bases of Z-DNA. This metal ion was found to bind to all guanines of $d(CG)_3$ in Z-DNA (Kagawa *et al.*, unpublished). The current study was designed to determine whether the adenine bases were also susceptible to covalent modification and, if so, under what circumstances, and what are the structural ramifications.

Copper ions and their associated ligands were added to the asymmetric unit during refinement of the 2.0 Å to 1.2 Å resolution shells. In general, the copper ions were distinguished from water molecules by their electron counts as observed in the electron density maps ($2F_{obs}$-F_{cal} maps). Copper(II) ions have a total of 27 electrons while waters have 10 electrons. Copper ions could thus be distinguished from the solvent molecules by their higher electron densities.

The various copper complexes in the $d(CG)_3$ structure were observed to be differentially occupied, with the degree of occupancy dependent on the crystal packing. The accessibility of each copper binding site, resulting from crystal packing, is nearly identical in the Z-DNA crystals of $d(CG)_3$ and $d(m^5CGUAm^5CG)$. Therefore, the degree of copper occupancy at each potential binding site in the $d(m^5CGUAm^5CG)$ structure should mirror those in the $d(CG)_3$ structure if the binding affinities of adenine and guanine were similar. A comparison of the copper occupancies at each purine base thus facilitates the actual assignment of the coppers and provides an estimate of the relative affinity of adenine and guanine bases for copper(II) binding. From the previous structure of copper-soaked $d(CG)_3$, each copper was observed to form a covalent coordinate bond to the N7 of the guanine bases (Kagawa *et al.*, unpublished). The average copper to N7 nitrogen distance was 2.27 Å ± 0.250 Å (± SD). With one exception, the copper-N7 bond was in the plane of the purine bases. Each copper was also in a complex with one or more solvent

molecules. The additional characteristics that distinguished a copper ion, therefore, were the distance from the center of the electron density to the purine N7 and the geometry of the surrounding atoms.

The following sections will describe the results of the copper occupancy calculations from the electron density maps at each purine base in the d(m^5CGUAm^5CG) structure and compare these to the analogous sites of the previous $d(CG)_3$ structure. From this, the copper binding sites in the d(m^5CGUAm^5CG) structure are defined, along with the specific geometry and nature of the ion complexes.

4.1 Total copper bound to d(m5CGUAm5CG) from electron density maps

Atomic absorption and UV absorption studies on a dissolved copper-soaked d(m^5CGUAm^5CG) crystal showed that there were approximately 1.1 copper(II) ions bound per hexamer duplex. The quantity of bound copper(II) can also be estimated from the electron density maps calculated from the collected X-ray diffraction data and the refined structure. A comparison of the copper present as determined by atomic absorption and by counting electrons in the electron density ($2F_{obs}$-F_{cal}) map calibrates the contours of the density map.

To calibrate the contours of the electron density map, the electron count from the map was compared to the electron count predicted from the chemical properties for various atoms in the structure. In this calculation the carbon and nitrogen atoms of the DNA were taken to be fully occupied (i. e., each unit cell in the crystal contains all the carbons and nitrogens of four hexamers with no defects). The contours around each atom of a purine and a pyrimidine base were counted. The volume for each atom was estimated from the width at half the maximum contour height, taking into account the volumes excluded when forming a covalent bond. By multiplying the number of contours by the volume, then dividing this value by the known number of electrons around each carbon and nitrogen atom, a contour increment set at 5 arbitrary units was found to correspond to an electron density of 0.10 electrons/$Å^3$. Using this value, a fully occupied copper(II) site having 27 electrons was predicted to show 278 contour lines * $Å^3$ in the electron density map. All the density calculated in the $2F_{obs}$-F_{cal} map whose center was approximately 2.2 Å from the N7 of the purine bases in the asymmetric unit added to 359 contour

lines * $Å^3$ (Table 7), showing that there were 359/278 = 1.3 copper(II) ions per hexamer in the d(m^5CGUAm^5CG) crystal. This value is nearly identical to the 1.1 copper(II) ions per hexamer as determined by atomic absorption spectroscopy and suggests that the method described for estimating the partial occupancies of the atoms from the electron density maps is fairly accurate.

4.2 Assigning copper(II) binding sites to d(m5CGUAm5CG) from partial occupancy calculations

As discussed above, the distribution of copper in the d(m^5CGUAm^5CG) structure should be identical to that of $d(CG)_3$ if copper(II) also binds specifically to adenine bases. To determine the copper distribution on the hexamers, the contours centered at approximately 2.2 Å from the N7 of each purine base of the d(m^5CGUAm^5CG) hexamer were counted for a set contour increment (5 arbitrary units) in the $2F_{obs}$-F_{cal} electron density map. No electron density was observed to be centered 2.2 Å from the N7 of adenine A4 (Figure 7). The closest set of electron density centered at 2.75 Å from this N7 was therefore used for the calculation. This set of density at the A4 will be shown later to be associated with a free water molecule and not a copper(II) ion.

The partial occupancy of copper(II) at each purine base was calculated from the $2F_{obs}$-F_{cal} map as previously described (see section Materials and Methods). The overall occupancy of copper(II) in the asymmetric unit of the d(m^5CGUAm^5CG) crystal was determined to be 1.7 fold lower than that of the $d(CG)_3$ crystal (Table 7). The calibration of the electron density map using the atomic absorption data above showed that the $d(CG)_3$ crystal contained 1.8 to 2.0 coppers per hexamer.

4.2.1 Copper(II) binding to the guanine bases

The relative partial occupancies at each copper guanine base of the d(m^5CGUAm^5CG) hexamer mirrored those of the analogous guanine bases of the $d(CG)_3$ crystal, taking into account the difference in the absolute quantity of copper within the Z-DNA crystals. Figure 8 compares the partial occupancies at each purine base within each of the two crystals. The sum of the electron counts for the copper site in each hexamer was set to 100 % in both structures (Table 7). Figure 9 is the same comparison, but the electron counts of each copper site were normalized to the electron count for a fully occupied copper(II) site (327 contour

Table 7. Partial occupancies of the copper binding sites in the copper(II)-soaked d(m^5CGUAm^5CG) and d(CG)$_3$ Z-DNA crystals as determined from the electron density maps.

A. d(CG)3 crystal:

Copper site:	[1]Number of contour lines	[2]'Atomic' volume in Å^3	[3]Electron count in contour lines * Å^3	[4]Relative partial occupancy in %	[5]Partial occupancy in %
Cu2 at G2	24	0.905	21.7	3.50	6.70
Cu4 at G4	54	1.20	65.0	10.5	19.9
Cu6 at G6	155	1.32	204	32.9	62.6
Cu8 at G8	48	1.56	75.0	12.1	23.0
Cu10 at G10	75	1.70	127	20.5	39.0
Cu12 at G12	75	1.70	127	20.5	39.0
Sum:			620	100	190 = 1.9 copper ions per hexamer

The electron count and the partial occupancies were determined from the electron density maps as described in the Methods section.

[1] The contour lines were counted for contour increment of 5 arbitraty units. The map settings were 35 arbitrary units for the minimum contour level and 800 arbitrary units for the maximum level.

[2]Volume of a sphere with the diameter of the contour line at half maximum peak height.

[3]Product of 'number of contour line' and ' atomic volume'. Relative measure for the number of electrons at a particular copper site.

Table 7. B. d(m5CGUAm5CG) crystal:

Copper site:	[1]Number of contour lines	[2]'Atomic' volume in Å^3	[3]Electron count in contour lines * Å^3	[4]Relative partial occupancy in %	[5]Partial occupancy in %
Cu2 at G2	48	1.22	58.5	16.3	17.9
Cu6 at G6	92	1.29	119	33.0	36.3
Cu8 at G8	32	1.52	48.5	13.5	14.9
Cu12 shared between G12 and A10	98	1.36	133	37.2	40.9
Sum:			359	100	110 = 1.1 copper ions per hexamer
Water next to N7 of adenine A4 (putative copper):	11	0.524	5.76	1.61	1.76

Continuation from Table 7. A.

[4]The relative partial occupancy is the electron count of the site i relative to the sum of the electron counts of all copper(II) sites in the hexamer duplex. The relative partial occupancy allows to compare copper binding affinities between crystals with different copper content.

[5]The partial occupancy is the electron count of the site i relative to the electron count for a fully occupied copper ion. Atomic absorption data from d(m^{5}CGUAm^{5}CG) allowed calibration of electron density map: 1.1 copper ions per hexamer duplex = 359 contour lines * Å^3 , therefore, 1 copper ion = 326 contour lines * Å^3 (=100 %). The partial occupancy gives the relative number of hexamer duplexes in a crystal in which the copper site i is occupied.

Figure 7. A 2.3 Å thick section along the z-axis of the $2F_{obs}$-F_{cal} electron density map showing the adenine A4/uridine U9 base pair and the surrounding solvent molecules of the copper(II)-soaked d(m^5CGUAm^5CG) crystal structure. The x-axis lies along the vertical axis and the y-axis along the horizontal axis of this figure. Five sections of the electron density map (1.5 unit cells along the x-axis and 0.75 unit cells along the y-axis) centered at 30.1 Å were overlapped to show all of the electron density associated with this base pair. The electron densities are shown as topological contours (in arbitrary units) and the model to fit the electron density shown as solid bonds. The solvent molecules assigned in the immediate area of this base pair are labeled as 'S'.

Figure 7.

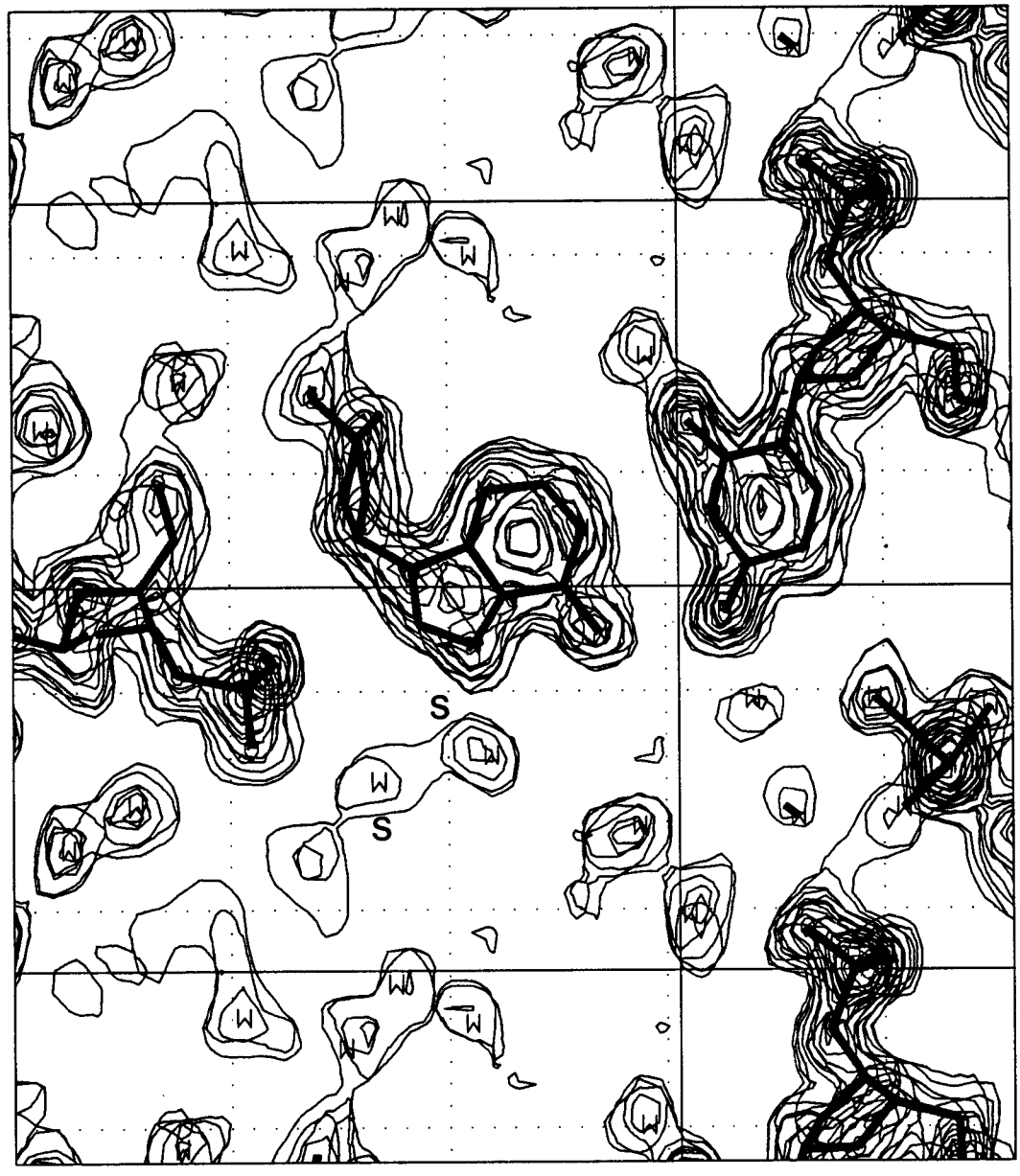

Figure 8. Comparison of the partial relative occupancies of the copper(II) sites along the hexamer chains in the copper(II)-soaked $d(CG)_3$ (Kagawa *et al.*, unpublished) and $d(m^5CGUAm^5CG)$ crystals, normalized to the total amount of copper(II) in each hexamer. The percent occupancy at each site is plotted along the vertical axis and the residue number of each purine residue that may be susceptible to copper binding is plotted along the horizontal axis. The occupancies at each guanine residue in the $d(CG)_3$ crystal are plotted as open squares. The occupancies of the coppers that overlap the G10 and G12 residues were added and plotted at residue number 11 to represent a 'shared' copper. The dashed lines connects the individual occupancy values of G10 and G12 with the remainder of the sites. The occupancies of the copper(II) ions assigned in the $d(m^5CGUAm^5CG)$ crystal are plotted as closed diamonds, with the copper shared between adenine A10 and guanine G12 plotted at residue 11 to show that it is a shared site. The putative copper at A4 was connected to the remainder of the sites in this crystal by a dotted line because it was later defined as a water molecule rather than a copper(II) ion, and is labeled as such. The relative uncertainty of the % occupancy values is approximately 20 %.

Figure 8.

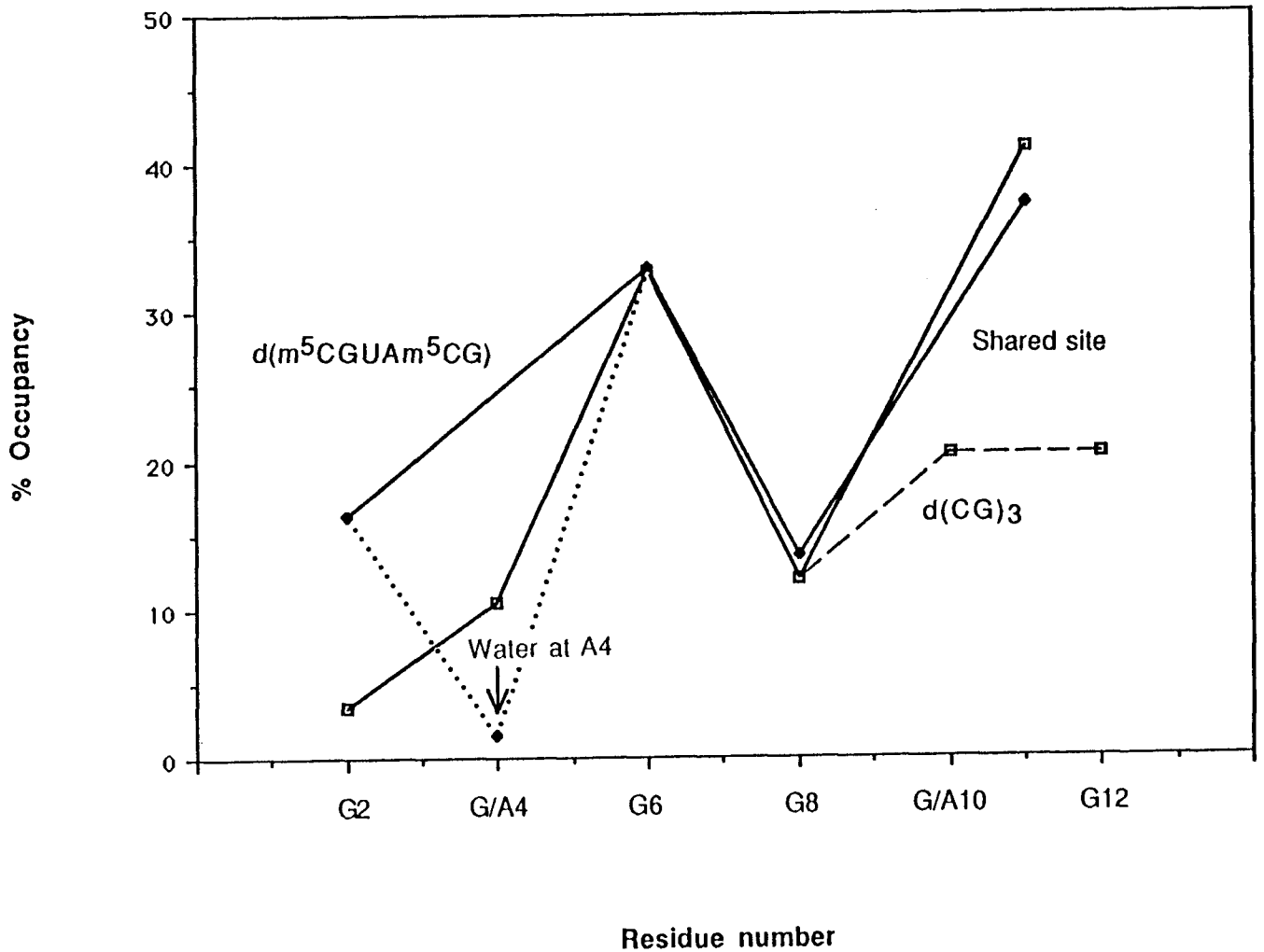
50
40
30
20
10
0
% Occupancy
d(m5CGUAm5CG)
Shared site
d(CG)3
Water at A4
G2
G/A4
G6
G8
G/A10
G12
Residue number

Figure 9. Comparison of the partial occupancies of the copper(II) sites along the hexamer chains in the copper(II)-soaked $d(CG)_3$ (Kagawa *et al.*, unpublished) and $d(m^5CGUAm^5CG)$ crystals, normalized to the electron count for a fully occupied copper(II) ion as determined by the calibration of the electron density map using the atomic absorption data from the $d(m^5CGUAm^5CG)$ crystal. All parameters are identical to those defined in Figure 8, except that the partial occupancies are represented as a percent of hexamer duplexes in the crystal in which a particular copper(II) site is occupied.

Figure 9.

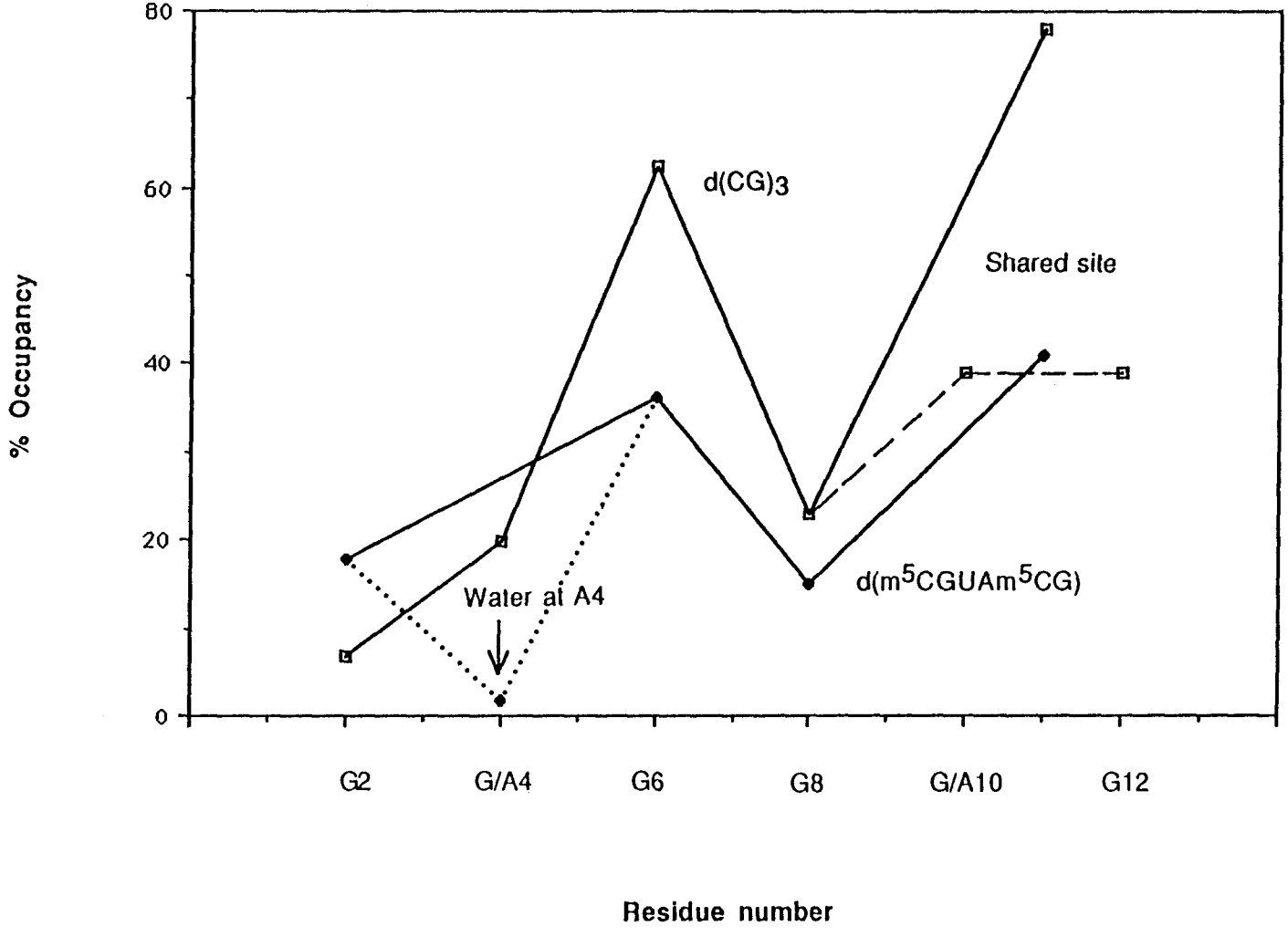
80
60
40
20
0
% Occupancy
d(CG)3
Shared site
Water at A4
d(m5CGUAm5CG)
G2
G/A4
G6
G8
G/A10
G12
Residue number

lines * $Å^3$) as determined by the calibration of the electron density map using atomic absorption data. Even the highest occupied copper site in both hexamers (the copper at the guanine G6 in $d(CG)_3$) is only occupied in 63 % of all hexamer duplexes in the crystal. The partial occupancy, relative to the total amount of copper per hexamer, was overall very low at guanine G2 and G8 (16 % and 14 % respectively) of the $d(m^5CGUAm^5CG)$ crystal (Table 7). The occupancy of the copper at G8 mirrors the value determined for the analogous site within the $d(CG)_3$ structure. The occupancy at the guanine G2 was significantly lower in the $d(CG)_3$ structure (3.5 %) due to differences in local crystal packing effects. This will be discussed in detail in a later section. The relative occupancies of the copper at G6 were identical in both structures. Thus, the partial occupancies at the copper sites at each guanine common to both copper-soaked structures are related, confirming that the reactivity of the accessible guanine N7 nitrogens are nearly identical in both crystals.

The second highest occupied site of the $d(CG)_3$ structure lies at a position shared between guanine G10 of one hexamer duplex and G12 of an adjacent hexamer duplex. The electron density showed that each of these guanine bases binds a distinct copper(II) ion (Figure 10). The two guanines are displaced by approximately 1.3 Å along the z-axis, but the two accompanying copper ions overlap to form two mutually exclusive binding sites. The sum of the occupancy at each site is equivalent to 41 % of the absolute amount of copper per hexamer (Table 7). The analogous position in the $d(m^5CGUAm^5CG)$ hexamer is shared between the adenine A10 and the guanine G12 base of two adjacent hexamer duplexes. These two purine bases, however, reside at essentially identical levels along the z-axis (Figure 11). The copper ion at this site actually coordinates to both purine bases with a partial occupancy of 37.2 % of the absolute amount of copper per hexamer (Table 7). The occupancies of these shared sites of the two structures were therefore nearly identical.

4.2.2 Copper(II) binding to adenine bases

The question concerning the ability of copper(II) to bind to adenine cannot be immediately resolved from the analysis of the site shared by A10 and G12 (Figure 11). By simple inspection it was unclear as to whether, at this site, the adenine acts identically as a guanine base, or whether copper binding to the adjacent guanine

Figure 10. A 2.3 Å thick section along the z-axis of the $2F_{obs}$-F_{cal} electron density map of the copper(II)-soaked $d(CG)_3$ crystal (Kagawa *et al.*, unpublished) showing the two mutually exclusive copper binding sites of guanines G10 and G12. Five overlapping sections of the electron density map (1.5 unit cells along the vertical x-axis, 1.0 unit cells along the horizontial y-axis, and centered at 26.13 Å along the z-axis) are plotted to show the copper(II) binding site at the guanine G10 (base pair C3-G10 is at the left side of the map) and at guanine G12 (base pair C1-G12 is at the right side of the map). The two copper(II) ions are shown as overlapping topological contours in the approximate center of the map, and lie between the N7 nitrogens of the two guanine bases. Bonds connect the copper ions with their N7 nitrogen ligands. A bond connects the two metal centers, showing that the centers of the electron densities assigned to the cations are closer than the sum of their van der Waal's radii. This was not strictly a shared copper, but represents two independent and mutually exclusive copper binding sites in the crystal.

Figure 10.

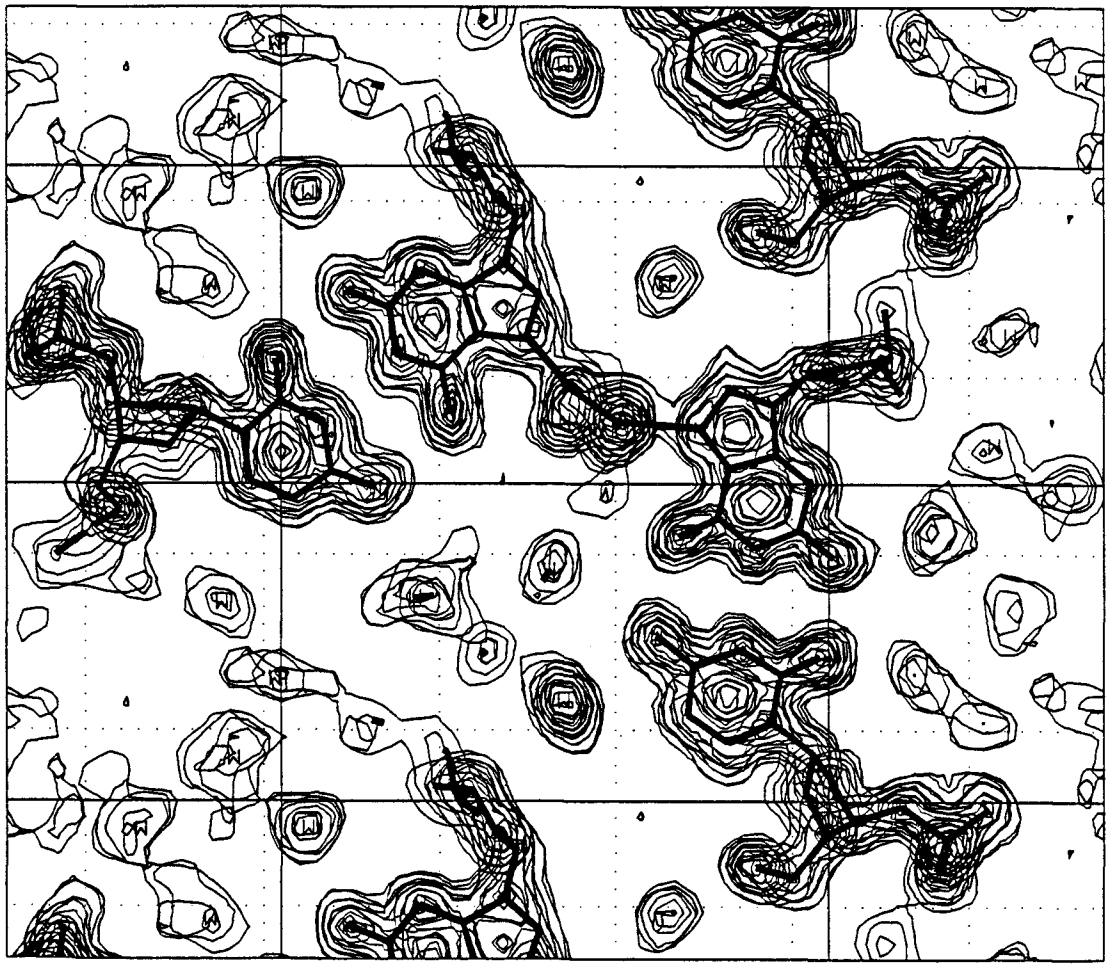

Figure 11. A 2.3 Å thick section of the $2F_{obs}$-F_{cal} electron density map of the copper(II)-soaked d(m^5CGUAm^5CG) crystal showing the single shared copper binding site at adenine A10 and guanine G12. Five overlapping sections of the electron density map (1.5 unit cells along the vertical x-axis, 1.0 unit cells along the horizontal y-axis, and centered at 26.13 Å along the z-axis) are plotted to show the copper(II) binding site shared by adenine A10 (base pair C3-G10 is at the left side of the map) and guanine G12 (base pair C1-G12 is at the right side of the map). The copper(II) ion is shown as a single set of topological contours in the approximate center of the map and lies between the N7 nitrogens of the two purine bases. Bonds connect copper ion to the N7 nitrogens of the purine bases. A bond connects the metal center to the water molecule that acts as the third ligand, along with the two purine bases, that form the equitorial plane of the trigonal bipyramidal coordination geometry of this copper site.

Figure 11.

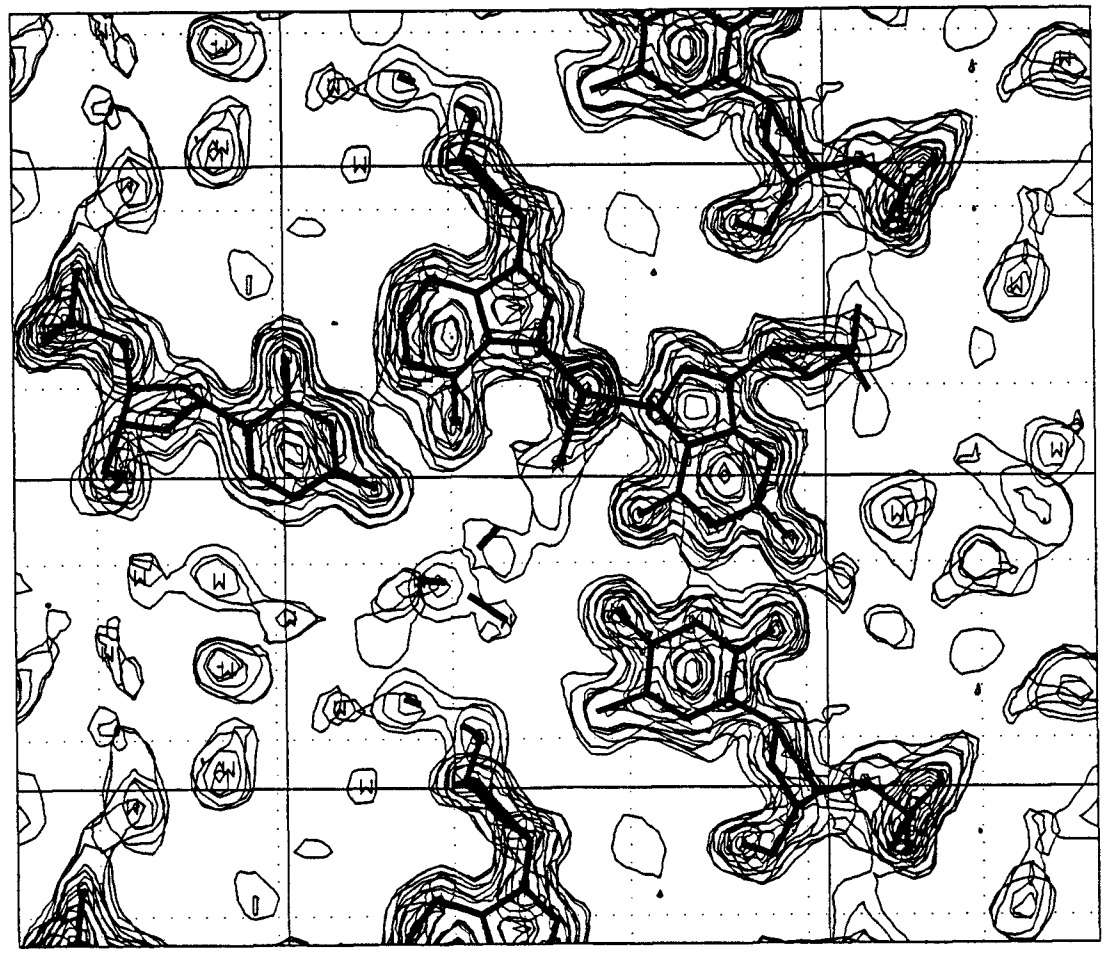

facilitates binding to the adenine, or that adenine binding is entirely a fortuitous event resulting from the relative distance and alignment of the two purine bases as a result of crystal packing. In binding copper(II) at this site, the adenine A10 and the guanine G12 purine bases were pulled 0.16 Å closer (the N7 to N7 distance was 4.04 Å in the native d(m^5CGUAm^5CG) structure versus 3.88 Å in the copper-soaked structure). The copper(II) to N7 nitrogen distance was 2.12 Å for guanine G12 and 1.92 Å for adenine A10. The relative angles between the bases remained identical between the two bases. The bond angle formed between the N9-N7-copper(II) atoms of G12 was 145.5^o and 148^o for the atoms of A10. These parameters are slightly distorted relative to the copper to N7 distance (2.15 Å) and N9-N7-copper angle (161^o) for the copper Cu6. This copper complex (Cu6) at guanine G6 represents the standard geometry of a copper-guanine complex in the absence of crystal packing effects, as will be discussed later. The guanine G12 copper to N7 distance of 2.12 Å is reasonably close to this distance for the standard copper geometry at a guanine bases. The copper to N7 distance of adenine A10 was much shorter. In addition, the angles formed between the G12 and A10 purine bases to the copper were both significantly smaller than expected. This suggests that the adenine plays more than just a passive role in binding a copper ion at this site. If a copper were placed at the guanine G12 using the average distances and geometries, with no involvement of the adenine, the resulting copper position would be predicted to be 2.52 Å from the N7, and would form a 157.5^o angle between N9-N7-copper for the A10 purine base. This is significantly different from the dimensions observed in the crystal. Both the A10 and the G12, therefore act in concert to define this copper(II) binding site.

There were no electron densities observed to be centered within 2.2 Å of the N7 of adenine A4 (Figure 7). The nearest electron density to this position, that was not previously assigned to atoms of the DNA, was centered 2.75 Å from the N7 nitrogen. This does not fall within the range of copper(II) N7 nitrogen bond distances (1.92 Å to 2.57 Å) observed for the copper complexes in either crystal (Table 8), suggesting that this density was not associated with a copper(II) binding site. If this set of electron densities were treated as a copper site, its partial occupancy (relative to the total amount of copper per each hexamer) would be 1.6 % relative to 10.5 % for the analogous guanine G4 site of the d(CG)$_3$ crystal. This value is much lower than would be predicted for this site and breaks the trend

Table 8. Geometry of copper complexes in the copper(II)-soaked d(m^5CGUAm^5CG) and d(CG)[3] (Kagawa *et al.*, unpublished) Z-DNA crystals.

A. Bond length.

Copper at base:	ligand:	Copper to ligand bond length in Å				
		d(m^5CGUAm^5CG)			d(CG)[3]	
				[1]Geometry:		[1]Geometry:
2Cu	G2	N7	2.30	Distorted	2.57	Not assigned
2Cu		W1	2.15	Tetrahedron	2.15	
2Cu		W2	2.03			
2Cu		W3	2.07		2.14	
2Cu		W4	2.20			
2Cu		W5	2.11			
4Cu	G4	N7			2.34	Not assigned
4Cu		W1			2.05	
4Cu/ water	A4	N7	2.75	[2]Putative copper/water		
6Cu	G6	N7	2.15	Undistorted	2.17	Undistorted
6Cu		W1	1.84	octahedron	2.13	octahedron
6Cu		W2	2.09		2.17	
6Cu		W3	2.01		2.35	
6Cu		W4	1.94		2.16	
6Cu		W5	2.31		2.22	
8Cu	G8	N7	2.38	Distorted	2.31	[3]bipyramid
8Cu		W1	1.99	octahedron,	2.14	W7
8Cu		W2	2.23	one water	1.99	W8
8Cu		W3	1.98	ligand	2.13	W9
8Cu		W5	2.21	missing	3.04	W10
10Cu	G10	N7			1.83	Not assigned,
10Cu		W1			2.07	site shared with G12
12Cu	A10	N7	1.98	Shared site,		
12Cu	G12	N7	2.12	trigonal	2.38	Not assigned,
12Cu		Cl A	3.10	bipyramid		site shared
12Cu		Cl B	2.69			with G10
12Cu		W1	2.30		2.02	
12Cu		W2			2.80	

Table 8.
B. Bond angles.

Copper at base:			Copper to ligand bond angle in ^{o}			
		angle between:	d(m^5CGUAm^5CG)	[1]Geometry:	d(CG)[3]	[1]Geometry:
2Cu	G2	N9N7Cu	152.98	Distorted	133.72	Not assigned
		N7CuW1	115.72	octahedron	107.49	
		N7CuW2	69.87			
		N7CuW3	80.79		94.30	
		N7CuW4	87.42			
		N7CuW5	165.63			
		W5CuW1	77.98			
		W5CuW2	96.04			
		W5CuW3	102.54			
		W5CuW4	87.90			
		W4CuW1	91.67			
		W4CuW2	82.44			
		W4CuW3	167.44			
		W3CuW1	97.29			
		W3CuW2	89.44			
		W2CuW1	171.81			
4Cu	G4	N9N7Cu			149.30	Not assigned
		N7CuW5			168.83	
	A4	N9N7Cu	142.84	[2]Putative	copper/water	
6Cu	G6	N9N7Cu	161.24	Undistorted	158.90	Undistorted
		N7CuW1	99.12	octahedron	98.07	octahedron
		N7CuW2	92.43		97.30	
		N7CuW3	94.29		98.49	
		N7CuW4	96.03		87.37	
		N7CuW5	172.83		174.52	
		W5CuW1	85.06		84.48	
		W5CuW2	83.06		90.33	
		W5CuW3	79.94		86.27	
		W5CuW4	88.09		87.68	
		W4CuW1	108.28		92.45	
		W4CuW3	88.71		172.61	
		W4CuW2	170.49		89.52	
		W3CuW1	156.95		91.18	
		W3CuW2	86.30		86.28	
		W2CuW1	74.53		174.36	

Table 8.
B. Bond angles. (Continuation)

Copper at base:			Copper to ligand bond angle in ^{o}			
		angle between:	d(m^5CGUAm^5CG)	[1]Geometry:	d(CG)[3]	[1]Geometry:
8Cu	G8	N9N7Cu	146.06	Distorted	152.63	[3]bipyramid
		N7CuW1	106.52	octahedron,	107.96	N7CuW7
		N7CuW2	78.67	one water	75.71	N7CuW8
		N7CuW3	87.11	ligand	100.37	N7CuW9
		N7CuW5	164.93	missing	163.79	N7CuW10
		W5CuW1	88.54		138.22	W7CuW8
		W5CuW2	86.68		101.12	W7CuW9
		W5CuW3	89.49		163.79	W7CuW10
		W3CuW1	104.99		119.29	W8CuW9
		W3CuW2	90.29		88.12	W8CuW10
		W2CuW1	163.91		88.46	W9CuW10
10Cu	G10	N9N7Cu			153.14	Not assigned,
		N7CuW1			131.46	shared site with G12
12Cu	A10	N9N7Cu	147.98	Shared site		
		N7CuW1	115.61	between A10		
		N7CuCL A	91.38	and G12,		
		N7CuCL B	94.87	trigonal		
12Cu	G12	N9N7Cu	145.50	bipyramid	156.07	Not assigned,
		N7CuW1	97.18			site shared
		N7CuCL A	98.01			with G10
		N7CuCL B	87.54		140.97	N7CuW1
		N7CuN7	147.22		94.92	N7CuW2
		CL ACuCL B	158.91			
		CL ACuW1	73.60			
		CL BCuW1	85.56			

[1]Geometry of the copper coordination complex. W5 is the axial ligand, ligand numbering may vary between the two structures, values can, therefore, not compared individually. Ligand numbers are given for the Cu8 complex in the d(CG)3 structure.

[2]No copper ion was found near the N7 of adenine A4 in d(m^5CGUAm^5CG). The closest water molecule is listed as putative copper.

[3]Trigonal bipyramid.

established for the partial occupancies along the strands of the hexamer duplexes (Figure 8). The observed distance and occupancy suggest that the set of electron density at the A4 was not associated with a copper(II) ion binding site. From this low electron density and the long bond distance, the most likely assignment of this density would be a water molecule hydrogen bonded to the N7 nitrogen of adenine A4. An analysis of the solvent electron density in the immediate vicinity of this putative water, as discussed in the next section, confirms that there was no regular coordination geometry associated with this site. This further supports the conclusion that this site was not occupied by a copper(II) ion.

A comparison of the partial occupancies of the copper sites in the $d(CG)_3$ and the $d(m^5CGUAm^5CG)$ crystals showed that overall, the structural differences between $d(CG)_3$ and $d(m^5CGUAm^5CG)$ in the Z-DNA crystal form do not significantly effect the binding of copper to Z-DNA (Table 7, Figure 8). The differences in occupancies between these crystals were related to the ability of the adenine bases to bind copper(II) ions.

4.3 Assigning coordination geometries to the copper(II) centers

Copper(II), as most metal ions in solution, forms regular geometric coordination complexes, with each vertex of the complex formed by nucleophilic ligands. The regularity of these complexes helps to define the observed electron densities as either metal ions or free solvent. Magnesium(II) ions in aqueous solution, for example, have been assigned to DNA structures according to their regular octahedral aqueous complexes. Transition metal ion complexes adopt a number of different regular geometries. Copper(II) ions in the $d(CG)_3$ Z-DNA structure have been found to adopt trigonal bipyramidal or octahedral coordination geometries. Even the poorly occupied ion sites show some evidence of a regular coordination geometry. The copper bound to guanine G4 of the $d(CG)_3$ structure shows a water ligand diametrically opposed to the guanine N7 nitrogen, suggesting either an octahedral or trigonal bipyramidal geometry (Figure 12).

Figure 12. A 2.3 Å thick section along the z-axis of the $2F_{obs}$-F_{cal} electron density map of the copper(II)-soaked $d(CG)_3$ crystal (Kagawa *et al.*, unpublished) showing the copper binding site at guanine G4. Five overlapping sections of the electron density map (1.5 unit cells along the vertical x-axis, 0.75 unit cells along the horizontal y-axis, and centered at 30.33 Å along the z-axis) are plotted to show the copper(II) binding site at guanine G4 (base pair G4-C9 is at the center of the map). The copper(II) ion is shown as a single set of topological contours in the approximate center of the map along the horizontal (y) axis. A bond connects the copper ion to the N7 nitrogen of the guanine base. A additional bond connects the metal center to the water molecule that acts as the axial ligand, of either a trigonal bipyramidal or octahedral coordination geometry for this copper site. No analogous copper was assigned at the adenine A4 of the $d(m^5CGUAm^5CG)$ crystal.

Figure 12.

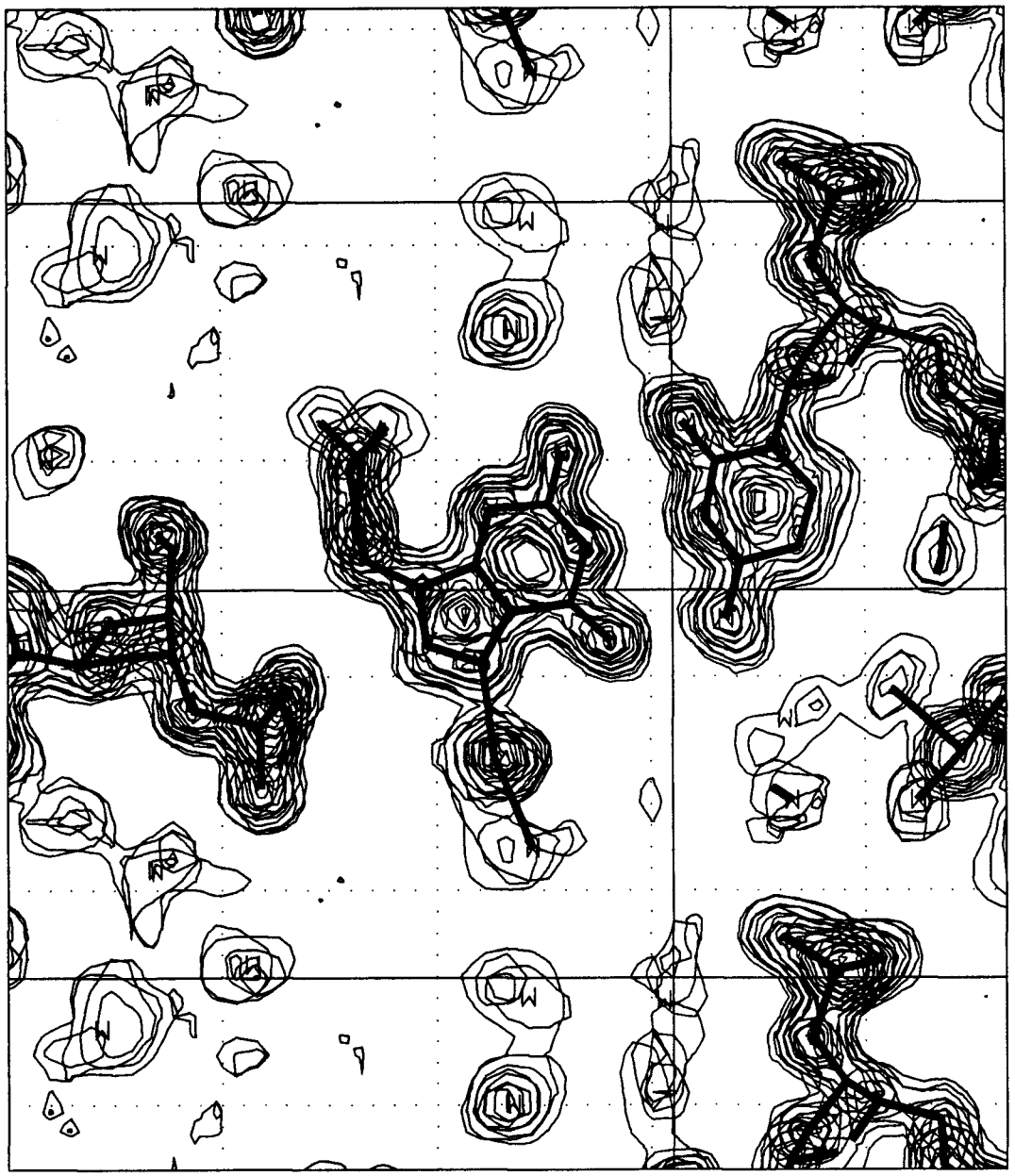

4.3.1 Copper(II) at guanine bases

All the sets of electron densities assigned to copper(II) in the soaked d(m^5CGUAm^5CG) structure show additional electron densities approximately 2.1 Å from the center that define a regular coordination geometry and, therefore, further supports their proper assignments (Figure 11, 13, 14, and 15). In general, the geometries of the d(m^5CGUAm^5CG) copper ions mirror those of the d(CG)$_3$ structure. The specific exceptions will be discussed in detail in a later section. In the next section, the electron density in the vicinity of the adenine A4 site, and shared between adenine A10 and guanine G12 of a adjacent hexamer will be analyzed.

4.3.2 Putative copper/water molecule at adenine A4

The electron density map showed a well defined set of electrons 2.75 Å from the N7 nitrogen of adenine A4 (Figure 7). From the discussion in the previous section, this putative copper could best be assigned as a water molecule hydrogen bonded to the N7 of the adenine base. An analysis of the electron density surrounding this A4 site will show that no regular coordination geometry exists for this putative copper, therefore supporting its assignment as a water molecule. The equivalent position in the d(CG)$_3$ structure was occupied by a set of electron density whose center was 2.34 Å from the N7 of the guanine base. This latter electron density showed an additional set of density that was diametrically opposed to the guanine N7 nitrogen, and positioned 2.05 Å from the copper center (Figure 12). Although the partial occupancy of this copper was low (10.5 %) (Table 7), this site at guanine G4 could be assigned as a copper(II) ion with two well defined ligands (the N7 of the guanine and a water molecule) at the axial positions of either an octahedral or trigonal bipyramidal coordination geometry.

The putative copper at the adenine A4 in the d(m^5CGUAm^5CG) structure was not surrounded by any additional sets of density within the range of observed copper-water ligand distances of 1.95 Å to 2.35 Å (Table 8, Figure 7). A single set of electron density, assigned to a water molecule, was within close proximity (2.66 Å) of the putative copper site at the adenine A4. This distance is much longer than any of the observed copper to water ligand bond lengths, but is within the range expected for hydrogen bonded water molecules (2.4 Å to 3.2 Å). The electron density assigned to the putative copper site at A4 showed the same maximum

Figure 13. A 3.22 Å thick section along the z-axis of the $2F_{obs}$-F_{cal} electron density map of the copper(II)-soaked d(m^5CGUAm^5CG) crystal showing the copper binding site at guanine G2. Seven overlapping sections of the electron density map (1.5 unit cells along the vertical x-axis, 0.75 unit cells along the horizontal y-axis, and centered at 23.65 Å along the z-axis) are plotted to show the copper(II) binding site at guanine G2 (base pair C5-G8 is left of center in the map). The copper(II) ion is shown as a single set of topological contours in the approximate center of the map along the horizontal (y) axis, and is connected by a bond to the N7 nitrogen of the guanine base. Three bonds connect the metal center to three of the five assigned water molecules that define the distorted octahedral coordination geometry for this copper site. A phosphate group (P) of a neighboring hexamer duplex is in close proximity of the copper complex. The N4 group (N) of a cytosine residue of a third hexamer duplex is in hydrogen bonding distance to one of the water ligands of the copper(II) complex.

Figure 13.

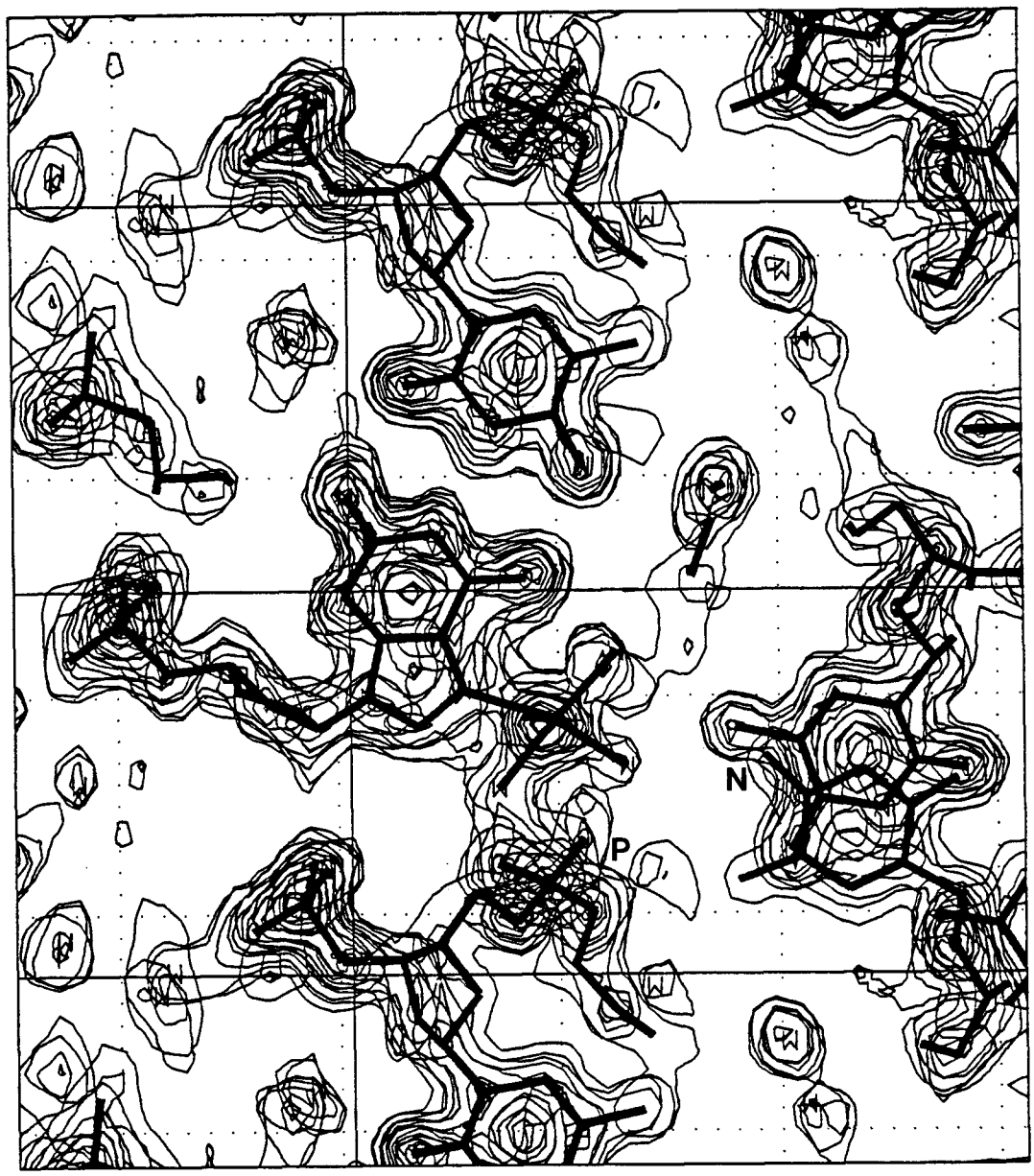

Figure 14. A 2.3 Å thick section along the z-axis of the $2F_{obs}$-F_{cal} electron density map of the copper(II)-soaked d(m^5CGUAm^5CG) crystal showing the copper binding site at guanine G6. Five overlapping sections of the electron density map (1.0 unit cell along the vertical x-axis, 1.0 unit cell along the horizontal y-axis, and centered at 30.14 Å along the z-axis) are plotted to show the copper(II) binding site at guanine G6 (base pair G6-C7 is right of center in the map). The copper(II) ion is shown as a single set of topological contours in the approximate center of the map axis, and is connect by a bond to the N7 nitrogen of the guanine base. Three bonds connect the metal center to three of the five assigned water molecules that define the octahedral coordination geometry for this copper site.

Figure 14.

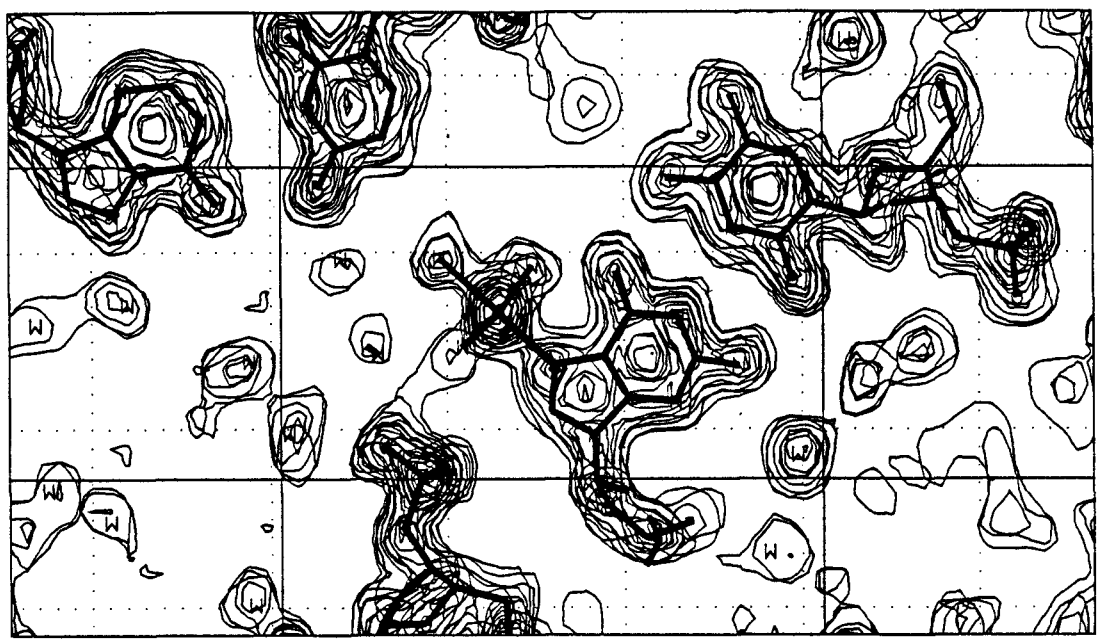

Figure 15. A 2.3 Å thick section along the z-axis of the $2F_{obs}$-F_{cal} electron density map of the copper(II)-soaked d(m^5CGUAm^5CG) crystal showing the copper binding site at guanine G8. Five overlapping sections of the electron density map (1.5 unit cells along the vertical x-axis, 1.0 unit cells along the horizontal y-axis, and centered at 33.39 Å along the z-axis) are plotted to show the copper(II) binding site at guanine G8 (base pair C5-G8 is at the center of the map). The copper(II) ion is shown as a single set of topological contours in the approximate center of the map along the horizontal (y) axis, and is connect by a bond to the N7 nitrogen of the guanine base. Two bonds connect the metal center to two of the four assigned water molecules that define most of the octahedral coordination geometry for this copper site.

Figure 15.

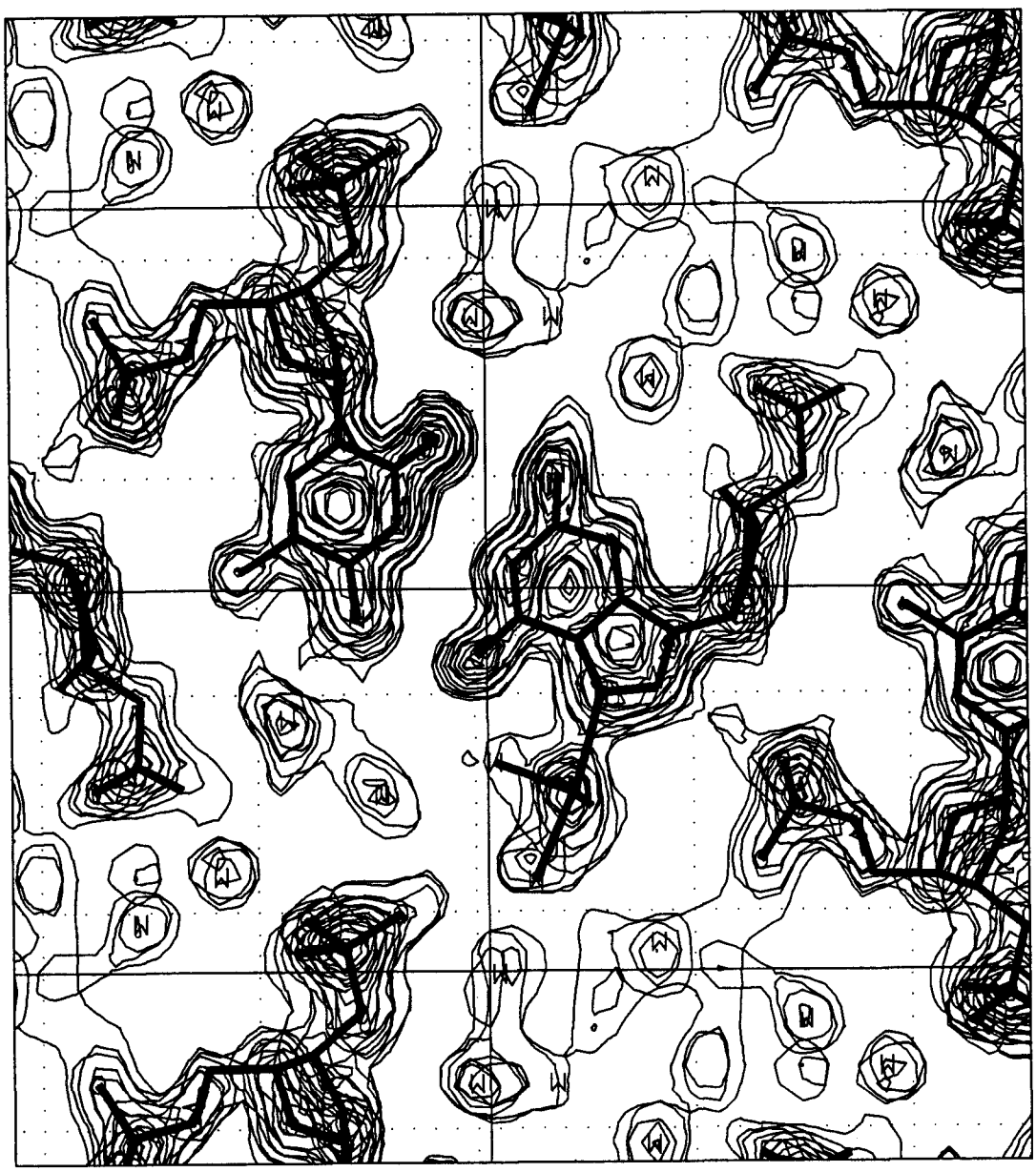

electron density as that assigned to this proximal free water molecule, and to other water molecules in the crystal. Furthermore, this proximal water does not lie in line with the N7 nitrogen of adenine A4 and the putative copper at A4 (Figure 7), as was the case for the G4 copper and its axial ligand found at the analogous site in the $d(CG)_3$ crystal (Figure 12). This proximal water, therefore, does not show the characteristics expected for a water ligand of a copper(II) complex.

The density closest to the N7 of adenine A4 does not appear to show any evidence of a regular coordination geometry defined by the surrounding solvent molecules. This suggests that this putative copper site is in fact not occupied by a copper(II) ion, but by a water molecule. Some additional considerations concerning the atoms surrounding this site support this conclusion. First, the center of the electron density at this A4 site does not lie in the same plane as the adenine base of A4 (Figure 16). This differs from all the well defined copper(II) sites at the guanines with one exception. This exception is the copper (Cu2) at the guanine G2 of both structures ($d(m^5CGUAm^5CG)$ and $d(CG)_3$), and its copper has been pulled out of the base plane by a closely positioned negatively charged phosphate group from a neighboring DNA duplex. The A4 position is not situated in a position to be so strongly influenced by this type of electrostatic interaction. Indeed, the analogous G4 site in the $d(CG)_3$ crystal that was defined as a copper(II) ion, is in the plane of the guanine base. Finally, the electron density at the putative A4 copper site was observed to be the same as that of surrounding solvent molecules. If the A4 site is a poorly occupied copper center, then the ligated molecules should also be poorly occupied. The relative ratio of electron density between the copper center and its ligands should remain the same regardless of the degree of occupancy at the site. The water next to the putative copper at the A4 (distance 2.66 Å), therefore, could not be assigned as ligands to a copper center. The accumulation of this data shows that there was no evidence for a regular coordination geometry that would be indicative of a copper(II) ion, and that the electron density at the major groove surface of adenine A4 could be best assigned as a water molecule.

Figure 16. Ball and stick model of the solvent molecules surrounding the N7 nitrogen of adenine A4 in the copper(II)-soaked d(m^5CGUAm^5CG) crystal structure. The N7 nitrogen of adenine A4 is shown as a dark shaded bonded sphere. The remainder of the atoms in the DNA bases are medium shaded bonded spheres and the atoms of the DNA backbone are shown as light shaded bonded spheres. The two solvent atoms in the proximity of the N7 nitrogen of adenine A4 are plotted as medium shaded unbonded spheres at the major groove surface. Of these, the solvent molecule that is closest to the N7 nitrogen (2.75 Å) is labeled with an 'S' and occupies a position similar to that of copper Cu4 in the copper(II)-soaked structure of the $d(CG)_3$ crystal (Kagawa *et al.*, unpublished). In contrast to the solvent molecule S, the copper Cu4 in the $d(CG)_3$ crystal lies in the purine base plane. Hydrogen bonds between the base pairs are drawn as dotted lines. A thin line connects the solvent molecule S with the N7 nitrogen, and the N7 nitrogen to the N9 nitrogen of the adenine base. The angle formed from the solvent molecule S to the N7 nitrogen to the N9 nitrogen is 142.82°.

Figure 16.

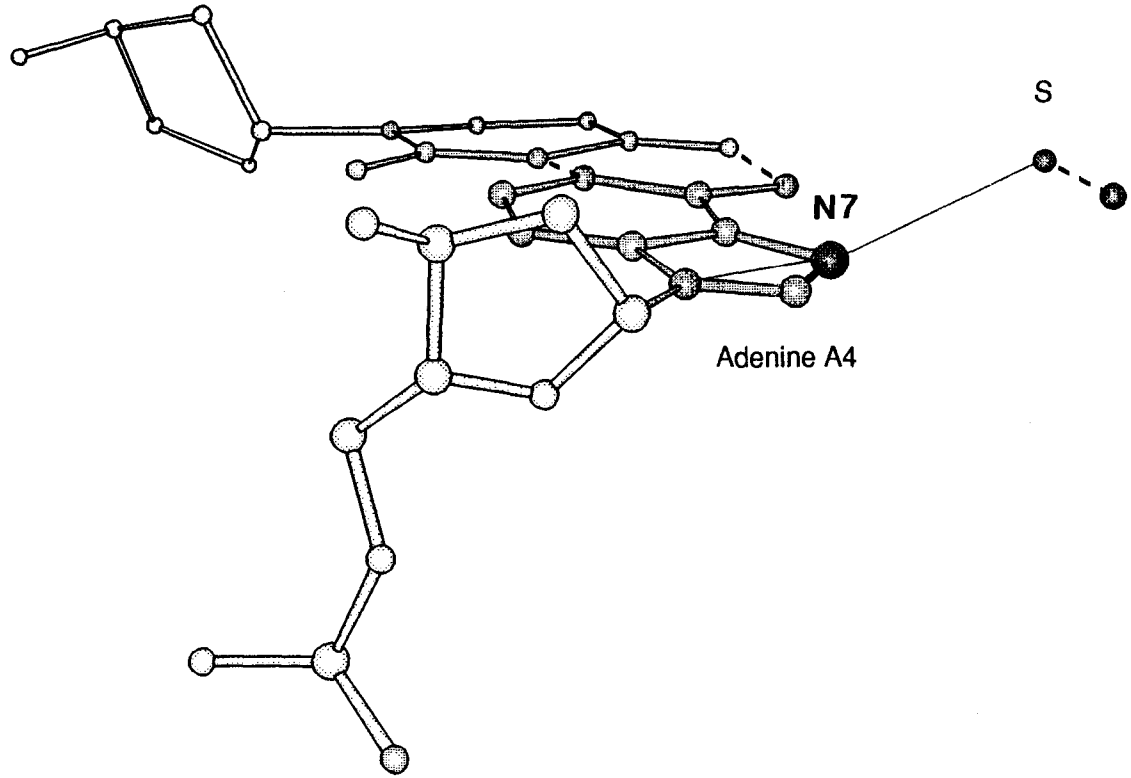

4.3.3 Copper(II) shared between adenine A10 and guanine G12

The copper(II) ion at the second adenine site (A10) is shared with the guanine G12 from an adjacent hexamer (Figure 11). This ion, therefore, has two purine bases functioning as ligands. The crystal packing of these hexamers places the two bases in an approximate angle of 82°. The angle formed between the N7 nitrogens of the two bases, with the copper acting as the common center, was 147.2°. This copper complex could, therefore, be either tetrahedral or trigonal bipyramidal. There would be insufficient room for the additional planar ligands to form an octahedral complex. A weak set of electron density was observed 2.30 Å from this copper center, forming bond angles of 115.6° to the adenine A10 ligand (N7-Cu-density) and 97.2° to the guanine G12 ligand (N7-Cu-density) (Figure 11). This suggests that the coordination geometry of this complex contains a trigonal plane. Copper(II) does generally not exist in a trigonal planar geometry (Huheey, 1978); a trigonal bipyramid is therefore more likely the geometry of this copper complex. In searching for the axial ligands of this copper complex, two sets of electron densities were observed at 2.69 Å above and 3.10 Å below the copper plane along the z-axis. The electron count of these additional sets of electron densities were significantly higher than that of water molecules in the structure. The electron count and the long distance from the copper center suggested that these axial ligands were chloride ions. Chloride ions have 18 electrons. The longest copper to chloride distance reported is 3.05 Å (Huheey, 1978). Thus, the geometry of this copper site was assigned as a trigonal bipyramid, with one water and the two purine bases forming the equitorial plane, and two chlorides at the axial positions.

The bond length of the chloride ligands to the copper center are at the upper limits of copper-chloride distances, which indicates a strong Jahn-Teller distortion to the axial ligands. This strong Jahn-Teller distortion along the axial coordination implies that the bond energies of the equitorial ligands must increase to compensate for the distortion. The copper to purine base bonds must therefore be stronger at this site, due to geometry, than for sites where no such distortion exists. This is supported by the short bond lengths for the ligands of the equitorial plane. This may also explain why a copper binds to adenine A10, but not to the adenine at A4. The crystal packing of the two hexamers forming the shared A10/G12 site plays a major role in defining the coordination geometry at this copper as a trigonal bipyramid and thus defines the bond strength of the equitorial ligands as stronger than one would

expect. Alternatively, one could argue that the geometric constraints of the adenine and guanine sites make the adenine N7 nitrogen more susceptible to copper attack than would be expected.

The assignment of the two axial ligands as chloride ions depended on the electron densities at each site being higher than that of water molecules. Since the plane of symmetry for the Jahn-Teller distortion bisects the purine bases and lies along the axial bonds, there is no *a priori* reason for both ligands being chloride ions. The axial ligands of a trigonal bipyramidal geometry are, however, generally identical. The axial chlorides, although being identical in most respects, do not have identical electron counts (Table 9). The electron count of the chloride at the more positive z-direction (i. e. above the copper center in the crystal), which will be named Cl B , has approximately twice the electron count as the lower axial chloride (Cl A). This can be explained as a difference in occupancy between the two sites. The rules of the Jahn-Teller distortion of axial ligands, however, require symmetric stretching of the axial bonds and, therefore, requires that the presence of one axial ligand be balanced by a second axial ligand. This disparity can be treated by two different models, both of which will be discussed in a later section. These models will take into account a number of different types of copper(II) complexes including the described trigonal bipyramid and a distorted tetrahedron with one chloride, one water and the two N7 of the purine base as ligands, that may possibly exist within the same crystal.

In conclusion the electron density maps showed that adenine A4 was not a copper binding site. Adenine A10 is a copper binding site by virtue of the geometry imposed on the copper coordination by the crystal packing. Adenine A4 represents an adenine base in an open solvent environment, while that of A10 is an example of a very specific DNA-DNA interaction. The N7 nitrogens of adenine bases, therefore, appear to be immune to covalent copper modification in free solution, while the geometry of a neighboring purine base, most likely a guanine base, facilitates copper binding to the N7 of adenines. The former case most closely models DNA in dilute solution. Both the open and geometrically constrained sites would be predicted to exist for DNA in a cellular matrix, suggesting that adenines may in fact be susceptible to copper(II) modification *in vivo*.

Table 9. Partial occupancies of the axial ligands of the copper Cu12 complex in the copper(II)-soaked d(m^5CGUAm^5CG) crystal as determined from the electron density maps.

Ligand:	[1]Number of contour lines	[2]'Atomic' volume in Å^3	[3]Electron count in contour lines * Å^3	[4]Relative partial occupancy in %
Cl A	28	0.905	43.4	48.8
Cl B	45	2.25	101	114

The electron count and the partial occupancies were determined from the electron density maps as described in the Methods section.

[1] The contour lines were counted for a contour increment of 5 arbitrarty units. The map settings were 35 arbitrary units for the minimum contour level and 800 arbitrary units for the maximum level.

[2]Volume of a sphere with the diameter of the contour line at half maximum peak height.

[3]Product of 'number of contour line' and 'atomic volume'. Relative measure for the number of electrons of a particular set of density in the electron density map.

[4]The relative partial occupancy is the occupancy of the ligand relative to the occupancy of the copper center Cu12. The electron count of Cu12 was 133 contour lines * Å^3. Cu2+ has 27 electrons, while Cl^- has 18 electrons. A chloride ligand occupied to the same extent as a copper has a electron count of: 133 contour lines * Å^3 * 18/27 = 88.9 contour lines * Å^3. A chloride ligand is occupied to 100 % if its electron density set results in a electron count of 88.9 contour lines * Å^3.

4.4 Comparison of corresponding copper site in the d(m5CGUAm5CG) and d(CG)3 structures

The previous Z-DNA structure of $d(CG)_3$ soaked with copper(II) chloride showed that copper(II) binds specifically to the N7 nitrogen of all guanine bases via a covalent coordinate bond. No direct binding of copper was observed at the phosphate groups. The partial occupancy and the coordination geometry of each copper in the $d(CG)_3$ structure varied widely along the hexamer chain, reflecting the effect of crystal packing on the accessibility of each binding site in the crystal unit cell. The present study explored the possibility of copper binding to the purine bases of adenine nucleotides by studying the copper-soaked structure of $d(m^5CGUAm^5CG)$ as Z-DNA.

A total of four copper binding sites was found in the structure of $d(m^5CGUAm^5CG)$ soaked with copper(II) chloride. The coppers form a covalent coordinate bond to the N7 nitrogen of guanine bases. In all cases the copper is further ligated to water molecules and, for one specific copper, is also ligated to chloride ions. The average copper to purine N7 bond length is 2.17 Å ± 0.178 Å (± SD) (Table 8). This is similar to the 2.29 Å ± 0.10 Å (± SD) copper-N7 bond lengths determined from the crystal structure of a polymeric copper(II) complex of guanine 5'-monophosphate (Aoki *et al.*, 1976). This also compares nicely to the 2.27 Å ± 0.25 Å (± SD) for the average copper-nitrogen bond length in the previously studied $d(CG)_3$ hexamer (Kagawa *et al.*, unpublished), although the bond lengths varied over a wider range in the d(CG)3 hexamer (1.83 Å to 2.57 Å). All the bond lengths for the copper complexes are compared in Table 8.

As expected from previous studies, no direct copper(II) binding was observed at the phosphate groups. However, all copper(II) complexes are indirectly bound to a phosphate group on either the same or a neighboring hexamer. At least one of the copper ligands in each copper(II) complex is hydrogen bonded to an oxygen of a phosphate group. With only one exception, the copper-N7 bond is essentially in the plane of the purine base. The copper to solvent ligand distances and bond angles are more variable, reflecting the diversity of coordination geometries found for copper complexes. The specific distances and geometries are dependent on the type of ligand at each copper and the interaction of the complexes with the DNA hexamer, with neighboring hexamers and with complexes on the same and neighboring hexamers.

The following section describes the geometry of each copper complex and the interactions with the DNA hexamer(s) that affect its geometry. Additionally, each copper site within the current d(m^5CGUAm^5CG) crystal structure will be compared to the equivalent site in the d(CG)$_3$ structure in terms of similarities and differences. This is followed by a discussion of the interactions between the copper ions within the crystals. The nomenclature of each copper site is defined by the guanine to which the copper has bound. For example, the complex Cu2 is the copper coordinated to guanine G2 along the hexamer chain. Since the guanine binding sites are common to both structures, this convention allows the same name to be used to describe analogous sites in both structures.

The copper complex Cu6 is discussed first because it, by virtue of the high occupancy and regular undistorted coordination geometry, represents the prototypical copper(II) complex covalently bound to the guanine N7 of an open site in both crystals. All the other sites are considered to be distortions caused by base substitutions and/or crystal packing.

4.4.1 Cu6 at guanine G6

In the present d(m^5CGUAm^5CG) structure the copper at position Cu6 forms a covalent coordinate bond to the N7 position of guanine G6. The copper assumes an octahedral geometry with four waters (W1, W2, W3, and W4) forming the ligands in the equitorial plane, and the guanine N7 and water W5 as the axial ligands (Figure 17). The copper sits only slightly above the plane defined by the G6 purine base, while the equitorial waters lie approximately 40^o to 50^o out-of-plane relative to the base plane. The bonds connecting the equitorial ligands to the copper center are 1.97 Å ± 0.105 Å (± SD) (Table 8). The W5 axial ligand, however, has a much longer bond length of 2.31 Å. The Cu6-N7 bond length is 2.15 Å. This suggests that the copper complex has undergone a slight Jahn-Teller distortion, pulling the two axial positions further from the ion center relative to the equitorial position. The closest phosphate group is the phosphate group of nucleotide C5 linking adenine A4 and cytosine C5. The W1 water ligand forms a hydrogen bond to the O2P oxygen atom of this phosphate group (distance: 3.09 Å). Water ligand W1 is also in hydrogen bonding distance of the O6 oxygen of the guanine G6 base (distance: 2.54 Å). A second phosphate group close in space is the phosphodiester linking uridine U9 and adenine A10 on a neighboring hexamer (Cu to P = 5.23 Å).

Figure 17. Ball and stick model of the copper(II) complex Cu6 bound to the N7 nitrogen of guanine G6 in the copper(II)-soaked d(m^5CGUAm^5CG) crystal structure. The atoms of the copper(II)-water complex are shown as dark shaded bonded spheres. The atoms in the DNA are shown as light shaded bonded spheres. The octahedral coordination geometry of this copper complex is shown as defined by four waters in the equitorial plane, and the N7 nitrogen and a fifth water at the axial positions.

Figure 17.

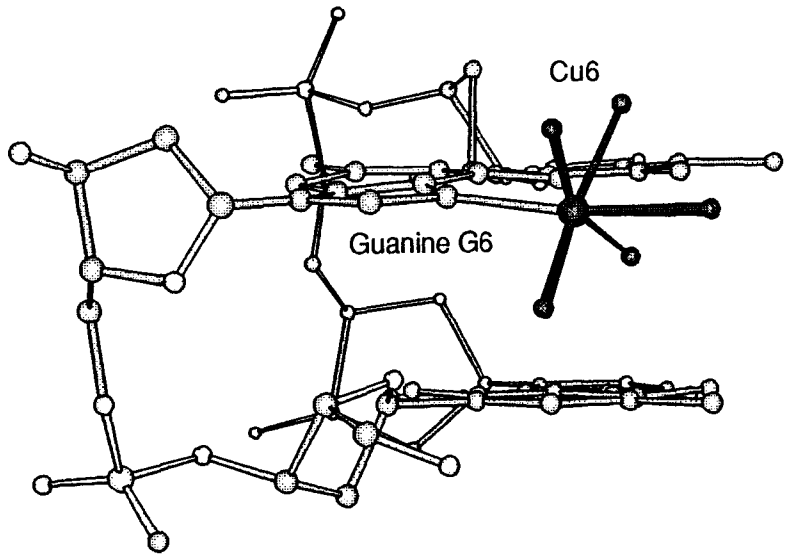

The distances of the water ligands of Cu6 to the oxygens of this phosphate group are, however, too long for hydrogen bonds (shortest distance: 3.58 Å). This Cu6 binding site is fairly open, but with several potentially stabilizing interactions with adjacent hexamers and copper complexes. This could account for the relatively high occupancy of this site.

The copper complex Cu6 at the guanine G6 of the $d(CG)_3$ structure exhibits an identical octahedral geometry as the Cu6 complex in the $d(m^5CGUAm^5CG)$ structure. The copper center lies approximately in the plane of the guanine base and one of the axial positions is occupied by the N7 nitrogen of the guanine base. The Cu-N7 distance is 2.17 Å, which is almost identical to the 2.15 Å in the $d(m^5CGUAm^5CG)$ structure. The bond length of the four equitorial water ligands are slightly longer, while the axial water ligand is closer to the copper center than in the comparable copper complex in the $d(m^5CGUAm^5CG)$ structure. The *equitorial water ligands are also* 40^o *to* 50^o *out of the base plane. The Cu6 site is* the highest occupied site in the $d(CG)_3$ due to the high accessibility of the site.

The absence of distortion defines the geometry of the Cu6 complex as the standard geometry guanine-copper(II) complex. The Cu6 site, by virtue of the crystal packing, the regular geometry and the high occupancy of its copper complex suggests that this is the prototypical copper binding motif for the guanines of double helical DNA in solution. An octahedral complex of this type can be placed at the N7 nitrogen of any guanine base of B-DNA without inducing any significant distortion to the DNA or the metal complex (Kagawa *et al.*, unpublished).

4.4.2 Cu2 at guanine G2

The overall copper site at guanine G2 of both the copper-soaked $d(CG)_3$ and $d(m^5CGUAm^5CG)$ crystal were similar in that they are crowded by a phosphate group from a neighboring DNA hexamer (related by translation of one unit cell along a) (Figure 18). This results in copper complexes that are pulled out of the purine base plane by approximately 30^o. The close proximity of the copper centers to the negatively charged phosphate groups (within 3.8 Å to 4.0 Å) suggests that an electrostatic attraction between the two ions is primarily responsible for this distortion in the copper-purine geometry. This distortion tends to weaken the coordination bond between the guanine N7 and the copper(II) ion, as evident from the longer nitrogen to copper bond length as compared to the average length for this

Figure 18. Ball and stick models of the copper(II) complexes Cu2 bound to the N7 nitrogen of guanine G2 in the (A.) copper(II)-soaked d(m^5CGUAm^5CG) and (B.) d$(CG)_3$ (Kagawa *et al.*, unpublished) crystal structures. The copper(II)-water complexes are shown as dark shaded bonded spheres. The atoms of the phosphate groups in the DNA backbones are medium shaded bonded spheres and the remainder of the atoms in the DNA are shown as light shaded bonded spheres. The potential hydrogen bonds that may be formed between the ligands of the copper complexes and the DNA are plotted as broken lines. In both structures a phosphate group from an adjacent DNA hexamer is shown to distort the N7 nitrogen to copper(II) coordinate bond out of the plane of the purine base. This was more pronounced in the d$(CG)_3$ (B.) crystal than in the d(m^5CGUAm^5CG) (A.) crystal.

Figure 18 A.

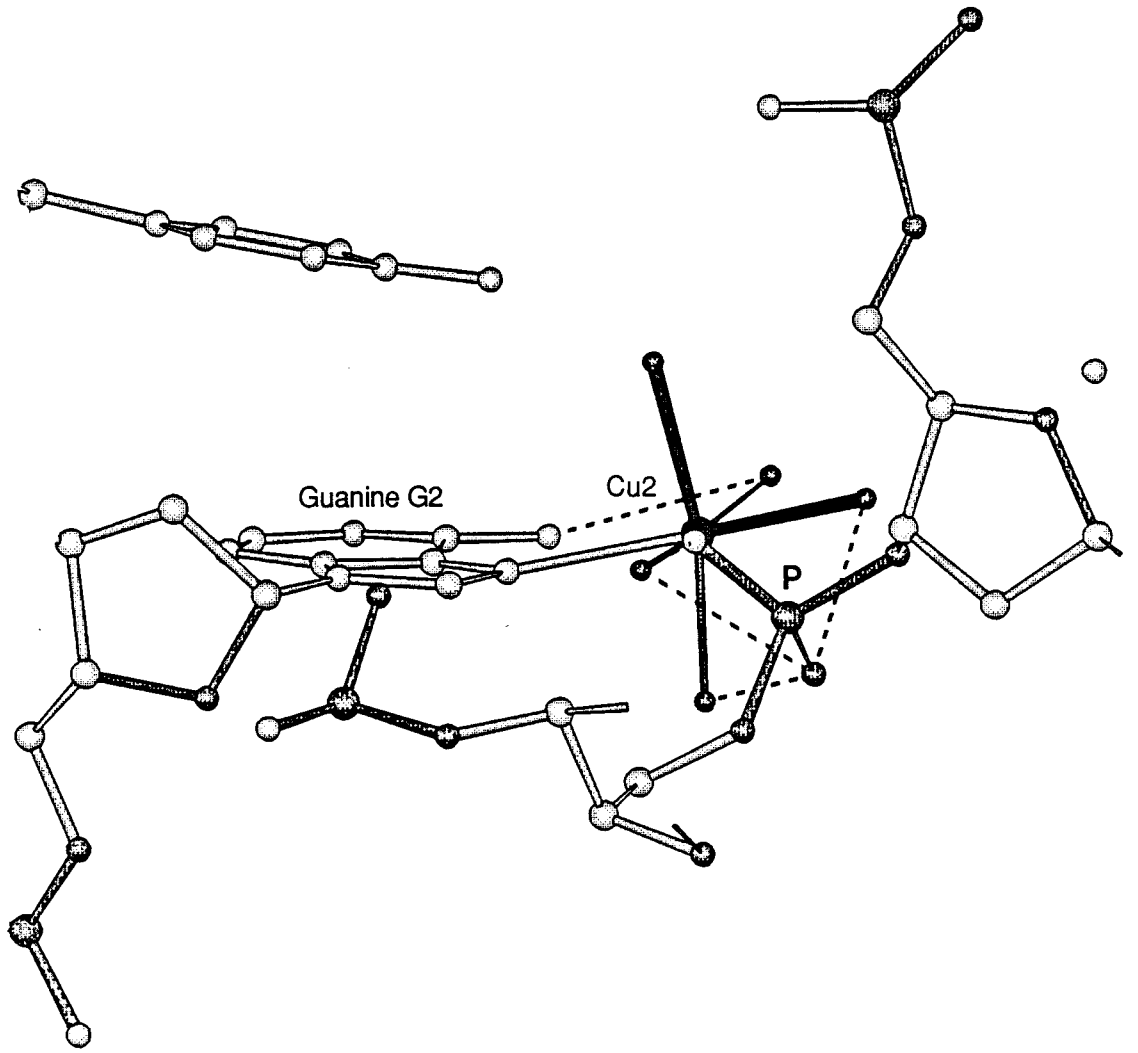

Figure 18 B.

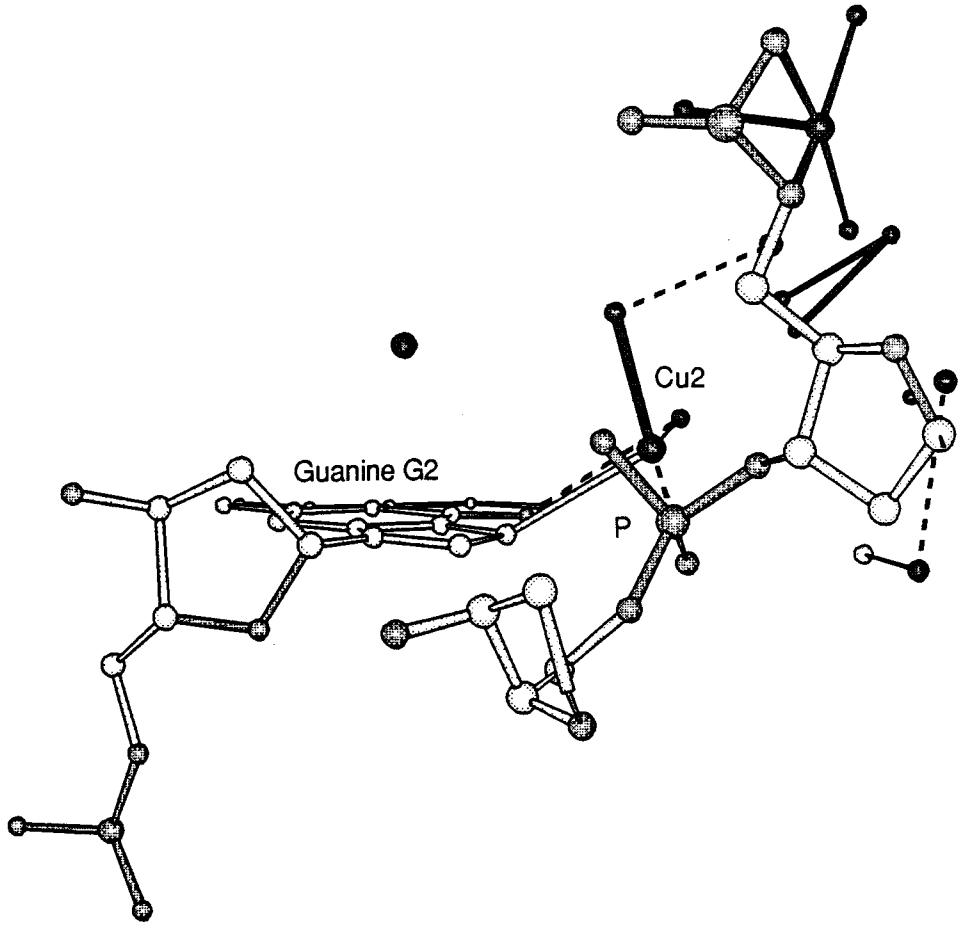

bond (2.30 Å compared to an average of 2.17 Å in the d(m^5CGUAm^5CG) structure and 2.57 Å compared to an average of 2.27 Å in the d(CG)$_3$ structure). Together the effect of the phosphate group in crowding and distorting this site act to decrease the relative occupancy of this copper complex in both structures (16 % in the d(m^5CGUAm^5CG) structure and 3.5 % in the d(CG)$_3$ structure relative to the total amount of copper(II) in each hexamer duplex).

The actual details of the binding sites between d(m^5CGUAm^5CG) and d(CG)$_3$ structures differ in the potential interactions available to the copper complexes and the surrounding solvent and DNA molecules. These differences can account for the differences in the occupancy of the two sites, as well as the observed differences in the coordination geometries of the copper complexes in the two Z-DNA crystals.

Within the previous d(CG)$_3$ crystal, the occupancy of the copper complex at this site was observed to be 3.5 % and only two water ligands were assigned. The analogous site in the d(m^5CGUAm^5CG) structure was occupied to 16 %, and displayed an octahedral geometry. The differences at this copper binding site include a shorter distance from the copper center to the closest phosphate group for the d(m^5CGUAm^5CG) structure (3.78 Å) as compared to the d(CG)$_3$ structure (3.93 Å). This closer distance would suggest that the electrostatic stabilization of this copper binding site is higher in the d(m^5CGUAm^5CG) crystal, and could account for the higher percentage of hexamer duplexes in the crystal that contain this copper ion (17.9 % for d(m^5CGUAm^5CG) and 6.7 % for d(CG)$_3$) (Table 7).

The comparison of the Cu2 copper binding sites in the previous copper-soaked d(CG)$_3$ structure, and in the d(m^5CGUAm^5CG) crystal (Figure 18 B and Figure 18 A), shows that the phosphate group was positioned much higher above the plane of the guanine base in the d(CG)$_3$ structure than in the d(m^5CGUAm^5CG) structure. The copper in the latter structure is closer to the N7 nitrogen of the base (2.30 Å versus 2.57 Å) and the copper complex is not pulled as far out of the base plane as in the d(CG)3 structure, indicating again, that local differences in crystal packing determine the different geometries and occupancies of the copper complexes in the two structures.

Interactions with a third hexamer may also contribute to the higher occupancy of the site in the d(m^5CGUAm^5CG) hexamer. The N4 amine group of a cytosine residue of this third hexamer is close enough (3.26 Å) for a potential hydrogen bond to the equitorial W1 ligand (Figure 13). The equivalent distance was

greater than 7 Å in the $d(CG)_3$ structure, and was, therefore, to long for any interaction (Figure 19). This additional interaction in the $d(m^5CGUAm^5CG)$ crystal could result in further stabilization of the copper complex in this structure.

Figure 18 A shows the interactions of the water ligands of Cu2 with the oxygens of the closest phosphate group in the $d(m^5CGUAm^5CG)$ structure. The O1P oxygen of the closest phosphate group of a neighboring hexamer duplex is within hydrogen bonding distance of the W2, W3 and W5 water ligand (2.42 Å, 2.85 Å and 2.68 Å) (Figure 18 A). Interactions between these three water ligands and the O1P oxygen further fixed and stabilized the position and orientation of the Cu2 copper complex in the $d(m^5CGUAm^5CG)$ structure. The opposing O2P oxygen of the phosphate group, however, is located within 1.86 Å from the equitorial water ligand W2. This implies that the O2P oxygen atom and the oxygen atom of the water are closer than the sum of their Van der Waal's radii (2 *1.5 Å). Their atomic positions would therefore be expected to be sterically hindered. A direct coordination bond of the copper center to the O2P oxygen is not possible because the copper-oxygen distance (3.58 Å) is too long for a bond. The close proximity of these two oxygen atoms would therefore be expected to have a destabilizing effect on the copper complex at this site. The copper complex is, however, only present in 18 % of all hexamer duplexes in the crystal (Table 8). Because the electron density map represents the electron distribution averaged for all hexamers in the crystal, one can argue that the observed position of the phosphate group is the position in the absence of copper at the Cu2 binding site, and the phosphate group may be slightly rotated in the presence of copper, resulting in a more favorable geometry. The observed steric hindrance between the oxygen atom of the phosphate group and the water ligand, therefore, may or may not apply to a fully occupied Cu2 binding site.

Only two water ligands were assigned to the Cu2 copper in the $d(CG)_3$ structure (Figure 18 B). Neither were within hydrogen bonding distance to the oxygen atoms of the neighboring phosphate group, and no stabilizing interactions were, therefore, observed. It may be possible that the O2P oxygen of the phosphate acts as a ligand to the metal center, thereby defining a tetrahedral geometry for Cu2 in the $d(CG)_3$ structure. A bond length of 1.95 Å was reported for a direct bond between copper and the oxygen of a phosphate group (Aoki *et al.*, 1976). A direct bond between the copper Cu2 center and the O2P oxygen of the phosphate group of a

Figure 19. A 3.22 Å thick section along the z-axis of the $2F_{obs}$-F_{cal} electron density map of the copper(II)-soaked $d(CG)_3$ crystal (Kagawa *et al.*, unpublished) showing the copper binding site at guanine G2. Seven overlapping sections of the electron density map (1.5 unit cells along the vertical x-axis, 0.75 unit cells along the horizontal y-axis, and centered at 23.33 Å along the z-axis) are plotted to show the copper(II) binding site at guanine G2 (base pair G2-C11 is left of center in the map). The copper(II) is shown as a set of topological contours centered in the map along the horizontal (y) axis, and is connected by a bond to the N7 nitrogen of the guanine base. One bond is shown connecting the cation center to one of the two waters assigned for this copper(II) complex. When the N7 nitrogen and an oxygen from a phosphate of a neighboring hexamer duplex is considered, the coordination geometry of this copper(II) complex is tetrahedral, as compared to the octahedral geometry of the analogous copper complex in the $d(m^5CGUAm^5CG)$ crystal (compare to Figure 13, and Figures 18 A and B). An additional set of free waters in this general vicinity is shown in the solvent channel (defined at the interface between three adjacent hexamer duplexes).

Figure 19.

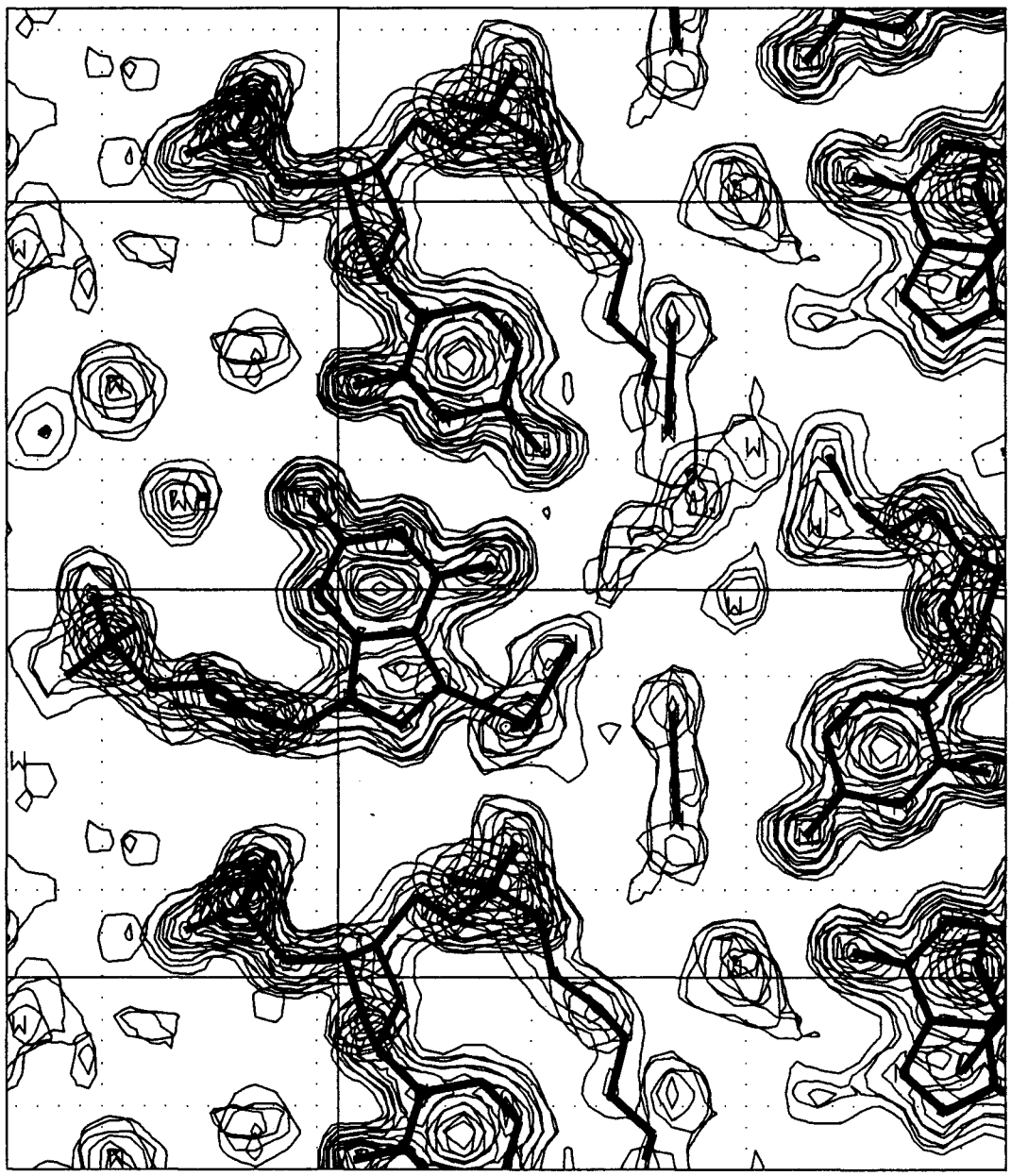

neighboring hexamer in the d(CG)$_3$ crystal would result in a bond length of 3.05 Å and, therefore, does not seem possible. The low occupancy of this site may, however, argue that the observed phosphate position is primarily for an unoccupied Cu2 site. In the occupied site, the phosphate could be twisted to accommodate either a coordinate bond to the metal center or a hydrogen bond to the ligands of Cu2.

Overall, the stabilizing effects of the electrostatic interactions and the hydrogen bonds must be greater than the loss in stability of the structure due to the distortion of the copper complex out of the G2 purine base plane (and to the possible steric hindrance between O2P and a water ligand in the d(m^{5}CGUAm^{5}CG) crystal). The specific geometry of the copper site within each crystal appears to be defined by the potential interactions between the water ligands of the complexes and the atoms of the DNA hexamers within the same strand or the adjacent strands, either directly or through water bridges. This also explains the observed differences in occupancy of the copper site in the two crystals.

4.4.3 Cu4 at guanine G4 in d(CG)3 and the potential binding site at adenine A4 in d(m5CGUAm5CG)

Only one water ligand was assigned to the copper Cu4 at the guanine G4 in the d(CG)$_3$ structure due to the relative low occupancy of the copper occupancy at this site. The bond length from the copper to the N7 nitrogen was 2.34 Å . The only water ligand observed was at the axial position with a copper to water bond length of 2.05 Å. Both an octahedral or a trigonal bipyramidal coordination geometry would be consistent with this observation (Figure 12). The partial occupancy of the copper ion at the G4 was about 10.5 % relative to the total amount of copper in the d(CG)$_3$ structure (Table 7).

The potential copper binding site at the adenine A4 in the d(m^{5}CGUAm^{5}CG) structure and also the corresponding site at guanine G4 d(CG)$_3$ is unique in its crystal packing. In both crystals this site is very open and freely accessible, due to the absence of any DNA-DNA contacts from crystal packing. In the d(m^{5}CGUAm^{5}CG) structure the water ligand W3 of the Cu8 copper complex is situated at a distance of 6.05 Å from the N7 nitrogen. The closest phosphate group is the phosphodiester linking cytosine C7 and guanine G8 of a neighboring hexamer. The distances separating the N7 of adenine A4 from the oxygen O2P and O1P are 5.64 Å and 4.90 Å. These distances would be short enough to provide potential interactions between

those groups and the water ligands if a copper complex was present at the adenine A4 site. Aside from these two possible interactions, a copper complex at the N7 of the adenine (or guanine) would be situated in an very open solvent channel that has fewest possibilities for interactions with neighboring hexamers and adjacent copper complexes than at any other site (Figure 7). This may disfavor copper binding to this site and may explain the low occupancy of the Cu4 at the G4 in the $d(CG)_3$ structure. The comparison of copper binding to this site in the two sequences, along with the arguments, in a previous section showed that copper(II) binding to Z-DNA is specific for guanine bases, barring additional mitigating interactions.

4.4.4 Cu8 bound to guanine G8

According to the ligand to copper bond length and the ligand-copper-ligand bond angles, the copper Cu8 complex in the $d(m^5CGUAm^5CG)$ structure is essentially an octahedral complex with the copper in the guanine G8 base plane (Figure 20). One of the equitorial waters, however, could not be assigned. This being the lowest occupied site within the hexamer duplex suggests that the data contributing to the position of this water is not of high enough quality to define its electron density at only 14 % occupancy. The axial water W5 is slightly distorted out-of-line from the Cu8-N7 bond as a result of a hydrogen bond formed with the O1P oxygen of the phosphodiester linking cytosine C5 and guanine G6 of an adjacent hexamer. The distance of 2.64 Å between the W1 ligand and the oxygen O2P of the phosphate group of adenine A10 of the same adjacent hexamer duplex defines a second hydrogen bond. An additional hydrogen bond between water ligand W1 and a water ligand of the Cu6 complex will be discussed in the section "Copper-copper interactions". Hydrogen bonding to the phosphate groups results in a longer than average copper to N7 bond length (2.38 Å, average: 2.17 Å) and may act to weaken this copper site. This may account for the observation that this copper site exhibits the lowest occupancy in the $d(m^5CGUAm^5CG)$ crystal.

In comparison, the copper at the guanine G8 was assigned as a trigonal bipyramidal complex in the $d(CG)_3$ structure with the N7 at one of the axial positions and three water ligands forming the equitorial plane. A additional water serves as the second axial ligand. This, however, was a highly distorted coordination geometry and may not be well defined. The relative occupancy of this site in the $d(CG)_3$ structure was similar to that in the $d(m^5CGUAm^5CG)$ structure.

Figure 20. Ball and stick model of the copper(II) complex Cu8 bound to the N7 nitrogen of guanine G8 in the copper(II)-soaked d(m^5CGUAm^5CG) crystal structure. The atoms of the copper(II)-water complex are shown as dark shaded bonded spheres. The atoms of the phosphates in the DNA backbone are shown as medium shaded bonded spheres and the remainder of the atoms in the DNA are light shaded bonded spheres. The partial octahedral coordination geometry of this copper complex is shown as defined by three of the four expected water in the equitorial plane, and the N7 nitrogen and a fourth water at the axial positions. The potential hydrogen bonds between this complex and the DNA of two adjoining hexamer duplexes are shown as broken bonds. The copper complex Cu6 is shown in close proximity to this site.

Figure 20.

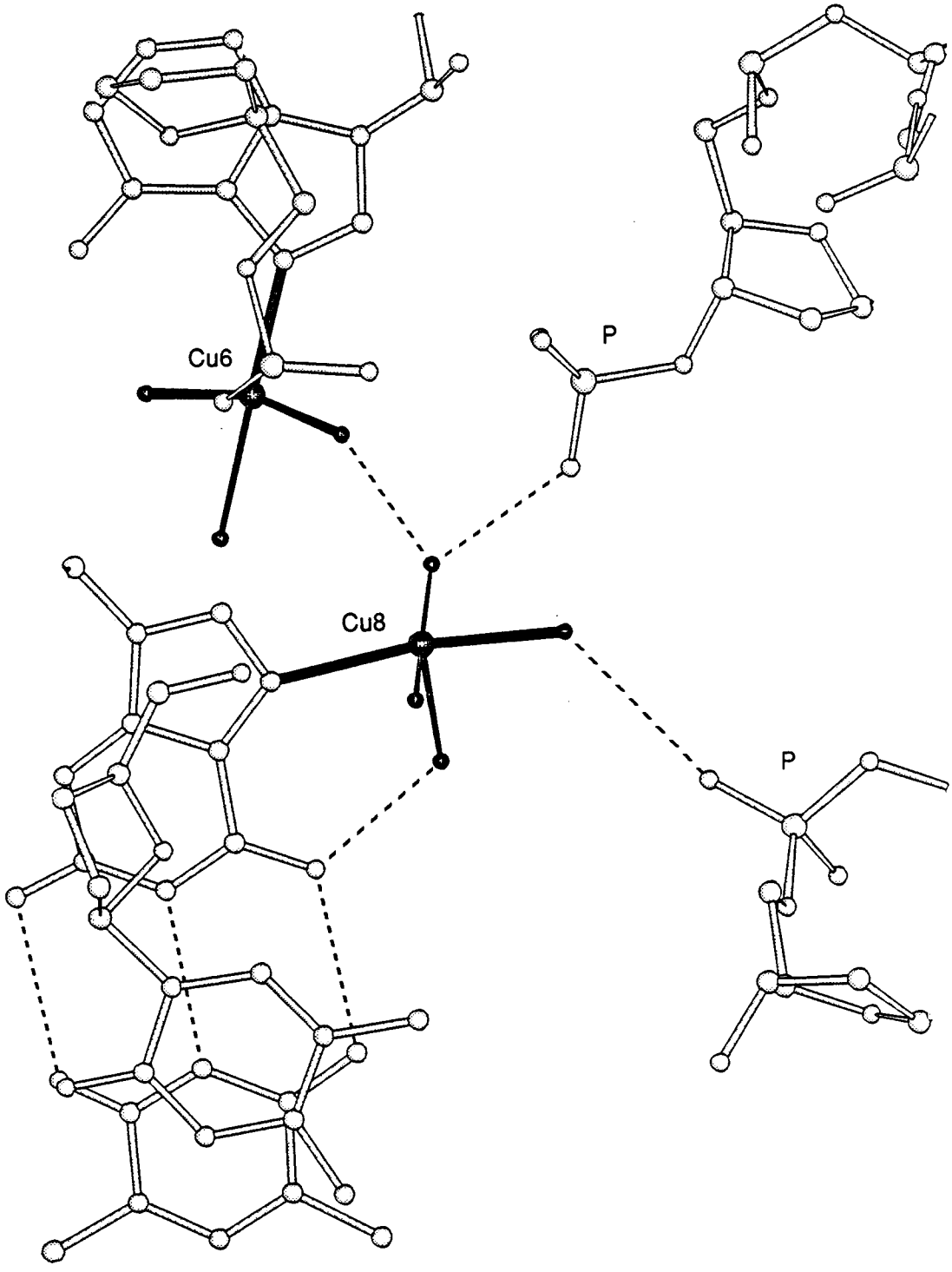

4.4.5 Cu12 at guanine G12

The Cu12 copper site is perhaps the most interesting in the d(m^5CGUAm^5CG) structure. Its geometry is clearly defined by the crystal packing. The G12 and A10 purine bases from two adjacent hexamer duplexes, along with one water molecule, define a triangular plane (Figure 21). The copper itself is in the plane of the two bases. This forms the equitorial plane of a trigonal bipyramidal coordination complex. The axial ligands appear to be two chloride ions (Cl A and Cl B) positioned 3.10 Å and 2.69 Å below and above this plane. Such a geometry is consistent with the general rule for d^n (n not equal 8) metal centers in trigonal bipyramidal geometries. The axial positions are the more electronegative chlorides and their bonds are weaker compared to the equitorial bonds. This is indicated by the length of the axial bonds, which is as long as the longest copper to chloride bonds observed in any inorganic complexes (Huheey, 1978). An alternative interpretation will be presented in a later section to suggest that Cl A may not in fact be a chloride ion, but a water molecule. The close proximity (distance between the N7 nitrogens: 3.88 Å) of two strong ligands, the N7 nitrogens of the purine bases of two neighboring hexamer duplexes, strongly favors copper binding to this site as indicated by the relative high occupancy. It is a crystal packing effect which causes the covalent binding of copper to the N7 of this particular adenine.

In the d$(CG)_3$ structure, the two purine bases G10 and G12 are not exactly coplanar, but are about 1 Å to 1.5 Å displaced along the z-axis (Figure 10). Two separate copper ions can be distinguished at the N7 nitrogens of both bases. The copper-N7 distance to G10 is 1.83 Å and 2.38 Å to guanine G12. Because of the close proximity of these fairly highly occupied sites (both 20.5 %) no particular geometry for a copper-ligand complex could be identified, although one water was assigned for each copper. The close proximity of the copper centers suggests that these are two mutually exclusive binding sites for copper(II).

In conclusion, the coordination geometries the geometries of the copper complexes in the copper-soaked d(m^5CGUAm^5CG) and d$(CG)_3$ structures appear overall very similar. Differences that are caused by local variation in the crystal packing can explain the variations in the occupancies at the guanine bases. The structural differences between d$(CG)_3$ and d(m^5CGUAm^5CG) in the Z-DNA crystal form, therefore, do not significantly effect the binding of copper. The Cu6 site can

Figure 21. Ball and stick model of the copper(II) complex Cu12 shared between the N7 nitrogen of adenine A10 and guanine G12 in the copper(II)-soaked d(m^5CGUAm^5CG) crystal structure. The atoms of the copper(II) complex are shown as dark shaded bonded spheres. The atoms in the DNA are light shaded bonded spheres. The trigonal bipyramidal coordination geometry of this copper complex is shown as defined by the two purine bases and one water molecule in a trigonal plane, and a chloride anion above the copper center (Cl B) and either a second chloride (Cl A) or a water below the copper center at the axial positions. The copper complex Cu2 is shown in close proximity to this site.

Figure 21.

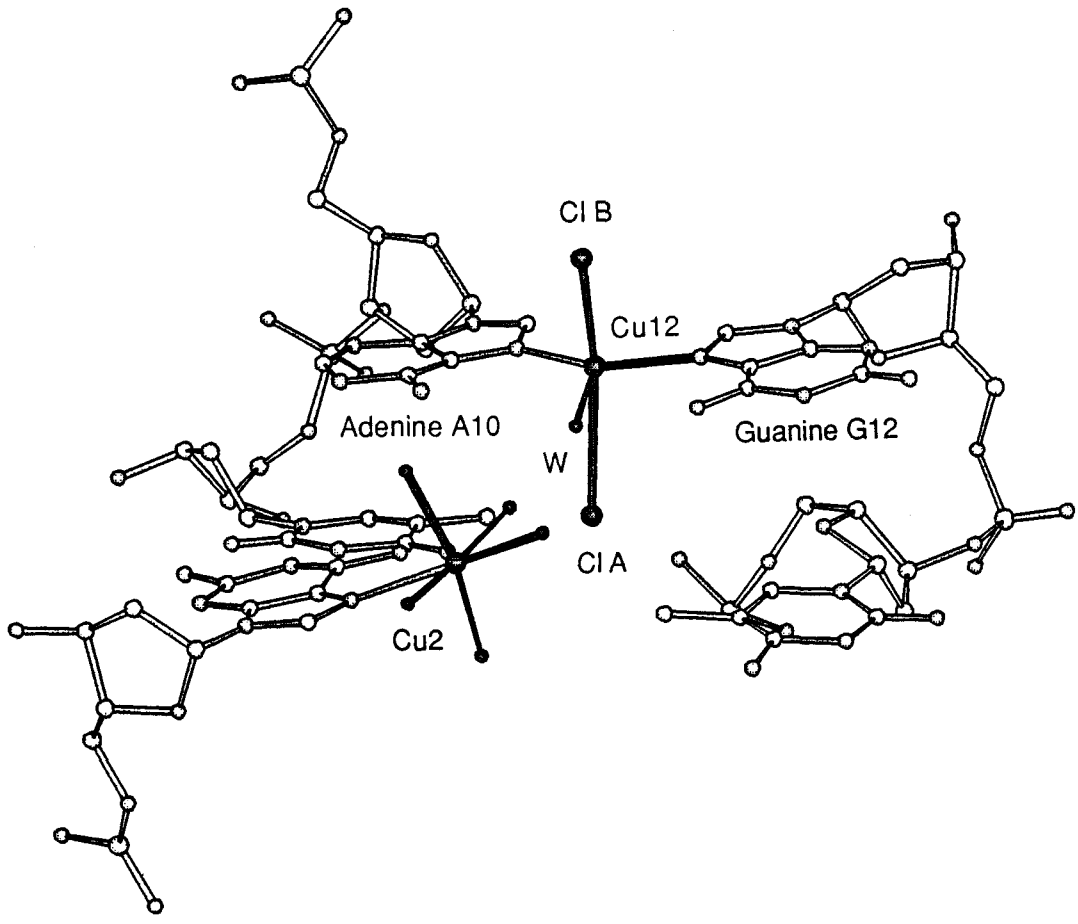

be considered to represent the prototypical copper complex at open and accessible guanine sites of DNA (Figure 14 and 17). The position is relatively free of crystal packing effects and accounts for the high occupancy within the crystal and essentially an undistorted octahedral coordination geometry of this copper complexes. The remainder of the copper complexes represent a range of complexes that are distortions of the prototypical structure resulting from copper-DNA interactions associated with crystal packing effects. In a similar fashion, there are some specific interactions between copper complexes along a hexamer duplex as well as across hexamer duplexes that either enhance or decrease the affinity of a particular binding site. No copper(II) ions were observed to bind to the N7 nitrogen of adenine A4, which sites in an open space. A well defined copper complex was observed to be shared between the purine bases of adenine A10 and guanine G12.

4.5 Copper-copper interactions in the d(m5CGUAm5CG) crystal

Crystal packing brings all four observed copper complexes in the d(m^5CGUAm^5CG) crystal in relative close proximity to each other. The interactions between the different copper sites are summarize in Figure 22 and 23. The copper complexes form a network at the interface of two neighboring hexamers (Figure 22). All four copper complexes are connected through hydrogen bonds. The distances separating each copper(II) center appear to be long enough to minimize charge repulsion between the cations (distances range from 5.38 Å to 6.88 Å at the interface between three neighboring hexamers). The negatively charged phosphate groups of the backbone of a third hexamer result in the distortion of the geometry of the copper complexes Cu2 and Cu8. The distances between the copper complexes are listed in Table 10.

The most prevalent interactions between copper complexes are between their ligands. The general result is a distortion of the geometry of the complexes from an ideal geometry, even for the well defined complex at Cu6. The equitorial W1 water of Cu8 is hydrogen bonded to W4 of Cu6 (distance 2.43 Å). This results in a slight distortion of the equitorial planes of both complexes. Although the distances between the water ligands of Cu6 and Cu2 are somewhat long, a hydrogen bond between W4 of Cu2 and water ligand W3 of Cu6 (3.05 Å distance) could be possible. Water ligand W1 of the Cu2 complex is hydrogen bonded to the water ligand of the Cu12 complex. Both copper-water bonds point towards each other and

Figure 22. Ball and stick model showing all of the assigned copper(II) complexes in the copper(II)-soaked d(m^5CGUAm^5CG) crystal structure, perpendicular to the helical axis of the crystal packing. The atoms of the copper(II)-water complex are shown as a dark shaded bonded spheres. The atoms in the DNA are light shaded bonded spheres. Shown are three hexamer duplexes, two of which are related by a translation along the crystallographic a-axis (vertical direction) and the third by the $P2_12_12_1$ packing along the b-axis (horizontal direction). The copper complexes are shown positioned at the interface between either two or three hexamer duplexes.

Figure 22.

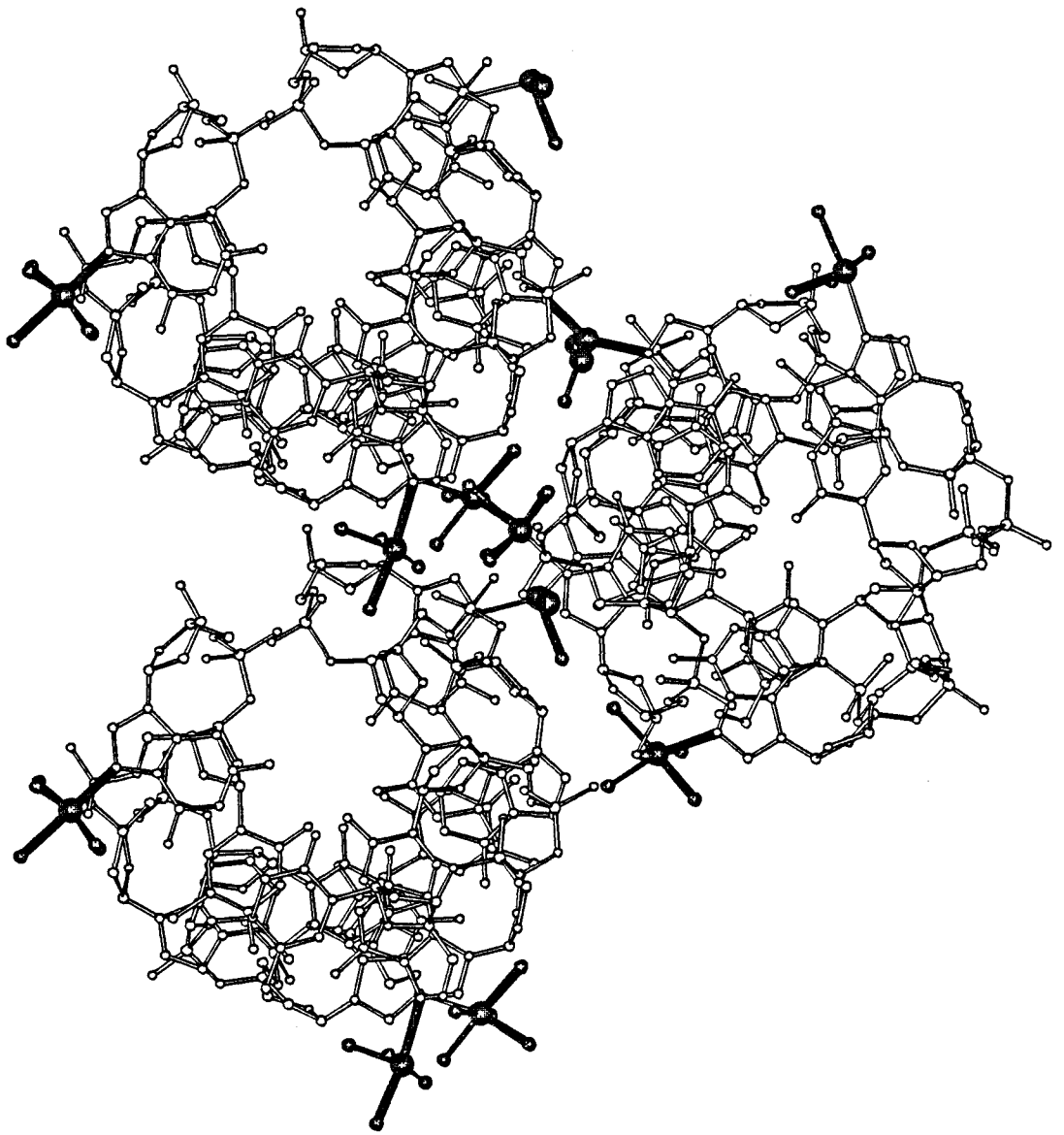

Figure 23. Ball and stick model showing all of the assigned copper(II) complexes in the copper(II)-soaked d(m^5CGUAm^5CG) crystal structure, approximately parallel to the helical axis of the crystal packing. The atoms of the copper(II)-water complex are shown as a dark shaded bonded spheres. The atoms in the DNA are light shaded bonded spheres. The four crystallographically unique copper complexes are shown positioned at the interface between two hexamer duplexes. A symmetry related Cu8 complex is shown in the far upper left hand corner. From top to bottom, the unique complexes are number Cu8, Cu6, Cu12, and Cu2. The complex Cu6 is shown to distort the position of the Cl B axial chloride ligand of complex Cu12 out of line relative to the opposing ligand below the Cu12 copper center. The hydrogen bonds connecting the copper complexes are shown as dashed lines. Possible interaction of the water ligands of Cu6 with the chloride ligand Cl B of the Cu12 complex are also indicated with dashed lines.

Figure 23.

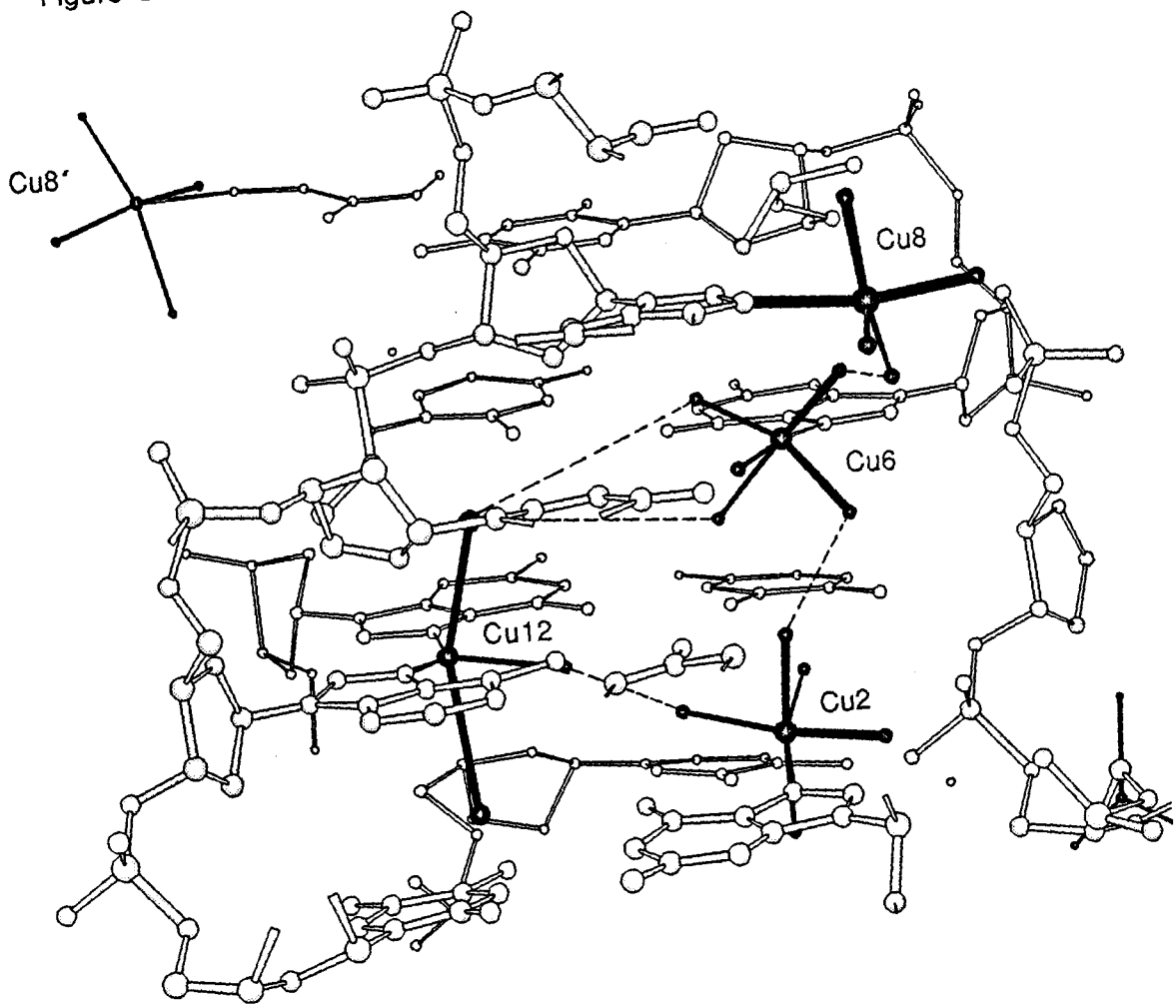

Table 10. Distances between the four different copper(II) complexes at the interface of two neighboring d(m^5CGUAm^5CG) hexamer duplexes.

Interaction between:		Distance in Å	Comments:
Cu2	Cu12	6.88	
Cu2W1	Cu12W1	2.58	Hydrogen bond
Cu2	Cu6	5.70	
Cu2W4	Cu6W3	3.05	
Cu2W5	Cu6W2	3.35	
Cu2W5	Cu6W3	3.45	
Cu6	Cu8	5.38	
CuW4	Cu8W1	2.43	Hydrogen bond
Cu6	Cu12	9.42	
Cu6	Cu12Cl B	6.26	Electrostatic attraction
Cu6W1	Cu12Cl B	4.98	Hydrogen bond through
Cu6W2	Cu12Cl B	4.84	water bridge possible.

this interaction may help to stabilize the position of the Cu2 complex above the plane of the guanine G2 base. At the other end, this interaction may be responsible for the observation, that the equitorial plane of the Cu12 complex is not identical with the plane defined by the N7 nitrogens of the purine bases and the copper center.

4.5.1 Effects of copper-copper interaction on the assignment of the ligands of the copper Cu12 complex

An interesting interaction was observed between the copper complexes Cu6 and Cu12. The geometry of Cu12 was assigned as that of a trigonal bipyramid, with the purines of G12 and A10, along with one water, forming the equitorial triangle, and two chloride ions at the axial positions. The interactions of these two coppers may account for the discrepant occupancies of the axial chloride ligands. The chloride at Cl B, which is closer to the Cu6 complex, is in a 1:1 molar ratio relative to the Cu12 center. The molar ratio of the opposing Cl A ligand to the Cu12 copper center was estimated to be only 1:2 (Table 11). How can the occupancies of two axial ligands differ so dramatically? There are two possible models to explain this observation, both of which rely on the interactions with the Cu6 complex that stabilizes the Cl B site.

In one model, the two fold difference in occupancy of the chlorides can be explained by considering individual unit cells and the presence or absence of specific ions within each unit cell. Within six individual unit cells, each cell could contain one of the combinations of ions shown in Figure 24.

According to the geometric requirements that satisfy the Jahn-Teller distortion for a trigonal bipyramid, the presence of one axial chloride ion at Cu12 requires the presence of a second axial chloride or other ligand. Therefore, assuming that all combinations are equally probable and that a trigonal planar coordination geometry as shown in Figure 24 E + F is possible for the Cu12 complex, one can count the number of coppers and chlorides and draw conclusions about the relative occupancies of each species averaged over the entire crystal (Table 11 and 12).

The ratios of the relative occupancies calculated from this model (Table 12) can, within the error of the calculations, account for the observed partial occupancies of the copper and chloride sites. There are, however, limitations of this simple model. The assumption that all combinations are equally probable is

Table 11. Ligand configuration of the copper Cu12 complex. Model for the possible occupation modes for the Cu12 complex (Figure 24). The appearance (number of atoms) of the atoms of interest in the six individual unit cells is listed and partial occupancies relative to Cu12 are calculated.

Number of atoms:		Electron counts* (contour lines * Å^3)	Occupancy relative to Cu12 in %	as molar ratio
4	Cu6	118.5	88.8	9:10
4	Cu12	133.4	100	- - -
2	Cl A	43.43	48.8	1:2
3	Cl B	101.1	114	1:1

*The electron counts (contour lines * Å^3) as a relative measure for the number of electrons was determined as previously described (section Methods). A chloride ion has 18 electrons, while Cu^{2+} has 27 electrons. If a chloride ligand is occupied to the same extent as its copper center, the ratio of electron counts (contour lines * Å^3) for Cu versus Cl should be 27/18 or 1.5. With the 133.4 contour lines * Å^3 for Cu12, a 100 % of the time occupied chloride should result in a product equal to 88.9 contour lines *Å^3. This value is, therefore, set to 100 %. Relative to Cu12, Cl A is only occupied in 50 % of the cases, while Cl B is occupied to about 100 % (considering the uncertainty of the estimation).

Figure 24. Model to explain the discrepant partial occupancies of the axial chloride ligands of the copper Cu12 complex in the copper(II)-soaked d(m^5CGUAm^5CG) crystal structure. Six panels are shown, each representing one possible combination of copper centers and ligand arrangements of the Cu12 and Cu6 copper complexes. The equitorial waters of the Cu6 complex is shown in a square plane and its axial waters above and below the plane. The equitorial purine and water ligands of the Cu 12 complex are shown in a trigonal plane and its axial ligands as Cl A below the plane and Cl B above the plane. A. All copper centers and ligands associated with copper complexes Cu12 and Cu6 are present. B. Only copper complex Cu6 and its associated ligands are present, as well as the chloride anion Cl B that is held in place by electrostatic attraction. C. Only copper complex Cu6 and its associated ligands are present. D. Only copper complex Cu12 and its associated ligands, including both chloride anions, are present. E. Only copper complex Cu12 and its associated equitorial ligands are present. The axial chloride anions are absent. F. Both the copper complexes Cu6 with its associated ligands, and Cu12 with its equitorial ligands are present. The axial chloride anions of Cu12 are absent. In the latter two panels, the coordination geometry of Cu12 is likely not trigonal planar, but may be tetrahedral.

Figure 24.

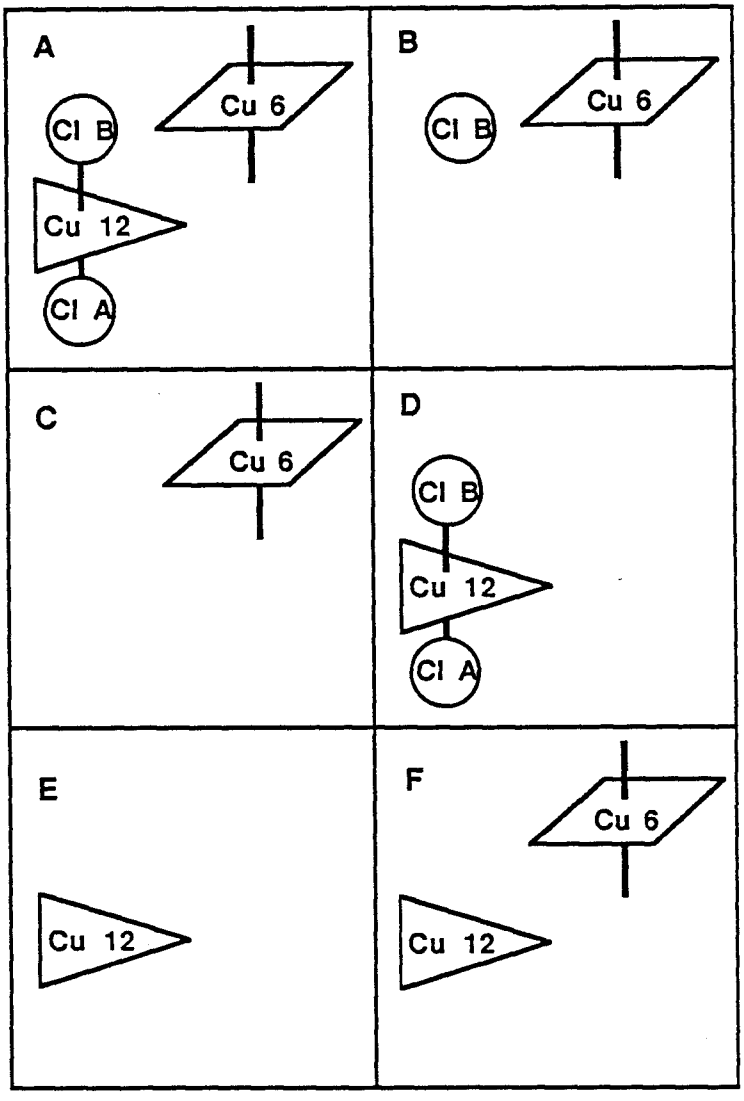

Table 12. Ligand configuration of the copper Cu12 complex. Estimation of the occupancies of two sites relative to each other from the number of appearances of the particular atom in the model for the possible occupation modes of the Cu12 complex (Figure 24).

Estimated relative occupancies from model	Observed relative occupancies
Cu12 : Cu6 = 4 : 4	133.4 : 118.5 = 10 : 9
Cl B : Cl A = 3 : 2	101.1 : 43.43 = 2 : 1
Cu12 : Cl A = 4 : 2	100 % : 48.8 % = 2 : 1
Cu12 : Cl B = 4 : 3	100 % : 114 % = 10 : 11
Cu6 : Cl B = 4 : 3	88.8 % : 114 % = 9 :12
Cu6 : Cl A = 4 : 2	88.8 % : 48.8 % = 9 : 5
Cu6-Cl A : Cu6 = 1 : 3	approximately 1 : 1

certainly not valid to the full extent. Secondly, the calculation of the electron count is particularly uncertain for the chlorides, because their electron contours have an elliptical shape and the level along z-axis with the maximum contour level laid between two available sections. The estimated volume is therefore highly uncertain. However, the large difference in occupancies for the chlorides cannot be explained by this uncertainty in the calculations. Despite these limitations, this model allows some conclusions to be drawn:

1. The Cu12 complex exists only to about 50 % of the time as $CuCl_2$ complex (Figure 24 E and F).
2. The higher occupancy of Cl B can be accounted for by the additional stability caused by Cu6 via electrostatic interactions possibly mediated through the presence of a water bridge between Cl B and the water ligands of Cu6 (Figure 24 B). This interaction may be favored by the absence of any negatively charged groups in that area. According to the observed occupancies this coordination could occur in about 50 % of the present Cu6 complexes (Figure 24 B).

The problem with this model is that copper(II) ions do not generally adopt a trigonal planar geometry (Huheey,1978). Therefore, it would be difficult to envision a unit cell in which Cu12 is present while the axial ligands are absent. One possibility would be that in the situations where the axial chlorides are absent, the copper(II) ion adopts a tetrahedral geometry by binding two water molecules, each about 50^{o} out of the plane of the purine bases. This could explain why the electron density of the equitorial water ligand is much weaker than expected, and why this electron density is not spherically symmetric but cylindrically distributed perpendicular to the equitorial plane.

An alternative model to explain the observed discrepancy in the occupancies of the chloride ligands would be one in which the axial ligands are always present when the Cu12 position is occupied. The Cl B ligand is always one of the axial ligands, because of electrostatic interactions with the Cu6 complex. The opposing ligand would, however, be occupied by either a water or a chloride ion. In this situation, there are no additional interactions to specifically define this as a chloride site. To estimate the preference of this site for a water versus a chloride ion, the number of electrons at the Cl A site was estimated from the electron density

map to be 9 relative to 27 electrons for the copper center at Cu12. The theoretical number of electrons for the oxygen of a water is 8, and that for a chloride ion is 18. By solving the equation 18 e^- * f + 8 e^- * (1-f) = 9 e^-, where f is the fractional occurrence of a chloride ion, the relative occurrence of water versus chloride ion was estimated to be 9:1. This high preference for a water molecule at this site suggests that the Cu12 complex may be a very heterogeneous complex in terms of the axial, as well as the equitorial ligands. The shortcoming of this model is that the copper to ligand distance for this site (3.10 Å) is much longer than any reported copper to water coordination bond. It can be argued, however, that the trigonal bipyramidal distortion of the axial bonds in this complex is extreme, thereby greatly weakening this bond.

A closer examination of the immediate environment surrounding the Cl A position suggests that the second model is a better description of the Cu12 copper complex. The phosphate group linking adenine A10 with cytosine C11 (on the same hexamer chain as the G12 linked to the copper Cu12 complex) has its O2P oxygen situated 2.47 Å from the Cl A ligand site (Figure 25). The environment of this ligand is already decidedly negative and would, therefore, disfavor the placement of a chloride at this position. A water situated at the Cl A position could, however, form hydrogen bonds to the phosphate group, and to a proximal (2.98 Å) nucleophilic N4 nitrogen of the cytosine C11 base that is on the same chain as the adenine A10 ligand of the copper complex (Figure 25). This strongly favors the assignment of a water at the Cl A ligand position of the Cu12 complex.

Regardless of the specific model or copper(II) coordination complex, it is clear that the interaction with Cu6 contributes to the observation of a chloride ligand at Cu12 and not at any of the other copper complexes. This is supported by the apparent distortion of this axial ligand bond in which the chloride leans towards the Cu6 complex (Figure 23). The specific interaction between the chloride ligand and Cu6 may be electrostatic or by hydrogen bonding through a bridging water, or both. The evidence for a bridging water that can form hydrogen bonds with both the chloride ion, and the two equitorial water ligands of Cu6 was found in the distance separating these ligands and in the weak electron density observed between the water ligands and the chloride ion. The distance separating the chloride of Cu12 from W1 and W2 of Cu6 are 4.98 Å and 4.84 Å, respectively. A single water molecule that is within hydrogen bonding distance (2.9 Å) to the chloride and either

Figure 25. Ball and stick model showing the interactions of the phosphodiester linking adenine A10 and cytosine C11 and the ligands of the copper(II) complexes Cu12 and Cu2 in the copper(II)-soaked d(m^5CGUAm^5CG) crystal structure. The copper(II) complexes at the interface of three adjacent hexamer duplexes are shown are shown as dark shaded unbonded spheres, while the atoms of the DNA are shown as light bonded spheres. The interacting phosphate group is shown in medium shaded bonded spheres. On the left, Cu12 is shown in its trigonal bipyramidal coordination geometry with the N7 of adenine A10 of one hexamer duplex (top) and the N7 of guanine G12 (bottom). The water ligands are labeled 'W', the chloride ligand are labeled 'Cl B' and 'Cl A'. Dashed lines connect the Cl A ligand of the Cu12 complex with the O2P oxygen (distance: 2.47 Å) and to the N4 nitrogen of the cytosine C11 (distance: 2.98 Å) of the top hexamer. Dashed lines connect the phosphate oxygens with those water ligands of Cu2 of a third hexamer (lower right corner) that are within hydrogen bonding distances (Distances are 1.86 Å to 2.9 Å).

Figure 25.

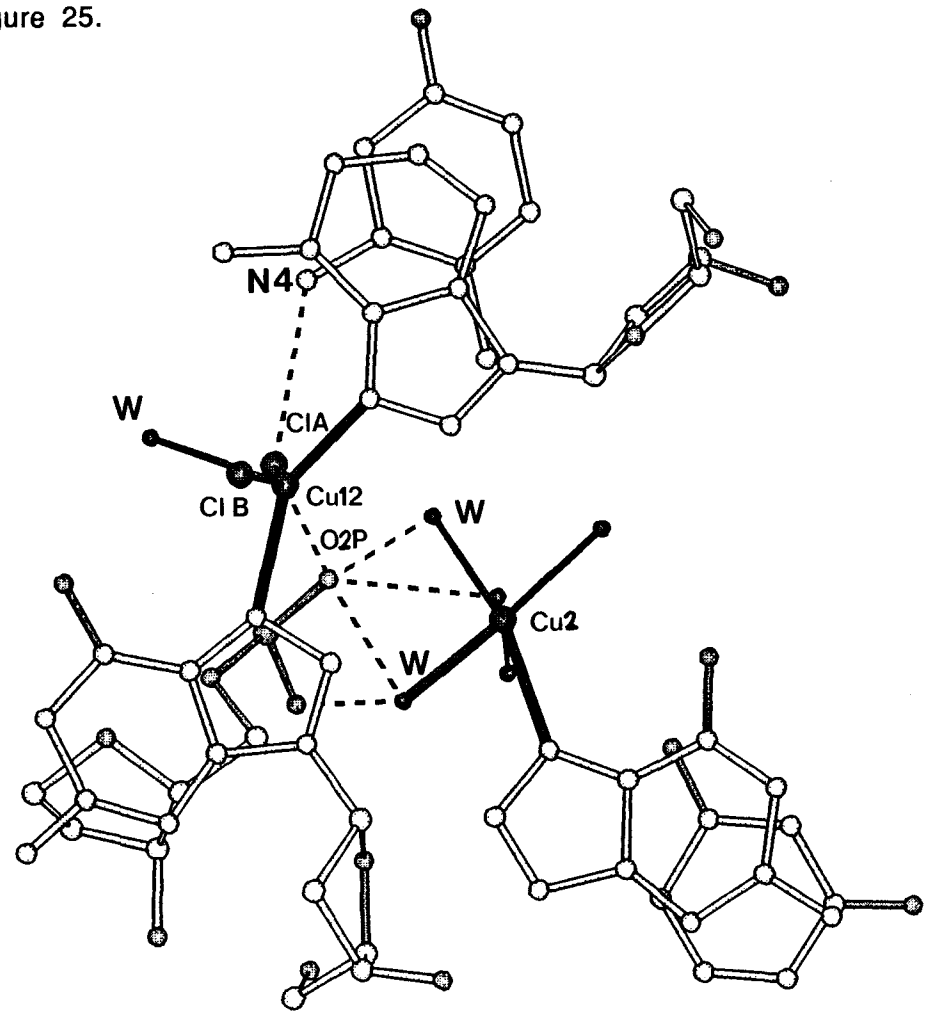

water ligand would form a 119^{o} angle. Geometrically, therefore, a bridging water could hydrogen bond with either water ligand, or both if this is a bifurcated hydrogen bond. To support this argument, a set of weak electron densities was observed at the position intermediate between these ligands.

In conclusion, the copper-copper interactions in this structure are solely the result of crystal packing. As shown in the above discussion, the interactions between neighboring coppers on the same as well as on adjacent hexamer duplexes affect the geometry of the copper-ligand complexes. Crystal packing was also shown to greatly affect the geometry of the copper complexes directly. Negatively charged phosphate groups of neighboring hexamers lead to distortion of the coordination geometry and affected the affinity of the Cu2 site for copper binding. On the other hand crystal packing can enhance the stability of copper complexes through hydrogen bonds of the water ligands to other hexamers, as it was the case for the same Cu2 complex, or by bringing two strong N7 purine ligands in a more favorable position for copper complex formation (Cu12). Crystal packing was clearly the reason for the observation of the shared G12/A10 site in the d(m^5CGUAm^5CG) crystal, while two distinct copper sites were detected in the $d(CG)_3$ structure in which the analogous purine bases were not as well aligned.

The most important conclusion, however, was that copper(II) does not bind to freely accessible N7 nitrogens of adenine bases in Z-DNA. Although the effect of crystal packing on the binding of copper to Z-DNA was described, the question of how copper binding affects the DNA structure remains open and will be discussed in the next section.

5. Effects of copper binding on DNA structure

The DNA structure of the copper-soaked and the native d(m^5CGUAm^5CG) structure were shown in a previous section to be very similar. The discussion of the overall DNA structure (see section 3.3, Figure 6), however, revealed several minor differences between the two structures. It is therefore of interest to discuss the effects of copper binding on the DNA structure in more detail. An analysis of the effects on the water structure in the minor groove crevice was of particular interest because of its significance for the stability of Z-DNA.

5.1 Effects of copper binding on base pairing

Copper ions were found to bind covalently to the N7 position of purine bases, particularly those of guanine nucleotides. The positive copper ions are expected to withdraw partial charges from the π-electron system of the bases. It is therefore likely that the ability to form hydrogen bonds will be somewhat altered. The bond lengths of the base pairing hydrogen bonds are compared in Table 13 for the copper-soaked and the native structure. No general conclusions about the redistribution of partial charges on the bases, however, could be drawn from the comparisons at this time. Most of the distortions to these hydrogen bond lengths appear to be associated with changes in the propeller twist of the base pairs, and will be discussed in this context.

The data in Table 14 compares the propeller twist angles of the base pairs in the copper-soaked and in the native d(m^5CGUAm^5CG) structures. While copper binding does not affect the propeller twist angles of the base pairs C5-G8 and G6-C7, it has a large effect on the base pairing of the C1-G12 and U3-A10 base pairs. The Cu12 complex that bridges the N7 nitrogens of the G12 and the A10 fixes the relative geometries of these purine bases. This may account for the large change in the propeller twist in both base pairs.

The copper Cu2 complex at the G2 is pulled out of the base plane by attractive forces of the phosphate group from a neighboring hexamer. Copper binding to the guanine G2, therefore, appears to significantly alter the propeller twist of the base pair. The central bond and the bond at the minor groove are shorter in the copper-soaked structure, while the O6-N4 distance is significantly longer. The propeller twist of this base pair may also be affected by an additional hydrogen bond from the O6 oxygen of guanine G2 to the water ligand W1 of the Cu2 copper complex (distance 2.92 Å).

The hydrogen bonds for the A4-U9 base pair are longer in the major groove and slightly shorter in the minor groove in the copper-soaked structure. No copper binding to the adenine A4 was observed and the propeller twist of the base pair is identical in the copper-soaked and native structure. Because copper does not bind to the adenine A4, copper binding can only indirectly effect the base pairing. The role of copper binding on the presence of a magnesium-water complex at the major groove surface of this base pair and its significance will be discussed later.

Table 13. Comparision of the base pair hydrogen bond lengths in the copper(II)-soaked and the native d(m^5CGUAm^5CG) Z-DNA structure.

Base pair:	Hydrogen bond between:	Bond length in Å		
		d(m^5CGUAm^5CG) copper(II)-soaked:	d(m^5CGUAm^5CG) without copper:	Difference (Cu)-(No Cu):
C1 - G12	O2 - N2	2.74	2.92	-0.18
	N3 - N1	2.80	2.79	0.01
	N4 - O6	2.79	2.91	-0.12
G2 - C11	N2 - O2	2.88	2.95	-0.07
	N1 - N3	2.84	2.95	-0.11
	O6 - N4	3.02	2.67	0.35
U3 - A10	N3 - N1	2.79	2.83	-0.04
	O4 - N6	2.92	2.98	-0.06
A4 - U9	N1 - N3	2.91	2.94	-0.03
	N6 - O4	3.03	2.87	0.16
C5 - G8	O2 - N2	2.92	2.84	0.08
	N3 - N1	2.82	2.84	-0.02
	N4 - O6	2.91	2.89	0.02
G6 - C7	N2 - O2	2.92	2.72	0.20
	N1 - N3	2.96	2.85	0.11
	O6 - N4	3.02	2.94	0.08

Table 14. Comparision of the propeller twist of the base pairs in the copper(II)-soaked and the native d(m^5CGUAm^5CG) Z-DNA structure.

Propeller twists were calculated from the torsion angles between ring atoms of the two bases along the line defined by the C6 of the pyrimidine base and the C8 of the purine base or the nearly identical C6/C5 line. The angle is defined relative to the pyrimidine base. A positive angle indicates a counter clockwise rotation around the intersecting line of the two base planes, bringing the plane of the pyrimidine base into the plane of the purine base.

Base pair:	Propeller twist angle in degrees (± SD)		
	d(m^5CGUAm^5CG), copper(II)-soaked:	d(m^5CGUAm^5CG) native (no copper):	Difference (Cu)-(No Cu):
C1 - G12	5.6 ± 4.7	-1.2 ± 5.7	6.8
G2 - C11	-10.4 ± 7.2	-6.0 ± 2.9	-4.4
U3- A10	-0.7 ± 3.7	8.1 ± 4.3	-8.8
A4 - U9	2.1 ± 3.1	2.4 ± 2.3	-0.3
C5 - G8	0.8 ± 4.7	0.5 ± 3.2	0.3
G6 - C7	3.1 ± 5.1	2.4 ± 5.1	0.7

In the C5-G8 base pair of the copper-soaked structure the bond length is longer in the minor groove but of similar values for the two other bonds. The hydrogen bonds in the G6-C7 base pair in the copper-soaked structure are generally longer by 0.1 Å. The propeller twist angles of the both base pairs did not change as a result of copper binding.

The effect of the copper binding on the ability to form hydrogen bonds cannot be easily discussed in a quantitative manner. Despite this, changes in the base pairing and changes in the orientation of the bases relative to each other (as indicated by the changes in propeller twist and in the bond length of the base pairing hydrogen bonds) are the result of copper binding to the DNA hexamer duplex. The effects are generally small and do not affect the overall DNA structure. The base pairs in the copper-soaked structure were still of the Watson-Crick type and no disruption of base pairing was observed.

5.2 Effects of copper binding on backbone conformation

Copper binding to the DNA in the d(m^5CGUAm^5CG) structure had overall only minor effects on the backbone conformation as previously shown (see section 3.3). There were, however, several local distortions to the backbone of the native structure observed upon copper binding (Figure 26).

As previously described, the ribose conformation of the nucleotide G12 inverts from a 3'-endo to a 2'-endo sugar pucker upon copper binding. The 2'-endo sugar pucker was also observed in the d(m^5CGTAm^5CG) structure in the absence of copper (Zhou and Ho, 1990, Wang *et al.*, 1984). The observed inversion of the sugar pucker in the d(m^5CGUAm^5CG) structure was not, however, a consequence of a direct copper to backbone interaction. This distortion appears to be a result of the large change in propeller twist induced by binding of a copper complex at the Cu12 site. This site is shared between the adenine A10 and the guanine G12 nucleotides of adjacent hexamer duplexes. The rigid coordination geometry of the copper forces the two purine bases to adopt a specific arrangement that induces large changes in the propeller twists in their base pairs. The inversion of the G12 ribose is evidently a result of the twisting of the C1-G12 base pair being translated to a distortion at the DNA backbone.

Copper binding to guanine G2 results in a significant change in the propeller twist of the G2-C11 base pair (Table 14). This is translated in a slight

Figure 26. Polar projection showing the interaction of the copper complexes with the copper-soaked (current study) and the native (Zhou and Ho, 1990) d(m^5CGUAm^5CG) structure. The polar projection is identical to that in Figure 6, except that the copper(II) complexes assigned in the d(m^5CGUAm^5CG) structure are shown as van der Waal's spheres. Both, the complexes covalently bound to the hexamer duplex and the symmetry related complexes for each copper center are shown to fill all the potential binding sites of the hexamer.

Figure 26.

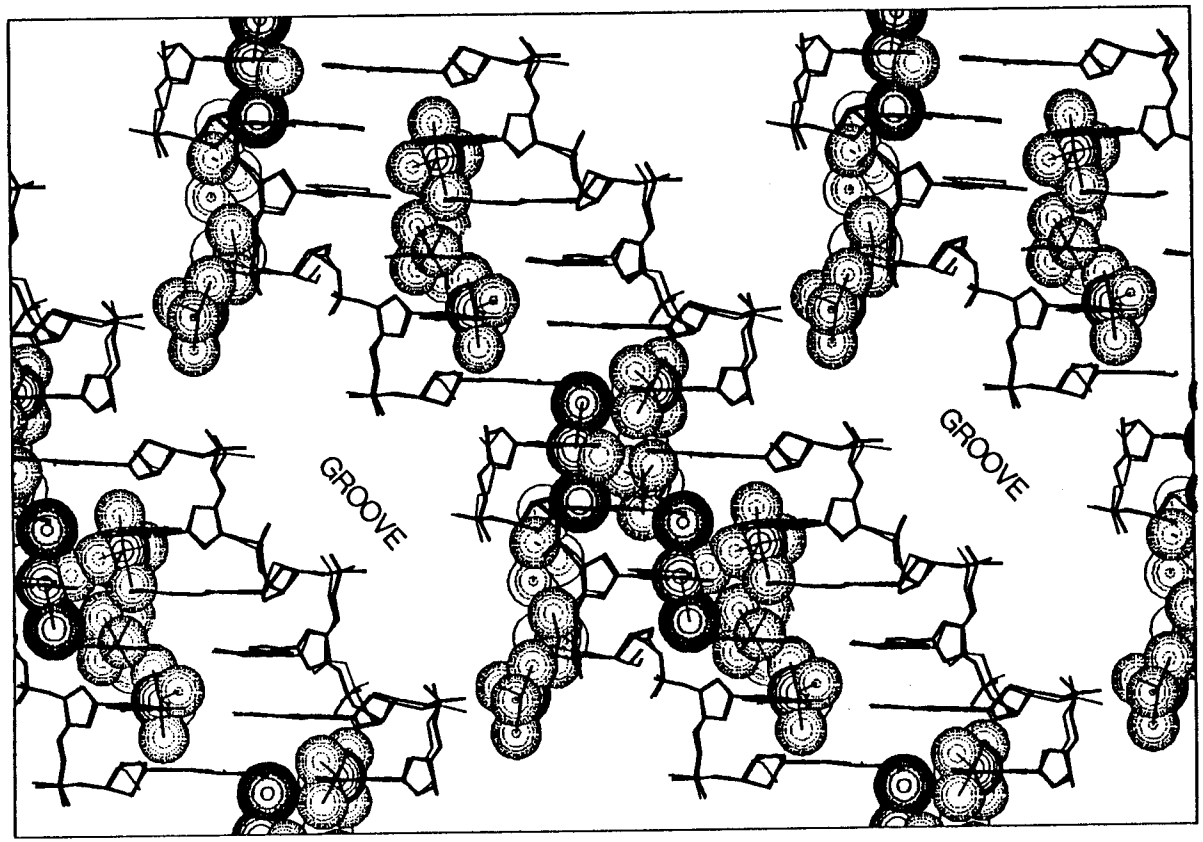

displacement of the phosphodiester linking cytosine C1 and guanine G2 and the phosphodiester linking G2 and uridine U3.

Although, the phosphate group linking cytosine C11 and adenine A10 distorted the coordination geometry of the Cu2 complex at the guanine G2 of a neighboring hexamer, this interaction had little or no effect on the position of this phosphodiester when compared with the native copper-free d(m^5CGTAm^5CG) structure (Figure 26). Strong interactions with the water ligands of a copper Cu2 complex at guanine G2 of a neighboring hexamer and ligand Cl A of the copper Cu12 complex at guanine G12 adjacent to cytosine C11 (Figure 25) appears to fix the position of this phosphodiester.

The large effects on the propeller twist of the U3-A10 base pair caused by the copper Cu12 at the shared site at G12 and A10 of an adjacent hexamer duplex appears to induce an additional change in the DNA backbone conformation. In this case, the phosphodiester linking A10 to uridine U9 along the hexamer chain was slightly displaced, resulting in a narrowing of the minor groove towards the helical center of the Z-DNA hexamer duplex. The O2P oxygen of this phosphodiester group is hydrogen bonded to the W1 water ligand of the Cu8 complex at the guanine G8 of an adjacent hexamer. This interaction may be partially responsible for the displacement of the phosphodiester bond as well.

The displacement of the phosphodiester linking uridine U3 and adenine A4 is an indirect effect of the copper complexes at Cu2, Cu12 and Cu8 along the hexamer chain, and Cu6 of an adjacent duplex. The special arrangement of these ions forms a positively charged pocket at the major groove surface of the adjacent U3-A10 and A4-U9 base pairs. This region in the native d(m^5CGUAm^5CG) structure was occupied by a hexaaquomagnesium(II) ion cluster. Two water ligands from this cluster form hydrogen bonds to each of the O4 oxygens of the stacked uridine bases. The two internal d(UA) base pairs in the native hexamer duplex, therefore, are physically linked and constrained in a specific conformation (Figure 27). The copper(II) ions in the soaked crystal displace this magnesium(II) cluster by electrostatic repulsion, thereby releasing the constraints on the two internal base pairs. The relaxation of these base pairs result in a slight rotation of the ribose sugar of uridine U3 and of adenine A4, a shifting of the phosphodiester linkage between U3 and A4 and concomitant narrowing of the minor groove crevice of the d(UA) base pairs by 0.5 Å.

Figure 27. Schematic summary of the structural differences between d(UA) and d(TA) dinucleotides in Z-DNA (Zhou and Ho, 1990). Planes represent the paired bases of U3-A10 and A4-U9 as viewed down the helical axis of the adjacent base pairs. The O4 oxygen of each uridine base is shown as stippled atoms. Dotted lines show the hydrogen bonding between the water ligands of the magnesium complex and the O4 oxygens of the uridine bases. The riboses are represented by triangles whose vertices are defined by the C1' carbon and the O3' and O5' oxygens. All points of free rotations between structurally rigid groups are indicated by a circled X, while points that are physically fixed by adjacent base pairs or metal clusters are indicated by closed circles. The straight arrow indicates the direction of the base shearing, while the curved arrows show the direction of rotation around points of free rotation. Upon binding the magnesium complex, the base pairs shear relative to each other resulting in concerted rotations of the riboses and phosphodiester linkages. This results in an overall widening of the minor groove crevice of Z-DNA and allows the specific binding of two water molecules per base pairs in the crevice.

Figure 27.

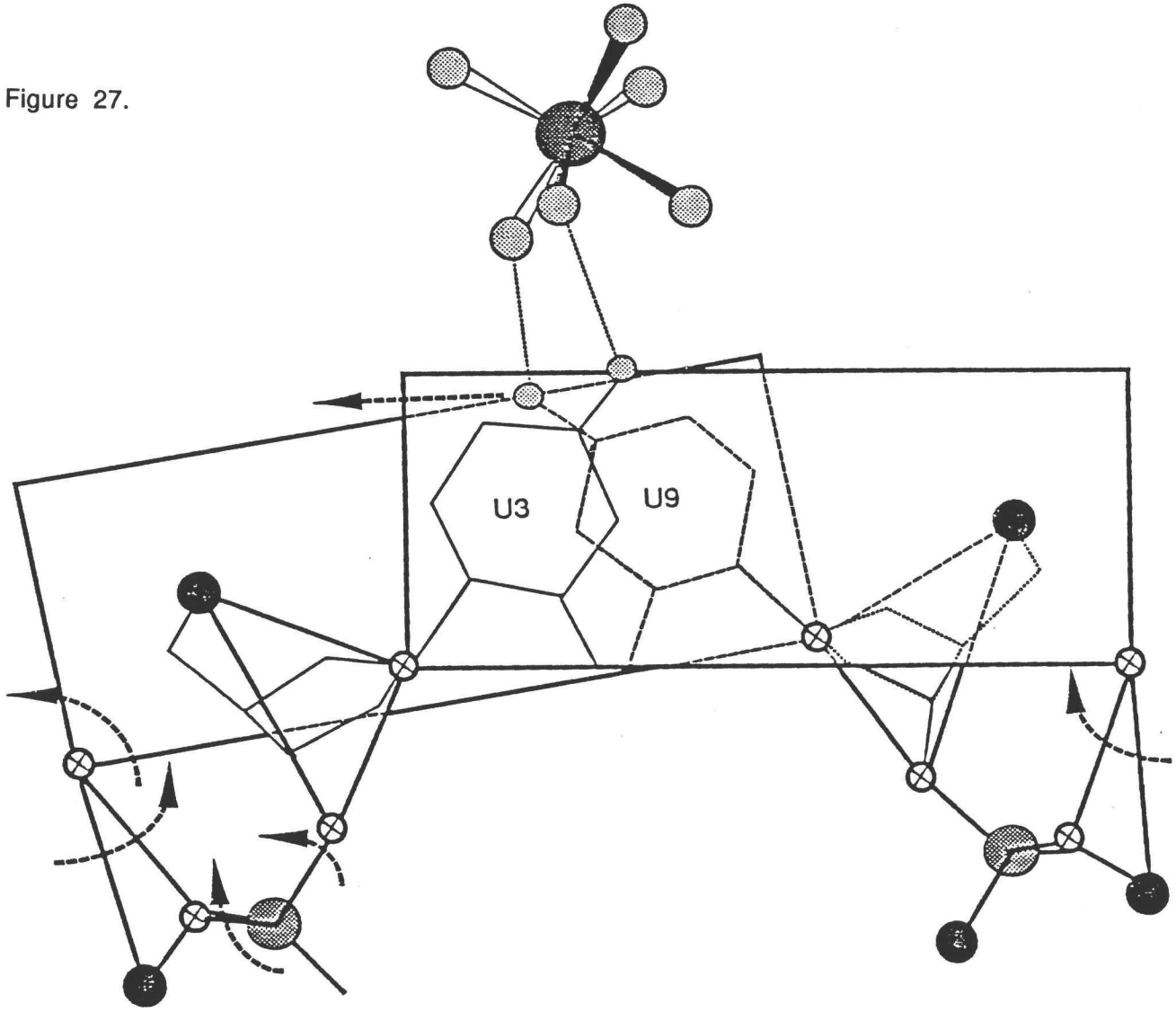

The most dramatic difference in the backbone, other than the sugar inversion, that was observed in the copper-soaked d(m^5CGUAm^5CG) structure, was at the phosphodiester linking adenine A4 to cytosine C5 along the hexamer chain. The O2P oxygen of this phosphodiester forms a hydrogen bond with the W1 (distance: 3.09 Å) of copper Cu6 on the adjacent guanine G6 residue. The long bond length of this hydrogen bond, and the regularity of the coordination geometry of Cu6 suggests that the distortion of this phosphate group is not a result of this single interaction, but may rely on electrostatic attraction between the charges as well.

The hydrogen bond between the W5 water ligand of the Cu8 complex of a neighboring hexamer duplex to the O1P of the phosphodiester linking cytosine C5 and guanine G6 causes a slight displacement and rotation of this part of the backbone, resulting in a narrower minor groove towards the end of the hexamer duplex. No interaction with copper complexes was observed with the phosphodiester linking cytosine C7 and guanine G8. The small displacement of this phosphodiester is, therefore, an indirect effect of copper binding to guanine G6 and/or G8.

Thus, the most significant change in the backbone structure upon copper(II) binding, other than the inversion of the sugar pucker, was the narrowing of the minor groove crevice mainly in the region of the internal d(UA) dinucleotides. This narrowing was a direct result of copper-DNA interactions and, indirectly, the result of displacing a magnesium complex at the major groove of the d(UA) dinucleotides in the native d(m^5CGUAm^5CG) structure. The effect of the narrowing of the minor groove crevice in the region of the d(UA) dinucleotide on the water structure and its implications on the stability of Z-DNA will be discussed in the next sections.

5.3 Effects of copper binding on water structure in the minor groove crevice

In comparing the atomic resolution structures of d(m^5CGUAm^5CG) and d(m^5CGTAm^5CG), both in the absence of copper ions, Zhou and Ho (1990) observed structural differences at the major and minor grooves of the two internal d(UA) and d(TA) base pairs. The differences in their primary DNA structures lie only in the C5-methyl of the thymine base. Removing this methyl group, to form the analogous deoxyuridine base, resulted in rearrangements in the solvent structure at the major groove surface, that were translated into rearrangements in the structure of the DNA and subsequently the waters of the minor groove. These structural

perturbations were used as a molecular model to explain why d(UA) base pairs would be more stable than d(TA) base pairs as Z-DNA. In soaking the d(m^5CGUAm^5CG) crystal with copper(II) chloride, a magnesium water cluster at the major groove surface of the two internal d(UA) base pairs was displaced through steric and electrostatic repulsion from neighboring copper complexes. This resulted in partial reversion of the rearrangements in the DNA and minor groove water structures that resulted from the original demethylation. A comparison of the water structure in the minor groove, and a discussion of the DNA rearrangements, between the copper-soaked and the native d(m^5CGUAm^5CG) crystal structures will, therefore, provide a system for testing the mechanisms proposed for the enhanced stability of Z-DNA caused by demethylation of thymine bases (Zhou and Ho, 1990). This comparison does not, however, attempt to draw conclusions concerning the direct effect of copper(II) binding on Z-DNA stability in general.

There were two structural motifs observed in the d(m^5CGUAm^5CG) Z-DNA crystal structure of Zhou and Ho (1990) that were not present in that of d(m^5CGTAm^5CG). These were not independent effects and, together showed how solvent rearrangements resulting from demethylation of thymine bases would stabilize Z-DNA. The first motif was that of a hexaaquomagnesium(II) complex at the major groove surface of the internal d(UA) dinucleotides (Figure 27 and 28). This was not present at the major groove of the d(TA) dinucleotides in the d(m^5CGTAm^5CG) structure, but was present at the same position of all Z-DNA crystal structures of hexamer sequences with internal d(CG) or d(m^5CG) dinucleotides (see Jovin *et al.*, 1987 for references). The earlier arguments for the Z-DNA stabilizing effect of this magnesium complex for the d(CG) or d(m^5CG) dinucleotide would hold for the complex in the d(UA) structure.

In the d(UA) structure two water ligands from this magnesium cluster formed hydrogen bonds with the O4 oxygens of each stacked deoxyuridine base (Figure 28). The analogous hydrogen bonds between this complex and the stacked cytosine bases were argued to stabilize Z-DNA by stabilizing the specific alternating syn-anti arrangement of the adjacent base pairs. The absence of this complex at the major groove surface of d(TA) dinucleotides in Z-DNA was attributed to steric and hydrophobic repulsion by the C5-methyl groups of the thymine bases.

The role of the magnesium cluster in stabilizing d(UA) dinucleotides as Z-DNA was not, however, limited to its direct effect on the conformation of stacked

Figure 28. Ball and stick model showing the solvent structure around the internal d(UA) dinucleotides in the native d(m^5CGUAm^5CG) crystal structure (Zhou and Ho, 1990). The paired bases of U3-A10 and A4-U9 are viewed down the helical axis of the adjacent base pairs. The magnesium centers of the magnesium(II)-water complexes are shown as a medium dark shaded bonded spheres. The water ligands are light shaded. Free water molecules are shown as unbonded light shaded spheres. Hydrogen bonds are shown as broken bonds. The atoms of the phosphates in the DNA backbone and oxygen atoms are shown as light shaded bonded spheres. The remainder atoms in the DNA are medium and dark shaded bonded spheres. A water ligand of an octahedral hexaaquomagnesium(II) complex is shown hydrogen bonded to an oxygen atom of a phosphate in the lower right corner. A second octahedral hexaaquomagnesium(II) complex binds in the major groove surface above the DNA molecule. Dashed lines show the hydrogen bonding between the water ligands of the magnesium complex and the O4 oxygens of the uridine bases. This results in an overall widening of the minor groove crevice of Z-DNA and allows the specific binding of two water molecules per base pairs in the minor groove crevice. Two of the waters are hydrogen bonded to the O2 oxygens of the uridine bases. The waters are interconnected by hydrogen bonds and are part of a continuous spine of water in the minor groove crevice, resulting in stabilization of Z-DNA. These waters were not observed in the by 1.5 Å narrower minor groove crevice in the d(m^5CGTAm^5CG) crystal (Wang *et al.*, 1984).

Figure 28.

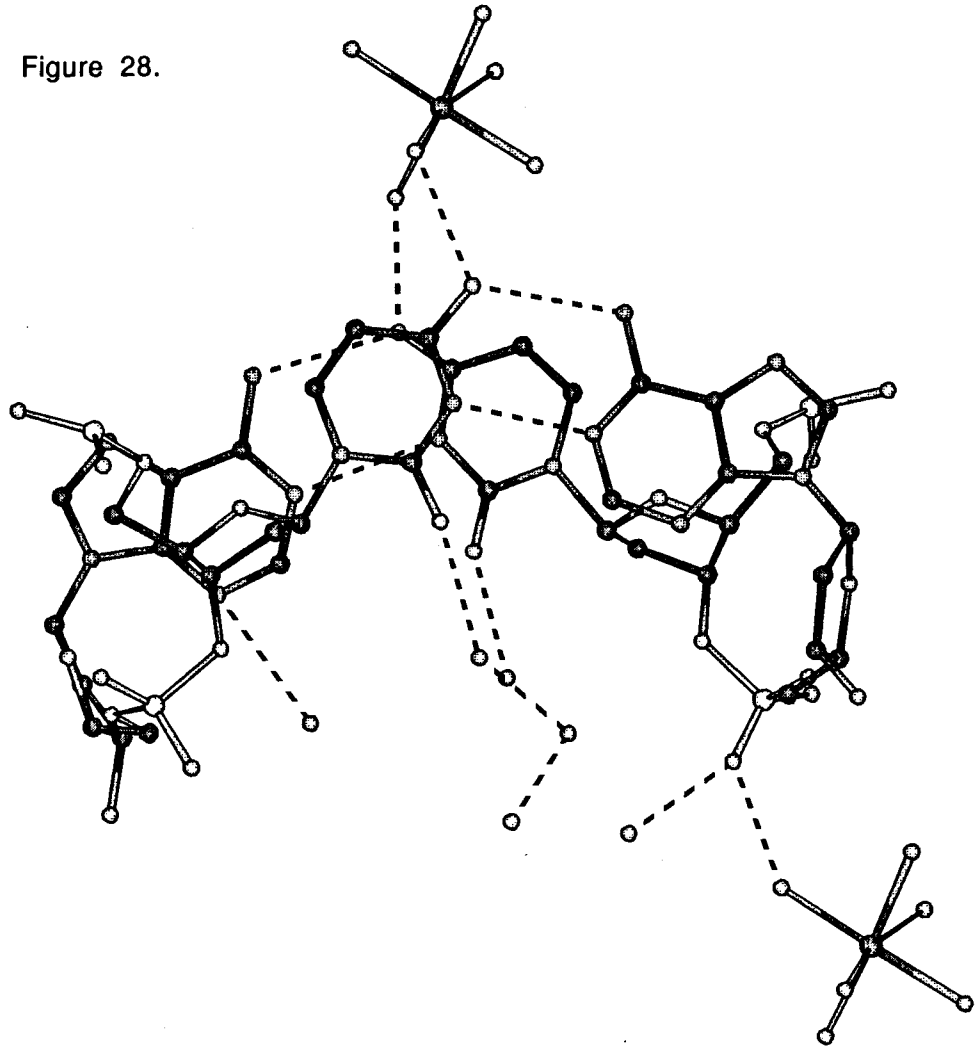

base pairs. In the binding to both uridine bases, the stacked base pairs were physically linked by the magnesium cluster. It was argued, that the rigid coordination geometry of the magnesium cluster forced the two base pairs into a conformation in which they were sheared causing a concomitant widening of the minor groove crevice (O1P to O2P: 11.13 Å in d(UA)dinucleotides) by 1.5 Å relative to the crevice of the d(TA) base pairs (O1P to O2P: 9.66 Å) in the absence of this magnesium cluster (Zhou and Ho, 1990) (Figure 27 and 29 A, Table 15). From this widening came the second structural motif that was deemed important for Z-DNA stability of d(UA) dinucleotides. By widening the minor groove, the crevice was able to accommodate additional water molecules (Figure 28), thereby extending the spine of waters in the minor groove that were initiated at both ends by the d(CG) dinucleotides (Zhou and Ho, 1990). This continuous spine of waters was observed in all Z-DNA hexamer sequences that contained internal d(CG) or d(m^5CG) dinucleotides (Gessner *et al.*, 1985). The spine of waters was interrupted, however, by d(TA) base pairs (Wang *et al.*, 1984), and was used to argue, again that the d(UA) base pairs would be more stable than the d(TA) base pairs as Z-DNA.

In this structure of the copper(II) soaked d(m^5CGUAm^5CG) Z-DNA crystal, the magnesium cluster at the major groove surface of the d(UA) dinucleotide was displaced by steric and electrostatic repulsions associated with the copper(II) complexes at adjacent base pairs (Cu2, Cu8), and copper sites on a neighboring hexamer duplex (Cu6, Cu12) (Figure 30). This provides an opportunity to analyze the actual role of the magnesium complex by comparing the DNA water structure in the absence of the bridging magnesium cluster.

As expected from the model of Zhou and Ho (1990) (Figure 27), displacing the magnesium cluster from the major groove surface resulted in an overall narrowing of the minor groove crevice (O1P to O2P: 10.68 Å) (Figure 29 B). This narrowing, however, did not result in a minor groove with the same dimensions as the d(TA) of the d(m^5CGTAm^5CG) structure. The width of the resulting crevice fell somewhere between the two values (Table 15). In addition, the details of the narrowing appear to not fall into a general trend. For example, although the phosphate-phosphate distances for this structure was intermediate between that of the native d(m^5CGUAm^5CG) and the d(m^5CGTAm^5CG) structures, the ribose-ribose and base-base distances were shorter then those in either of the noncopper containing structures (Table 15). This suggests that some additional effects may be

Figure 29. Comparison of the dimensions of the minor groove crevice at the internal d(U{T}A) dinucleotides of the native d(m^5CGUAm^5CG) (Zhou and Ho, 1990) and d(m^5CGTAm^5CG) (Wang *et al.*, 1984) with those of the present copper(II)-soaked d(m^5CGUAm^5CG) structure. A. Ortep drawing showing the base pair stacking down the helical axis of the native d(m^5CGUAm^5CG) and (m^5CGTAm^5CG) (Zhou and Ho, 1990) structures. The dimensions are labeled for the O4 to O4 oxygen, O2 to O2 oxygen, and the C3' to C3' carbon distances of the uridine nucleotides, and the O3' to O3' oxygen and O1P to O2P oxygen distances of the phosphodiesters linking the stacked base pairs. B. The analogous distances are shown for the present copper(II)-soaked d(m^5CGUAm^5CG) structure. Hydrogen bonds are indicated with dotted lines.

Figure 29 A.

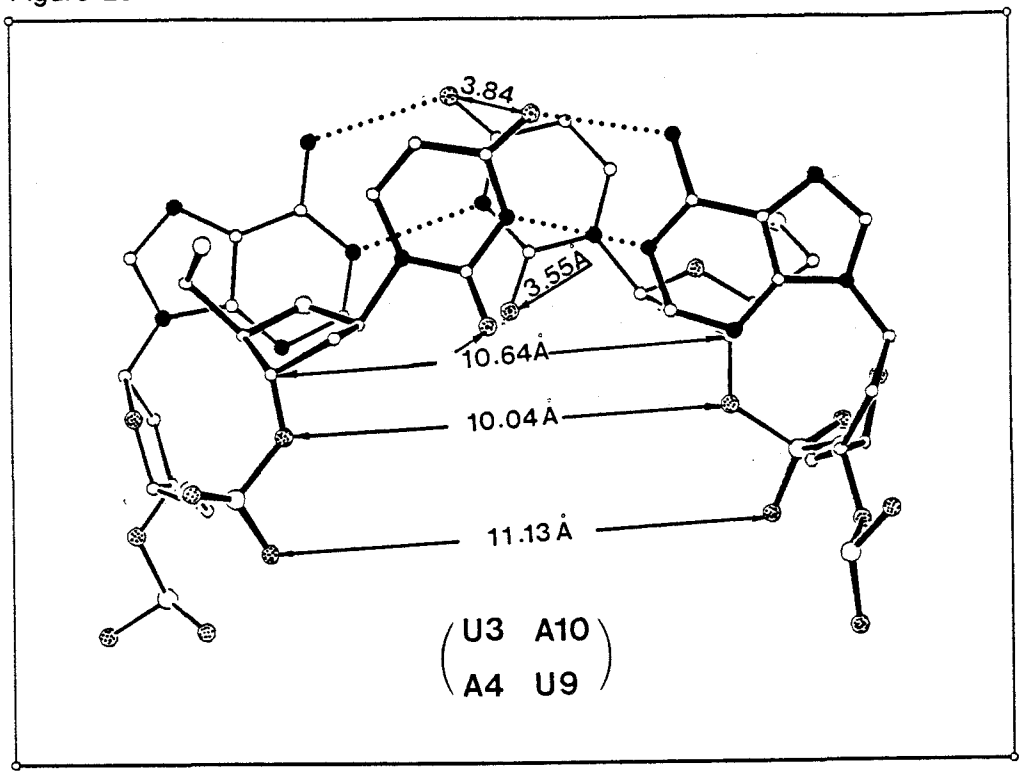
3.84
3.55Å
10.64Å
10.04Å
11.13Å
U3 A10
A4 U9

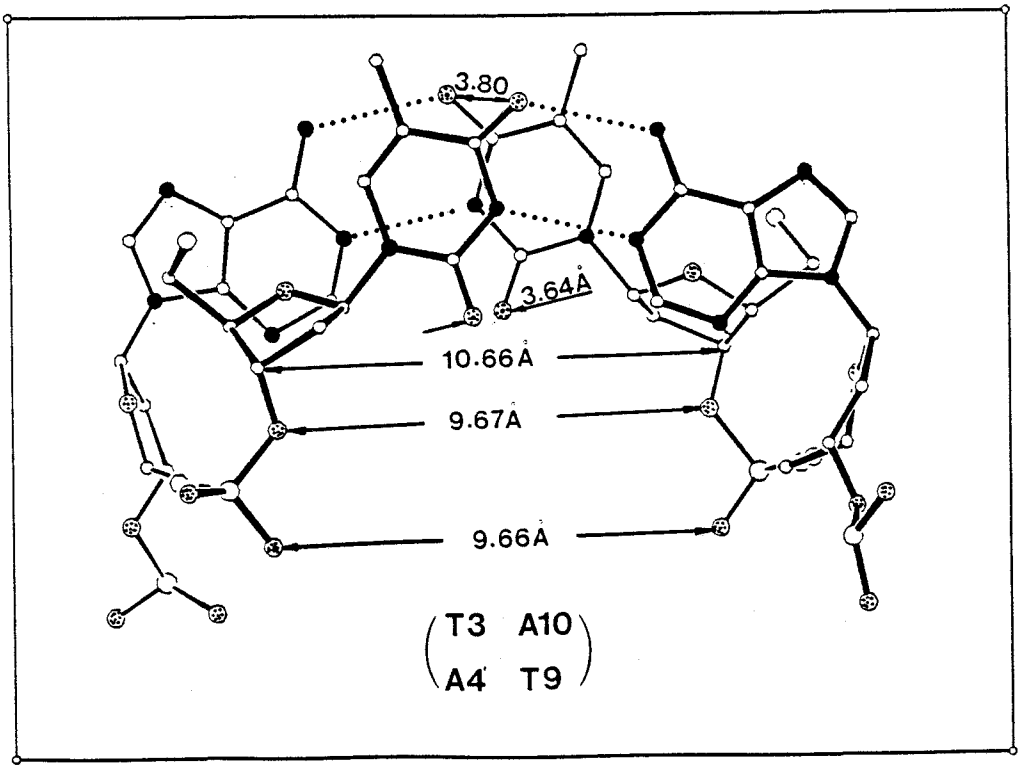
3.80
3.64Å
10.66Å
9.67Å
9.66Å
T3 A10
A4 T9

Figure 29 B.

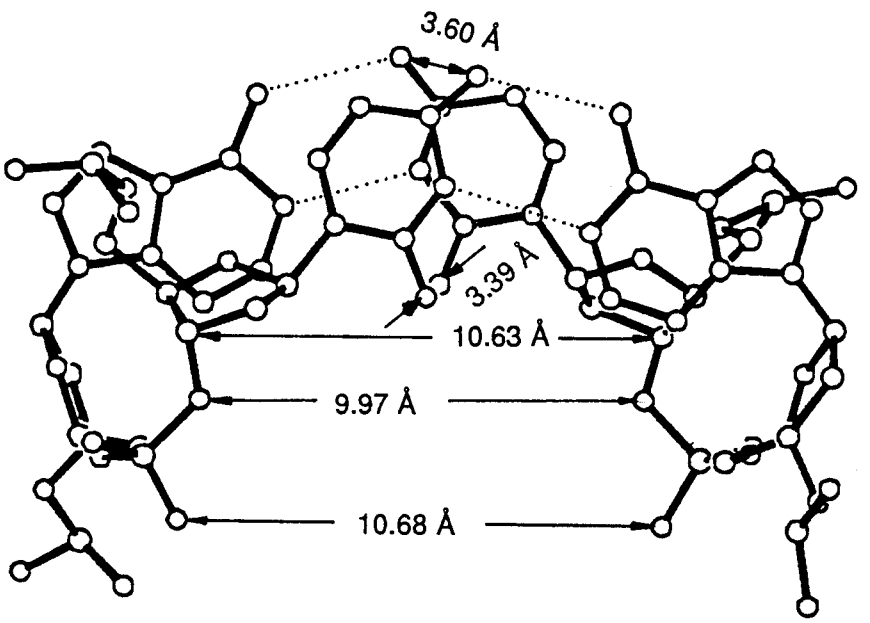

(U3 A10)
(A4 U9)

Table 15. Comparision of the width of the minor groove crevice at the d(UA) dinucleotide in the native (no copper) and copper(II)-soaked d(m^5CGUAm^5CG) structure and at the d(TA) dinucleotide in the d(m^5CGTAm^5CG) structure (no copper) (see Figure 29).

Atoms	Distances in Å		
	d(m^5CGUAm^5CG)[1]	d(m^5CGUAm^5CG) + Cu[2]	d(m^5CGUAm^5CG)[3]
O1P-O2P*	11.13	10.68	9.66
O3'-O3'	10.04	9.97	9.67
C3'-C3'	10.66	10.63	10.66
O2-O2	3.55	3.39	3.64
O4-O4	3.84	3.60	3.80

[1] Zhou and Ho, 1990

[2] Present study

[3] Wang *et al.*, 1984

* O1P to O2P distance measures the narrowest linear separation at the minor groove crevice.

Figure 30. Ball and stick model of the copper(II) complex Cu2 near the major groove surface of the internal d(UA) dinucleotide in the copper(II)-soaked d(m^5CGUAm^5CG) crystal structure. The atoms of the copper(II) complex are shown as dark shaded bonded spheres. The atoms in the DNA are light shaded bonded spheres. This figure shows the proximity of this copper complex to the major groove surface of this dinucleotide, in relationship to the magnesium complex observed at the major groove in the native d(m^5CGUAm^5CG) structure (compare to Figure 28). The copper(II) complexes Cu8, Cu12 of the same hexamer duplex and Cu6 of a neighboring hexamer duplex are also in close proximity of this major groove surface (not shown). One of the water ligands of the Cu2 complex is hydrogen bonded to the O4 oxygen ot the uridine base (dashed line).

Figure 30.

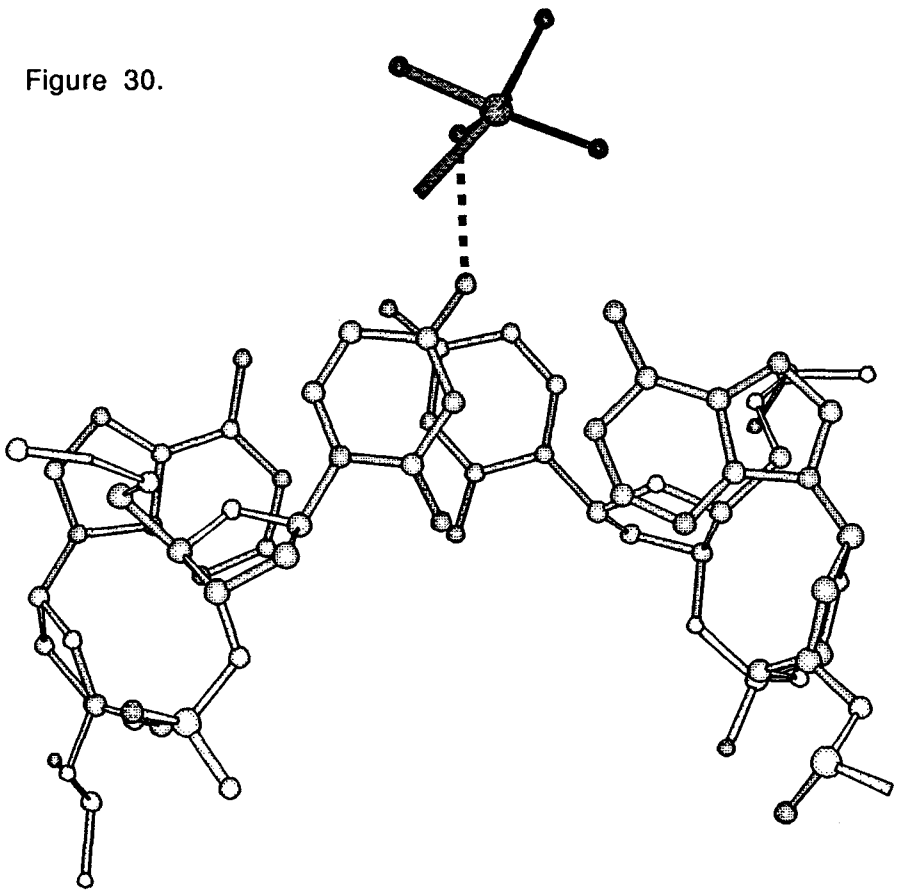

induced by the proximal copper(II) complexes, even though these do not play the same structural role as did the magnesium complex at the major groove surface.

These induced DNA rearrangements, particularly the change of the width of the minor groove crevice, have some significant effects on the second structural motif that should affect Z-DNA stability. This motif is defined by the structure of the waters in the minor groove crevice of Z-DNA. At least two water molecules have been observed in the minor groove crevice of every d(CG) base pair crystallized in Z-DNA (Gessner *et al.*, 1985). For a continuous sequence of alternating d(CG) base pairs, these waters from a continuous spine of hydrogen bonded waters along in the minor groove crevice. The only interruption of this spine has been with the introduction of d(TA) base pairs in the sequence, suggesting that the network of waters act to stabilize d(CG) base pairs as Z-DNA (Wang *et al.*, 1984). In the d(UA) containing structure, two waters were also observed in the minor groove crevice at each d(UA) base pair (Zhou and Ho, 1990). Thus, even though the differences between the d(UA) and d(TA) base pairs is only a C5-methyl group at the major groove, the spine of waters in the minor groove crevice is interrupted by the d(TA), but not by the d(UA) base pairs in Z-DNA. An explanation to account for the transmission of major groove modifications across the helix to affect the minor groove waters would be that the narrower minor groove crevice of the d(TA) base pairs in Z-DNA cannot accommodate the waters required to continue the network of waters. The presence of the magnesium cluster at the major groove of the d(UA) base pairs, however, widens the minor groove, allowing additional waters to reside in the minor grooves in Z-DNA.

In the copper-soaked d(m^5CGUAm^5CG) structure the magnesium cluster has been displaced by the neighboring copper complexes, resulting in a minor groove that is narrower than that of the native d(UA) dinucleotide (O1P to O2P: 10.68 Å versus 11.13 Å in the native structure) (Figure 29). An analysis of the waters in the minor groove crevice of this current structure, in context of the native structure and the d(m^5CGTAm^5CG) structures in Z-DNA, may help elucidate the effects of the minor groove dimensions on their water structures. It will also serve to test the model presented by Zhou and Ho (1990) in which the effect of the C5-methyl group of thymine on the minor groove structure and their waters is primarily mediated by the displacement of a magnesium water complex at the major groove surface of Z-DNA.

Figure 31. Comparison of the water structure surrounding the base pairs of the copper(II)-soaked and native (Zhou and Ho, 1990) d(m^5CGUAm^5CG) crystal structures. This figure shows six panels (A through F), each representing sections along the z-axis of the $2F_{obs}$-F_{cal} electron density maps containing each base pair in the two structures. From A to F, the panels show the electron density sections for the base pairs C1-G12, G2-C11, U3-A10, A4-U9, C5-G8, and G6-C7 along the hexamer duplex. The copper soaked structure is shown on the left and the native structure is shown on the right in each panel. Water molecules in the minor groove crevice are labeled 'W'.

Figure 31 A. C1-G12 base pair.

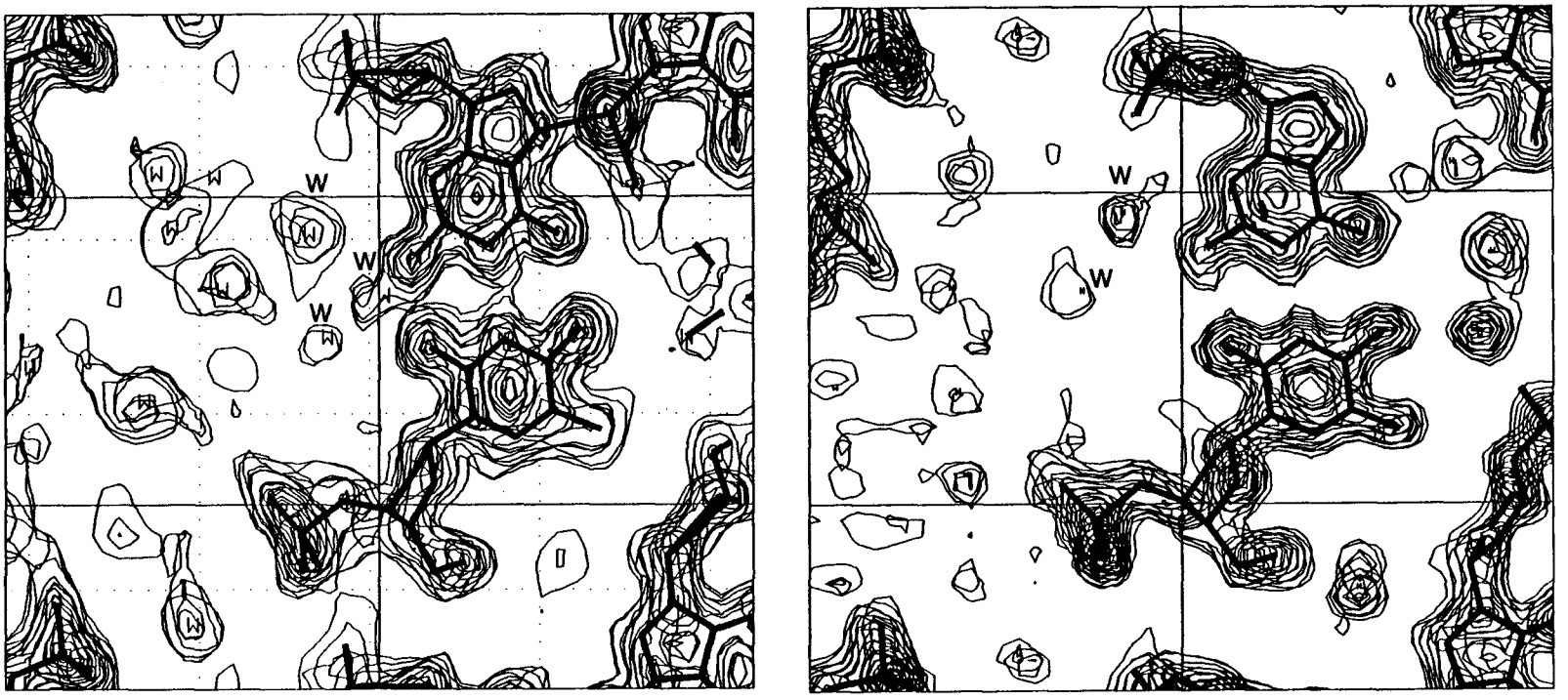

Figure 31 B. G2-C11 base pair.

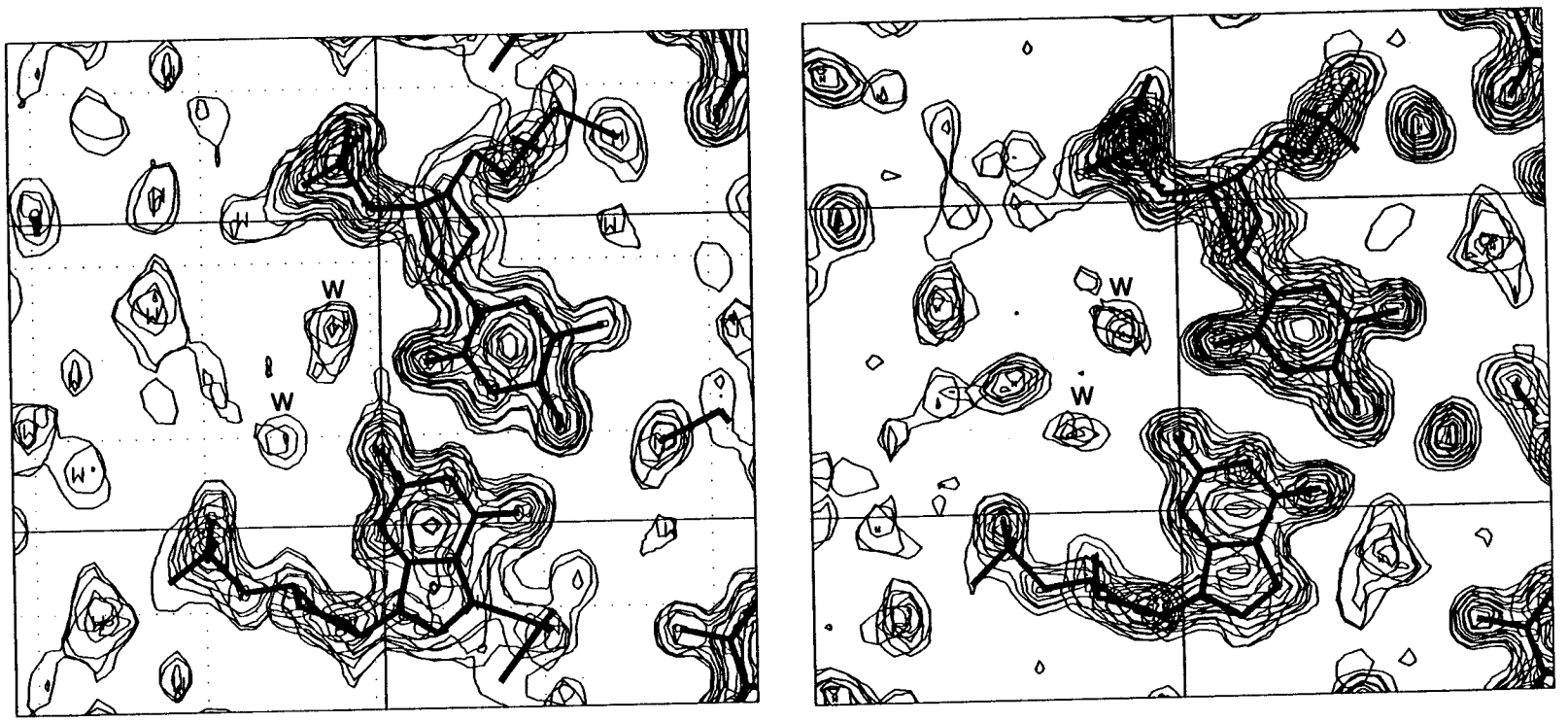

Figure 31 C. U3-A10 base pair.

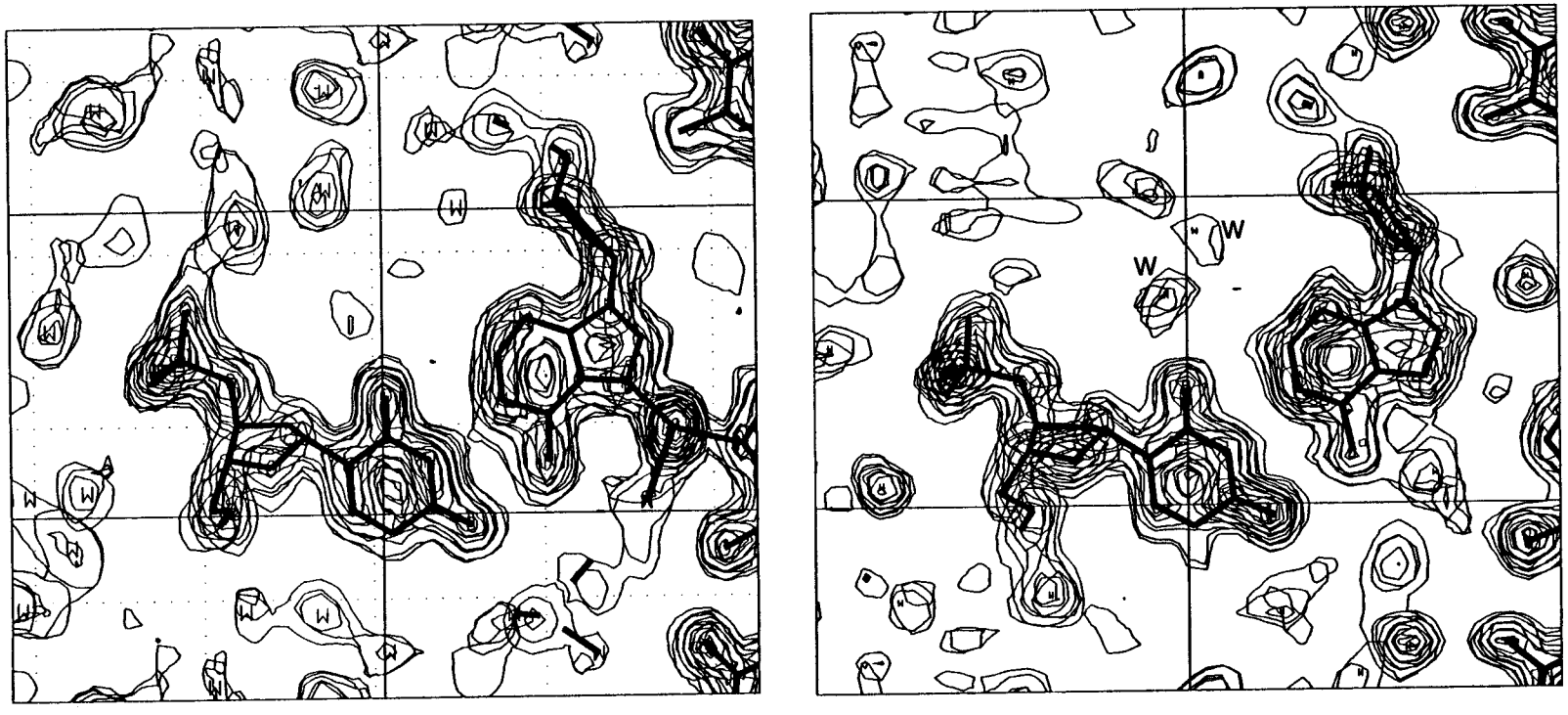

Figure 31 D. A4-U9 base pair.

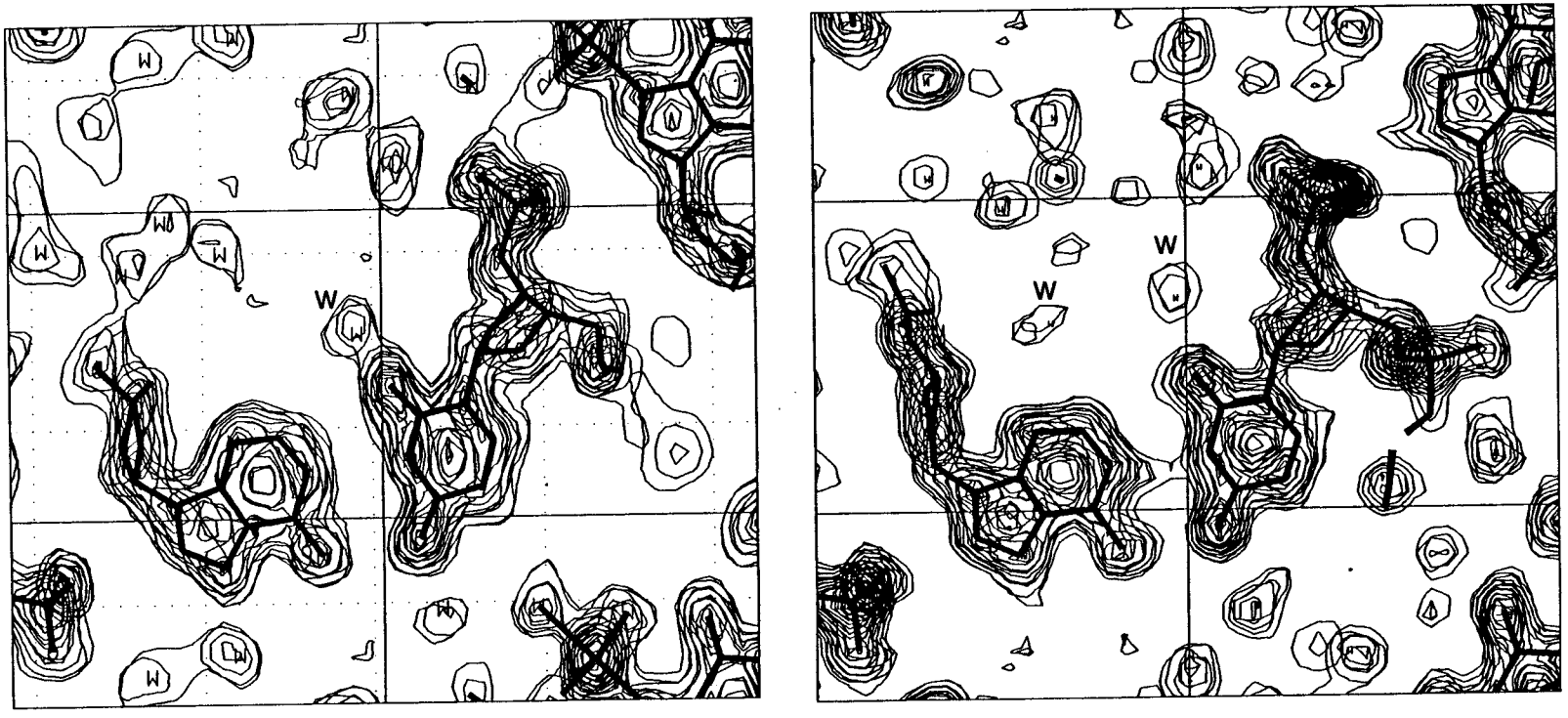

Figure 31 E. C5-G8 base pair.

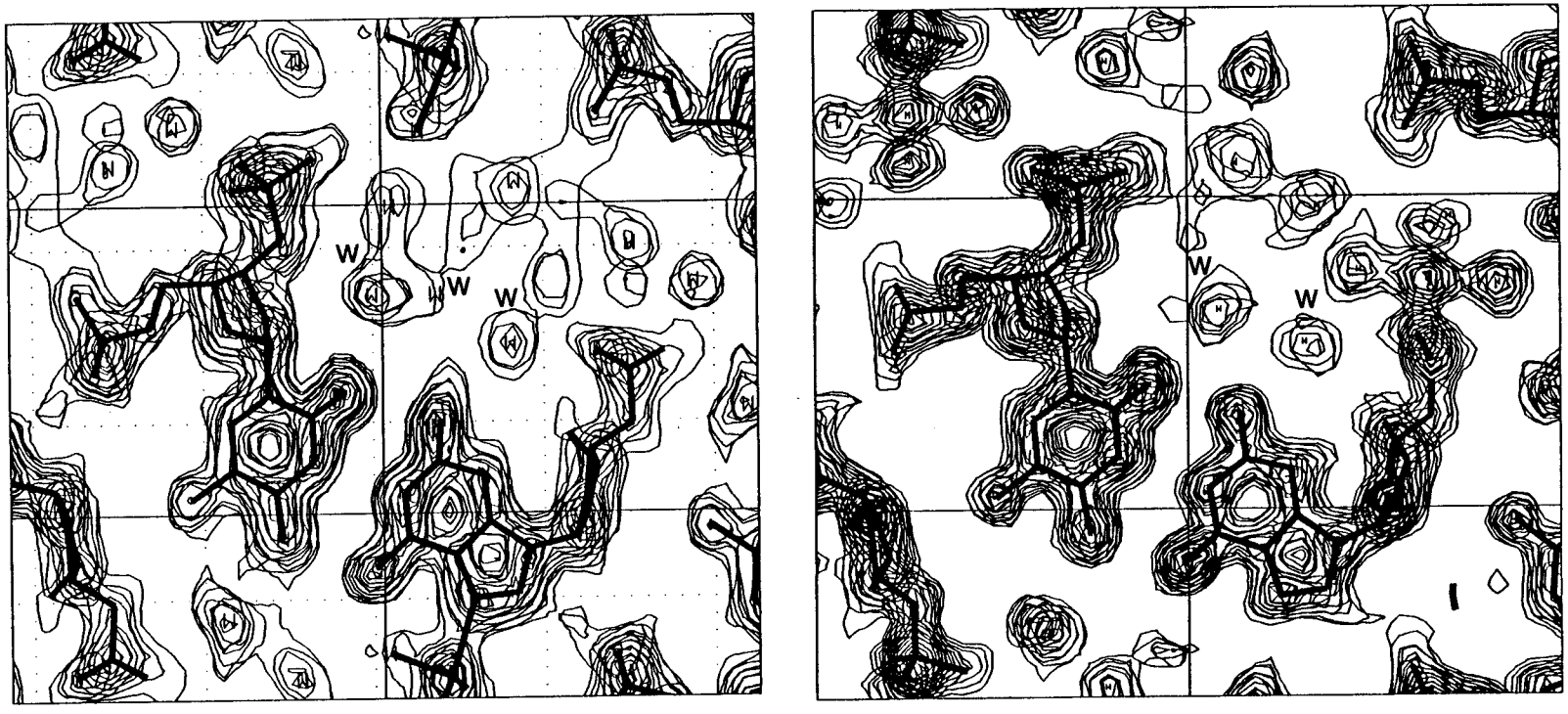

Figure 31 F. G6-C7 base pair.

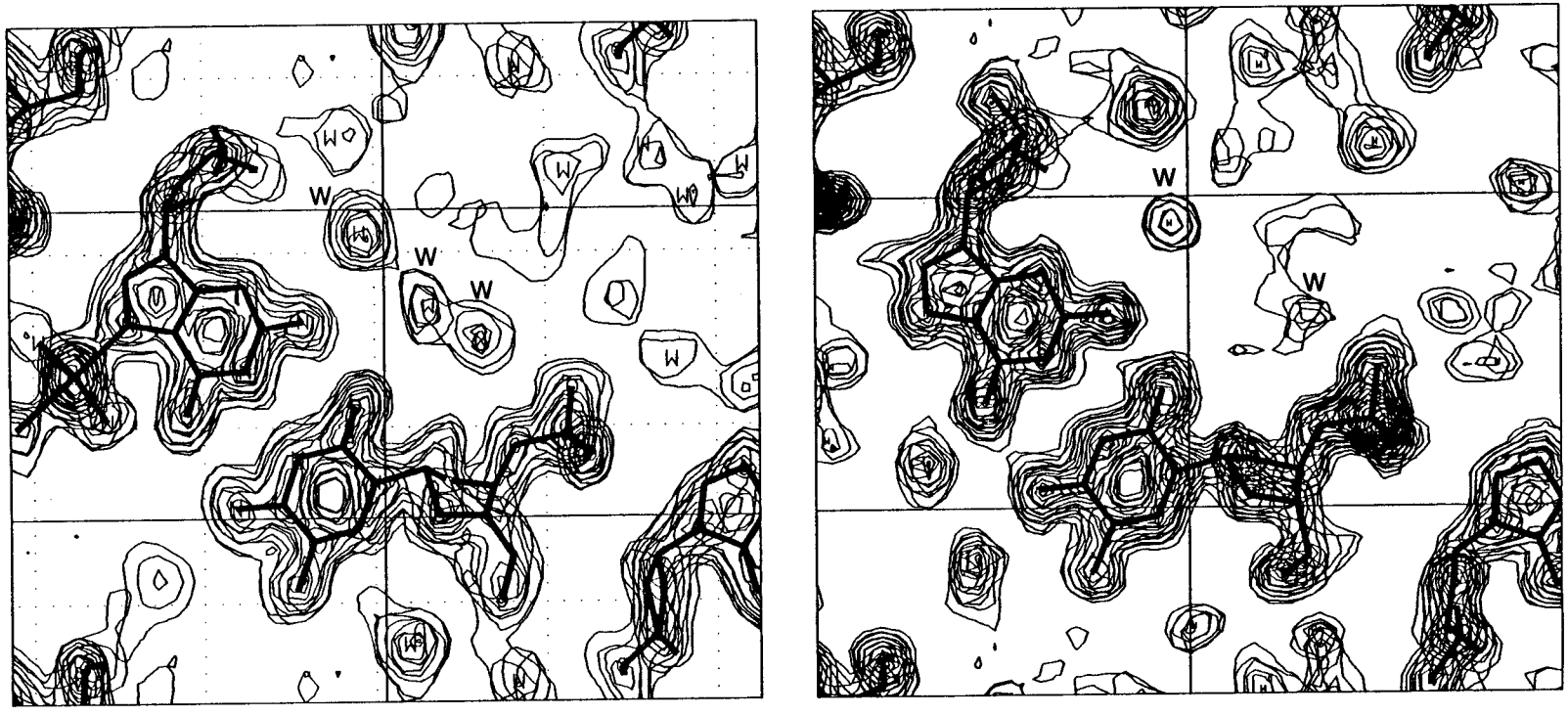

Figure 32. Ball and stick model showing the water structure in the minor groove of one hexamer duplex in the copper(II)-soaked d(m^5CGUAm^5CG) crystal structure. The assigned water molecules are shown as dark shaded unbonded spheres, while the atoms of the DNA are shown as light bonded spheres. Dashed lines connect the waters that are within hydrogen bonding distances of each other.

Figure 32.

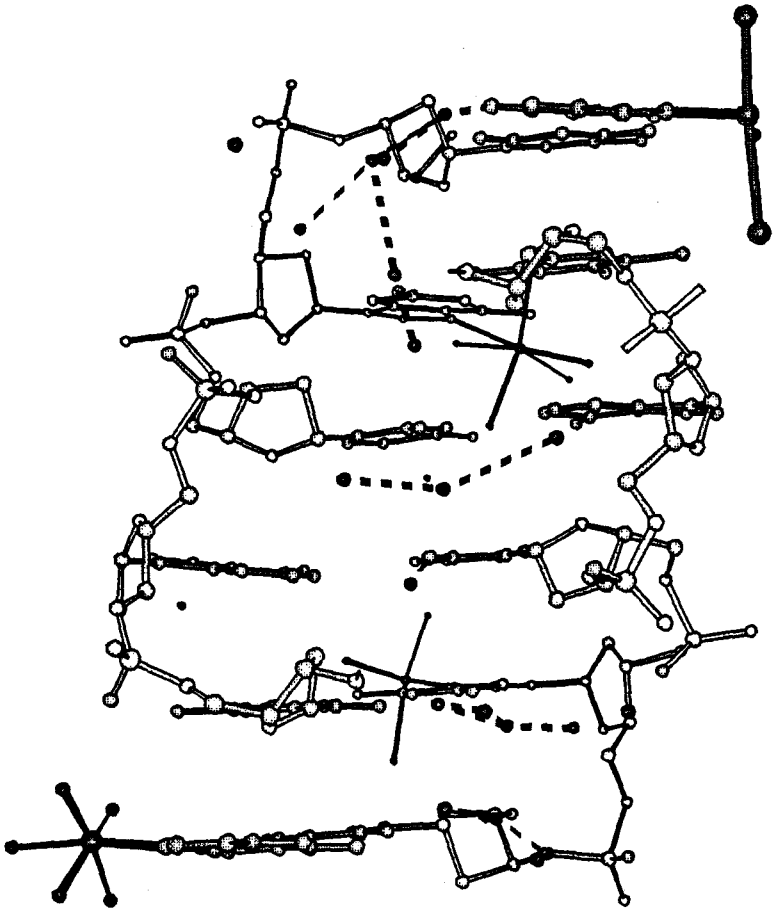

The most dramatic effects of the copper binding on the water structure in the minor groove were observed at the two internal d(UA) base pairs (Figure 31 C and 31 D). In the native structure, there were essentially two waters in the base plane of each d(UA) base pair, giving four waters total for the internal d(UA) dinucleotide (Figure 28). The total number of waters at the dinucleotide remained the same in the copper soaked crystal, but they were redistributed among the base pairs. In the current structure, one water each appeared to be essentially in the same plane of the d(UA) base pairs, but two waters were displaced along the helical axis such that they sit between the base planes. These waters remain within proper hydrogen bonding distances with each other; therefore within the cluster of UA waters, the spine stays intact (Figure 32). Relative to the remainder of the hexamer structure, however, there were some disruptions to the continuity of the water network in the minor groove crevice. The closest water from the G2-C11 base pair to this UA cluster was 4.05 Å away, while at the opposing end, the closest water from the C5-G8 base pair was 3.39 Å away. These are too long to form strong hydrogen bonds. The waters in the minor groove at the d(UA) dinucleotide appear to form an isolated cluster that is not well connected to the remainder of the waters in the minor groove crevice of the hexamer. The narrower minor groove crevice, resulting from the displacement of the magnesium cluster by copper complexes, therefore, squeezes the waters in the minor groove into different positions than in the native structure, but not to the extent of actually squeezing out any water molecules, as was observed in the case of the even narrower minor groove of the d(TA) dinucleotide in the d(m^5CGTAm^5CG) structure (Wang *et al.*, 1984). Thus, even though the number of waters in the minor groove crevice stayed constant, the continuity of the spine of waters was disrupted by the slight narrowing of the minor groove crevice. This would be predicted to destabilize Z-DNA, but not to the extent that the exclusion of waters from the minor groove would destabilize Z-DNA. Copper binding to the guanine, therefore, appears to negate some, but not all, of the Z-DNA stabilizing effects observed in the native d(m^5CGUAm^5CG) crystal.

DISCUSSION

The comparison of the structure of the copper(II) soaked d(m^5CGUAm^5CG) Z-DNA crystal with the previous copper-soaked d(CG)$_3$ structure (Kagawa *et al.*, unpublished), demonstrates that copper modification of DNA duplexes is dependent on base composition and on potential interactions with neighboring DNA molecules. The results from the d(CG)$_3$ crystal showed that all guanines of Z-DNA were susceptible to copper(II) modification, and that the coordination geometries of the specific sites were dependent on interactions with the atoms surrounding the binding site. The current results from the d(m^5CGUAm^5CG) structure were similar, except that an adenine base in a open solvent channel was found to be insensitive to copper(II) modification. However, under special, perhaps unique, circumstances when an adenine base is positioned near a guanine base from an adjacent DNA hexamer such that the two purine bases can form two legs of the equitorial plane of a trigonal bipyramid, the guanine base appears to facilitates binding to the adenine N7 nitrogen. Under no circumstances, in either crystal, were copper ions found to bind directly to the phosphate groups along the backbone.

To place these X-ray diffraction results into the physiologically relevant environment of DNA in the nuclear matrix of a cell, the significance of the binding modes in Z-DNA must be extended to other conformations, in particular the right-handed B-conformation. In addition, the DNA must be discussed in terms of the noncrystalline environment of the nuclear matrix.

Z-DNA crystals were chosen for these studies because of the high resolution of the data and structures that could be obtained from these crystals. The specific coordination geometries and, indeed, the confidence in assigning a site as a copper binding or noncopper binding site could not be accomplished without the ability to resolve the electron densities surrounding each copper center. This requires data of resolution shells beyond the 2.3 Å limit of the current B-DNA crystals (Drew and Dickerson, 1981). The 1.3 Å resolution of this current crystal and the previous d(CG)$_3$ crystal allowed definitive conclusions to be drawn concerning which bases of the DNA duplex were susceptible to copper modifications, and what the structure requirements for and ramifications resulting from this modifications were. To extrapolate these results to B-DNA, which is the conformation that the majority of the DNA is generally believed to adopt in the cell, consideration of the differences in

the accessibility and nucleophilicity at each group between the two conformations are required.

The accessibility of DNA conformations is dependent on the dimensions and shapes of the major and minor groove of the double helix. For B-DNA both the major and minor grooves are accessible to electrophiles. The wider groove is the major groove (17 Å in width). The atoms lining the major groove include the nucleophilic N7 and N6 (or O6) of the purine bases, and O4 (or N4) of the pyrimidine bases. Using an octahedrally complexed copper(II) as the prototypical copper, Kagawa *et al.* (unpublished) found that the major groove of B-DNA can bind copper complexes without significant distortion to the DNA structure. From electrostatic calculations, Pullman and Pullman (1981) determined that the major groove surface contains the most electronegative atoms of the B-DNA double helix. Interestingly the N7 position in the major groove of the guanine bases is overall the most electronegative site of the B-DNA double helix. Together these studies suggest that the major groove surface of B-DNA is most susceptible to electrophilic attack.

The major and minor grooves of Z-DNA are exaggerated in their differences as compared to that of B-DNA. The major groove is essentially a broad convex surface rather than a true groove, while the minor groove is a deep narrow crevice and is essentially inaccessible to copper complexes. The minor groove crevice in contrast, is more electronegative in Z-DNA (Pullman and Pullman, 1981) than the major groove surface. This increase is likely the result of the close proximity of the phosphate groups lining the minor groove crevice, and not a function of the partial charge distribution of the base pairing. When the effect of counter ions are included in the calculations of the electrostatic potential, the major groove surface is the most electronegative part even in the left-handed Z-DNA conformation. In any case, considering the accessibility of the sites of Z-DNA, the N7 nitrogen of guanine bases is the most electronegative and accessible site of Z-DNA, and, therefore most likely the site of electrophilic attack.

The Z-DNA crystals used in these studies can, therefore, be considered to be good models for the major groove in B-DNA in terms of steric accessibility and electrophilicity.

These studies on the d(m^{5}CGUAm^{5}CG) and the d(CG)$_3$ crystal showed that, for the prototypical guanine site, covalent copper binding occurs only at the N7 of the guanine bases, and not the phosphates or any other nucleophilic group of the Z-

DNA duplex. One of the water ligands of the copper complex, however, is hydrogen bonded to an oxygen atom of an adjacent phosphate group. The coordination geometry of the prototypical copper complex is octahedral and its coordination geometry and relative orientation to the guanine base would be considered to represent the structure of a copper-complex to Z-DNA in solution, and would hold true for B-DNA in solution. Electrostatic and accessibility calculations (Pullman and Pullman, 1981) showed that the atoms most susceptible to electrophilic attack are the N7 nitrogens of the purines, and not the phosphate groups. The electronegativity of the N7 of guanine in B-DNA is larger than that of the N7 of adenine. The adenine A4 of the d(m^5CGUAm^5CG) structure shows that the N7 of adenine bases are not susceptible to copper(II) modification for Z-DNA in solution.

Extrapolating these results to B-DNA in solution, these observations suggest that copper(II) ions would covalently modify the N7 of guanines at the major groove, but not of adenines and not at the phosphate groups. This would be consistent with the previous observations that plasmid DNAs and DNA digestion fragments are most susceptible to copper(II) facilitated hydrogen peroxide cleavage at guanine bases, and not adenines (Sagripanti and Kraemer, 1989, Yamamoto and Kawanishi, 1989). The other binding sites for copper that are affected by crystal packing in the d(m^5CGUAm^5CG) and the d$(CG)_3$ crystal represent some, but not all, of the possible DNA-DNA interactions in the nuclear matrix of cells that may affect the ability of purines to bind copper(II). The tight packing of DNA in a cell or cell nucleus suggests that DNA *in vivo* is likely not in a solution environment but more closely resembles a distorted crystal. The variations and distortions of the copper geometries observed in the d(m^5CGUAm^5CG) and the d$(CG)_3$ crystal, resulting from crystal packing effects, indicate the ability of the copper(II) complexes to adopt to given geometric constraints by DNA-DNA interactions. The Cu2 copper site showed that steric crowding decreases the accessibility of a site for copper, and that electrostatic attraction can compensate for some of the binding energy lost from pulling the ion out of the base plane of the guanine. More interestingly, the Cu12 site of the d(m^5CGUAm^5CG) structure demonstrates that proper positioning of an adenine and a guanine base from adjacent DNA strands can induce the N7 of adenine to share a copper binding site. Thus, DNA-DNA interactions that are likely found in a cell could induce susceptibility to copper modification and crosslinking between

guanines and adenines, and perhaps other bases, simply by providing a proper coordination geometry to the metal ion.

The same line of arguments can be followed for the cleavage specificity of DNA/copper/drug complexes (see Introduction, Table 1). Both guanine and adenine bases appeared to be the main targets for binding of the copper ion, which functions as a redox center to generate DNA cleaving oxygen radicals. DNA interactions with the copper/drug complexes constrain the geometry and allow the drug bound copper to attack at sites that are not susceptible on DNA in solution.

In conclusion, the answer to the question of whether adenine N7 in double helical DNA is susceptible to covalent modification by copper(II) ions is "it depends". It depends on whether the DNA is in solution or closely packed, as in a cell. It depends on specific DNA-DNA interactions. In solution, in the absence of DNA-DNA interactions, it appears that adenines are not susceptible to modification. In a cell, or in a supercoiled plasmid where the potential for the proper DNA-DNA interactions are increased, a guanine base can facilitate copper binding to a spatially adjacent adenine base. This may account for the low level of nonspecific copper facilitated oxidative cleavage of supercoiled DNA by hydrogen peroxide at bases other that guanines.

A comparison of the solvent structure in the native (Zhou and Ho, 1990) and the current d(m^5CGUAm^5CG) crystal structure provided some additional insight into the structural factors that stabilize Z-DNA, that were not originally designed into these studies. A previous comparison of the crystal structures of d(m^5CGUAm^5CG) and its methylated analogue d(m^5CGTAm^5CG) (Wang *et al.*, 1984) showed that the C5-methyl group of thymine destabilized Z-DNA by displacing a magnesium water complex at the major groove surface of the d(UA) dinucleotide (Zhou and Ho, 1990). The presence of this cation complex in the d(UA) containing sequence resulted in a wider minor groove that could accommodate two well structured waters at each of the two internal d(UA) base pairs. In the current copper soaked d(m^5CGUAm^5CG) crystal, the magnesium complex was displaced from the major groove by electrostatic and steric repulsion from copper complexes at the guanines of adjacent base pairs along the hexamer chain and across from a neighboring chain. A comparison of the current structure with the native d(m^5CGUAm^5CG) and the d(m^5CGTAm^5CG) structures, therefore, serves as a test of the model that the magnesium complex at the major groove helps to stabilize

d(UA) dinucleotides as Z-DNA not only in terms of its direct effect on the DNA base conformations, but also by affecting the solvent structure across the helix in the minor groove crevice.

Copper(II) binding to the d(m^5CGUAm^5CG) structure displaced the magnesium cluster that bridged the stacked uridines of the two adjacent d(UA) base pairs. The structural geometry of these two base pairs were thus, no longer constrained by the geometry of the magnesium water cluster. In relieving this constraint, the DNA minor groove of the d(UA) dinucleotide partially relaxed back to a narrower crevice, but still not as narrow as the observed at the d(TA) dinucleotides in Z-DNA. The narrower crevice "squeezed" the spine of water in the minor groove at the d(UA) dinucleotide enough to disrupt the continuity of the water network, but not enough to dislodge any of the waters, as was the case for the d(TA) dinucleotides (Wang *et al.*, 1984). This suggests that, indeed, the magnesium cluster at the major groove surface of the d(UA) dinucleotide of the native d(m^5CGUAm^5CG) Z-DNA structure was responsible for the width of the minor groove and the continuity of the spine of water in the groove. It does not, however, definitively answer the question of whether the effect of the magnesium on the minor groove is actually rooted in the constraints imposed by the coordination geometry of the complex or through electrostatic interactions. The copper complexes that were responsible for displacing the magnesium cluster may act to partially compensate for the loss of the cationic charge at the major groove surface, and may account for the intermediacy of the minor groove width and disruptions of the spine of water in relationship to the native d(m^5CGUAm^5CG) and the d(m^5CGTAm^5CG) Z-DNA structures. Alternatively, the direct crosslinking of the adenine A10 of one hexamer to the guanine G12 of a neighboring hexamer may impose additional geometric constraints that may not allow the d(UA) base pair to entirely relax to the d(TA) conformation.

The observation that the minor groove in the current structure is intermediate in width relative to the native d(UA) and the d(TA) dinucleotides, and the correlation of this to the degree of distortion imposed on the integrity of the spine of waters in the minor groove helps to answer a "chicken and egg" question concerning the relationship of the minor groove dimensions and the water structure in the groove. The comparison of the native d(UA) and the d(TA) dinucleotide structure demonstrated this correlation, but was not capable of deciphering which

was the cause and which was the effect. Does distortion of the DNA structure alter the structure of the spine of water, or do waters find their way into the crevice of a susceptible Z-DNA duplex and widen the minor groove in the process of forming a spine of water? The observation from this current structure that removing the structural constraints imposed by the magnesium cluster induces at least a partial relaxation in the Z-DNA structure, which in turn disrupts the continuity of the water spine, suggests that the DNA structure defines the structure of the spine of water, and not the other way around. Therefore, even though the spine of water in the minor groove crevice may help to stabilize the structure of Z-DNA, it cannot induce formation of Z-DNA.

In conclusion, the current structure of the d(m^5CGUAm^5CG) soaked with copper(II) chloride demonstrated that copper(II) does not modify the purine bases of adenine in the same manner as that of guanine bases. Although both types of purines are susceptible to electrophilic attack at the N7 nitrogen at the major groove in Z-DNA, and probably in B-DNA as well, DNA in dilute solution would likely be modified only at the guanine bases. Modifications at the adenine bases require additional, perhaps very specific, DNA-DNA interactions that occur in the crystal environment and perhaps in the more densely packed environment of the nuclear matrix in a cell. This structure also demonstrates the significance of cationic interactions on Z-DNA stability. The direct effect of copper(II) binding to the guanine bases on Z-DNA stability was not discussed, but the structure did help to answer some mechanistic questions concerning the effect of the physiologically important magnesium ions on Z-DNA stability.

BIBLIOGRAPHY

Aoki, K., Clark, G. R., & Orbell, J. D., Metal-Phosphate Bonding in Transition Metal-Nucleotide Complexes. The Crystal and Molecular Structure of the Polymeric Copper(II) Complex of Guanosine 5'-Monophosphate, (1976) Biochimica et Biophysica Acta, 425, 369-371.

Barton, J. K., & Lippard, S. J., Heavy Metal Interactions with Nucleic Acids, (1980) Nucleic Acid-Metal Ion Interactions, (Spiro, T. G., ed.) John Wiley & Sons, Inc., New York, 38-39.

Bram S., Froussard, P., Guichard, M., Jasmin, C., Augery, Y., Sinoussi-Barre, F., & Wray, W., Vitamin C Preferential Toxicity for Malignant Melanoma Cells, (1980) Nature, 284, 629-631.

Cantor, C. R., & Schimmel, P. R., Biophysical Chemistry, (1980), W. H. Freeman and Company, New York, part II, 687-792.

Chiou, S.-H., Chang, W.-C., Jou, Y.-S., Chung, H.-M. M., & Lo, T.-B., Specific Cleavage of DNA by Ascorbate in the Presence of Copper Ion or Copper Chelates, (1985) J. Biochem., 98, 1723-1726.

Drew, H. R., & Dickerson, R. E., Structure of a B-DNA Dodecamer, (1981) J. Mol. Biol., 151, 535-556.

Eichhorn, G. L., & Shin, Y. A., Interaction of Metal Ions with Polynucleotides and Related Compounds. XII. The Relative Effect of Various Metal Ions on DNA Helicity, (1968) J. Am. Chem. Soc., 90, 7323-7328.

Fujimoto, S., Adachi, Y.,Ishimitsu, S., & Ohara, A., Release of Bases from Deoxyribonucleic Acid by Ascorbic Acid in the Presence of Cu^{2+}, (1986) Chem. Pharm. Bull., 34, 11, 4848-4851.

Gessner, R. V., Quigley, G. J., Wang, A. H.-J., van der Marel, G. A., van Boom, J. H., & Rich, A., Structural Basis for Stabilization of Z-DNA by Cobalt Hexaammine and Magnesium Cations, (1985) Biochemistry, 24, 2, 237-240.

Goldstein, S., & Czapski, G., Mechanisms of the Reactions of some Copper Complexes in the Presence of DNA with O_2^-, H_2O_2, and Molecular Oxygen, (1986) J. Am. Chem. Soc., 108, 2244-2250.

Graham, D. R., Marshall, L. E., Reich, K. A., & Sigman, D. S., Cleavage of DNA by Coordination Complexes. Superoxide Formation in the Oxidation of 1,10-Phenanthroline-Cuprous Complexes by Oxygen-Relevance to DNA-Cleavage Reaction, (1980) J. Am. Chem. Soc., 102, 5419-5421.

Hecht, S. M., DNA Strand Scission by Activated Bleomycin Group Antibiotics, (1986) Federation Proceedings, 45, 212, 2784-2791.

Hendrickson, W. A., & Konnert, J., Stereochemically Restrained Crystallographic Least-Squared Refinement of Macromolecule Structures, (1981) Biomolecular Structure, Conformation, Function and Structure, (Srinivasan, R., ed.) Pergamon Press, Ltd., Oxford, 43-57.

Ho, P. S., Zhou, G., & Clark, L. B., Polarized Electronic Spectra of Z-DNA Single Crystals, (1990) Biopolymers, in press.

Huheey, J. E., Inorganic Chemistry, (1978) Harper & Row, Publishers, Inc., New York, 379-433.

Johnson, G. R. A., Nazhat, N. B., & Saadalla-Nazhat, R. A., Reaction of the Aquocopper(I) Ion with Hydrogen Peroxide: Evidence against Hydroxyl Free Radical Formation, (1985) J. Chem. Soc., Chem. Commun., 7, 407-408.

Jovin, T. M., Soumpasis, D. M., & McIntosh, L. P., The Transition between B-DNA and Z-DNA, (1987), Ann. Rev. Phys. Chem., 38, 521-560.

Kagawa, T., Ho, P. S., Stoddard, D., Rich., A., & Wang, A. H.-J., Covalent Modification of Guanine Bases of Z-DNA by Copper(II): 1.3 Å Structure of $d(CG)_3$ Soaked with $CuCl_2$, (unpublished) in preparation.

Kim, S. H., Quigley, G., Suddath, A., McPherson, A., Sneden, D., Kim, J. J., Weinzierl J., & Rich, A., X-ray Crystallographic Studies of Polymorphic Forms of Yeast Phenylalanine Transfer RNA, (1973), J. Mol. Biol., 75, 421-428.

Kuwahara, J., Suzuki, T., Funakoshi, K., & Sugiura, Y., Photosensitive DNA Cleavage and Phage Inactivation by Copper(II)-Camptothecin, (1985) Biochemistry, 25, 1216-1221.

Lehninger, A. L., Biochemistry, (1975) Worth Publishers, Inc., New York, Second edition, 873-874.

Levy, M. J., & Hecht, S. M., Copper(II) Facilitates Bleomycin-Mediated Unwinding of Plasmid DNA, (1988) Biochemistry, 27, 2647-2650.

Marshall, L. E., Graham, D. R., Reich, K. A., & Sigman, D. S., Cleavage of Deoxyribonucleic Acid by the 1,10-Phenanthroline-Cuprous Complex. Hydrogen Peroxide Requirement and Primary and Secondary Structure Specificity, (1981) Biochemistry, 20, 244-250.

Marshall Pope, L. E., Reich, K. A., Graham, D. R., & Sigman, D. S., Products of DNA Cleavage by the 1,10-Phenanthroline-Copper Complex, (1982) J. Biological Chemistry, 257, 20, 12121-12128.

Marzilli, L. G., Kistenmacher, T. J., & Eichhorn, G. L., Structural Principles of Metal Ion-Nucleotide and Metal Ion-Nucleic Acid Interactions, (1980) Nucleic Acid-Metal Ion Interactions, (Spiro, T. G., ed.), John Wiley & Sons, Inc., New York, 181-250.

Masarwa, M., Cohen, H., Meyerstein, D., Hickman, D. L. Bakac, A., & Espenson, J. H., Reactions of Low-Valent Transition-Metal Complexes with Hydrogen Peroxide. Are They "Fenton-Like" or not? 1. The Case of Cu+aq and Cr2+ aq, (1988) J. Am. Chem. Soc., 110, 4293-4297.

Morita, J., Ueda, K., Nanjo, S., & Komano, T., Sequence Specific Damage of DNA Induced by Reducing Sugars, (1985) Nucleic Acids Research, 13, 2, 449-458.

Nanjou, S., Fujii, S., Tanaka, K., Ueda, K., & Komano, T., Induction of Single Strand Scission in ØX174 RFI DNA by D-Isoglucosamine, (1985) Agric. Biol. Chem., 49, 2, 459-466.

Ponganis, K. V., de Araujo, M. A., & Hodges, H. L., Electron-Transfer Reactions of Copper Complexes. 1. A Kinetic Investigation of the Oxidation of Bis(1,10-Phenanthroline)Copper(I) by Hydrogen Peroxide in Aqueous and Sodium Dodecyl Sulfate Solution, (1980) Inorg. Chem., 19, 2704-2709.

Pullman, A., & Pullman B., Molecular Electrostatic Potential of the Nucleic Acids, (1981) Quarterly Reviews of Biophysics, 14, 3, 289-380.

Quinlan, G. J., & Gutteridge, J. M. C., Oxygen Radical Damage to DNA by Rifamycin SV and Copper ions, (1987) Biochemical Pharmacology, 36, 21, 3629-3633.

Rabow, L. E., Stubbe, J. A., & Kozarich, J. W., Identification and Quantitation of the Lesion Accompanying Base Release in Bleomycin-Mediated DNA Degradation, (1990a) J. Am. Chem. Soc., 112, 3196-3203.

Rabow, L. E., McGall, G. H., Stubbe, J. A., & Kozarich, J. W., Identification of the Source of Oxygen in the Alkaline-Labile Product Accompanying Cytosine Release During Bleomycin-Mediated Oxidative Degradation of d(CGCGCG), (1990b) J. Am. Chem. Soc., 112, 3203-3208.

Sagripanti, J.-L., & Kraemer, K. H., Site-Specific Oxidative DNA Damage at Polyguanosines Produced by Copper plus Hydrogen Peroxide, (1989) J. Biological Chemistry, 264, 3, 1729-1734.

Schaaper, R. M., Koplitz, R. M., Tkeshelashvili, L. K., & Loeb, L. A., Metal-Induced Lethality and Mutagenesis: Possible Role of Apurinic Intermediates, (1987) Mutation Research, 177, 179-188.

Sigman, D. S., Nuclease Activity of 1,10-Phenanthroline-Copper Ion, (1986) Acc. Chem. Res., 19, 180-186.

Sissoeff, I., Grisvard, J., & Guille/, E., Studies on Metal Ions-DNA Interactions: Specific Behaviour of Reiterative DNA Sequences, (1976) Prog. Biophys. Molec. Biol., 31, 165-199.

Stoewe, R., & Prutz, W. A., Copper-Catalyzed DNA Damage by Ascorbate and Hydrogen Peroxide: Kinetics and Yield, (1987) Free Radical Biology & Medicine, 3 , 97-105.

Veal, J. M., & Rill, R. L., Sequence Specificity of DNA Cleavage by Bis(1,10-Phenanthroline)Copper(I), (1988) Biochemistry, 27, 1822-1827.

Veal, J. M., & Rill, R. L., Sequence Specificity of DNA Cleavage by Bis(1,10-Phenanthroline)Copper(I): Effects of Single Base Pair Transitions on the Cleavage of Preferred Pyrimidine-Purine-Pyrimidine Triplets, (1989) Biochemistry, 28, 3243-3250.

Wang, A. H.-J., Quigley, G. J., Kolpak, F. J., Crawford, J. L., van Boom, J. H., van der Marel, G., & Rich, A., AT Base Pairs are Less Stable than GC Base Pairs in Z-DNA: The Crystal Structure of d(m^5CGTAm^5CG), (1984) Cell, 37, 321-331.

Wendrychowski, A., Schmidt, W. N., & Hnilica, L. S., The *In Vivo* Cross-Linking of Proteins and DNA by Heavy Metals, (1986) J. Biological Chemistry, 261, 7, 3370-3376.

Wong, A., Cheng, H.-Y., & Crooke, S. T., Identification of the Active Species in Deoxyribonucleic Acid Breakage Induced by 4'-(9-Acridinylamino)Methanesulfon-m-Anisidide and Copper, (1986) Biochemical Pharmacology, 35, 7, 1071-1078.

Yamamoto, K., & Kawanishi, S., Hydroxyl Free Radical is not the Main Active Species in Site-Specific DNA Damage Induced by Copper(II) Ion and Hydrogen Peroxide, (1989) J. Biological Chemistry, 264, 26, 15435-15440.

Zhou, G. & Ho, P. S. , Stabilization of Z-DNA by Demethylation of Thymine Bases: 1.3 Å Single Crystal Structure of d(m^5CGUAm^5CG), (1990) Biochemistry, in press.

Zimmer, Ch., Luck, G., Fritzsche, H., & Triebel, H., DNA-Copper(II) Complex and the DNA Conformation, (1971) Biopolymers, 10, 441-463.